

https://dspace.org/

An evaluation of chromitiferous layers and their host rocks in the Platreef, on the Turfspruit and Zwartfontein properties: a comparative study with the main Bushveld Complex

Cronje, Louwrens

2017

https://hdl.handle.net/10539/24847

Cronje, Louwrens Johannes (2017) An evaluation of the chromitiferous layers on the Turfspriut and Zwartfontein properties : a comparative study with the main Bushveld Complex, University of the Witwatersrand, Johannesburg, https://hdl.handle.net/10539/24847

Downloaded from a DSpace repository. https://dspace.org/



An evaluation of chromitiferous layers and their host rocks in the Platreef, on the Turfspruit and Zwartfontein properties: A comparative study with the main Bushveld Complex.

By

Louwrens J Cronje

A research report submitted to the Faculty of Science, University of the Witwatersrand, Johannesburg, in partial fulfilment of the requirements for the degree of Master of Science.

University of the Witwatersrand, Johannesburg

2017

Declaration

I declare that this thesis is my own, unaided work. It is being submitted for degree of Master of Science in the University of the Witwatersrand, Johannesburg. It has not been submitted before for any degree or examination in any other University.

Signature of candidate

day of 2017

Acknowledgements

First and foremost, my utmost thanks to both Professor Judith Kinnaird and Dr Marina Yudovskaya for their supervision, support and travelling with me to Mokopane to sample and log material for this study. Secondly, I would like to thank my parents for their continual support in assisting and encouraging me to further my studies. A great deal of appreciation goes to Ivanplats for providing me with the opportunity to study and sample their core. Lastly, a great deal of appreciation goes to Sandy Little for her ceaseless support during difficult times.

Abstract

The origin of the Platreef in the northern limb of the Bushveld Igneous Complex remains a topic of debate. Its relationship with that of the PGE-reefs of the Main Bushveld Complex is disputed and there is currently no widely accepted theory available, as both parties have valid arguments. This study involves the stratigraphic, petrographic and chemical investigation of the chromitiferous layers and their hosts, in the Platreef, on both the Turfspruit and Zwartfontein properties. The work in this study has shown that the conventional stratigraphy that defines the upper Critical Zone is not present in the study areas, which lack the sophisticated layering and cycles present in the main complex and generally, rocks are significantly more heterogenous in the Platreef than elsewhere in the Bushveld Complex. A large number of petrographic similarities were identified in the study area, when compared to known textures and morphologies published by previous workers, especially on the Upper Group chromitite layers. The chemistry of the Platreef reflect a more primitive magma responsible for the deposition of these rocks, which is demonstrated through higher Mg contents, and lower Ti, indicating less fractionation when compared to the main Bushveld Complex. It must be stated that the influence of contamination on Mg-rich lithologies may have altered their composition, which could have generated misleading results. Statistically, the results obtained may not be entirely representative of the true chemical character of the entire northern limb, and the opinions and assumptions made are very localised. This study concludes that the upper Critical Zone magma was probably not responsible for the deposition of the Platreef, while rocks were locally altered due to contamination from country rock.

Table of Contents

Abstract iv
List of Figures vii
List of Tables xi
Chapter 1 12
General Geology of the Bushveld Igneous Complex 12
1.1 Background Geology of the Bushveld Complex 12
1.2 The Rustenburg layered suite 13
1.3 Marginal Zone (MaZ) 15
1.4 Lower Zone (LZ) 15
1.5 Critical Zone (CZ) 16
1.6 Main Zone (MZ) 16
1.7 Upper Zone (UZ) 18
Chapter 2 19
Location and aim of study 19
2.1 General Geology of the Northern Limb 19
2.2 Location 21
2.3 Aim 23
2.4 Objectives 24
Chapter 3 26
Field observations 26
3.1 Introduction 26
3.2 Stratigraphy of the area 26
3.3 Methodology 28
3.2 Lithologies of the Study area 29
3.4 Stratigraphy of the Turfspruit area 34
3.5 Lithologies of the Turfspruit Area 38
3.6 Stratigraphy of Zwartfontein 41
3.7 Discussion 44
3.7.1 Comparison between Akanani and Turfspruit 46
3.7.2 Comparison with the Main Bushveld Complex 47
Chapter 4 50
Petrography 50
4.1 Introduction 50
4.1.1 Pyroxenite 50

4.1.2 Feldspathic Pyroxenite 56
4.1.3 Parapyroxenite 57
4.1.4 Harzburgite 59
4.2 Petrography of Chromitiferous horizons 60
4.2.1 Atoll-type chromites 63
4.2.2 Chain-textured 63
4.3 Petrography of sulphide minerals 64
4.4 Discussion 67
4.4.1 Pyroxenite 67
4.4.2 Feldspathic Pyroxenite 68
4.4.3 Parapyroxenite 68
Harzburgite 69
Chromite 70
Sulphides 73
Comparison between the Main Bushveld Complex and the study areas 73
Chapter 5 76
Chemistry 76
Introduction 76
Techniques 76
5.1 Mineral Chemistry 76
5.1.1 Chromite 76
5.1.2 Olivine Chemistry 79
5.2 Mineralisation 82
5.3 Geochemistry of hole UMT366 85
5.4 Discussion 89
5.4.1 Chromite 89
5.4.2 Olivine 90
5.4.3 Mineralisation 91
5.5 Comparison between the study areas and the Main Bushveld Complex 91
Chapter 6 93
Conclusion 93
References 95
Appendix 105

List of Figures

Figure 1. 1: Map of the Bushveld Igneous Complex, showing the position of the various limbs, lithologies and major structures (Reczko et al. 1995; Cawthorn and Lee, 1998). The dotted lines outlining the Southern and Northern limbs are interpreted from aeromagnetic and gravity data..... 13
Figure 1. 2: Stratigraphic column of the Bushveld Complex, with a summary of mineral compositions and initial Sr isotopic ratio through the complex (Cawthorn, 2015). 14
Figure 1. 3: Stratigraphy through the Critical Zone, showing the position of chromitite layers and the cyclic nature of the rocks (Schürmann et al., 1998). 17

Figure 2. 1: Schematic illustration of the geology of the northern limb of the Bushveld Complex. (A) The complete northern limb indicating all the lithologies and major structures (Van der Merwe, 1978; Ashwal et al., 2005). (B) Geological map of the northern limb with the position of the farms indicated as well (Viljoen and Schürmann, 1998) and the four sectors (Kinnaird et al., 2005). 20
Figure 2. 2: Location of the Akanani project on the farm Zwartfontein 814 LR. Open cast mining is currently taking place up dip on the farms Sandsloot 236KR, Vaalkop 819 LR, Zwartfontein, 818 LR and Overysel 815 LR. (Van der Merwe et al., 2012; Mitchell and Scoon, 2012). 22
Figure 2. 3: Location of the Ivanplats Underground Mining project on Turfspruit. The areas highlighted in red delineate the location of the boreholes used in this study (Van der Merwe, 1978; Ivanplats, 2013)..... 23

Figure 3. 1: Traditional correlation of stratigraphic columns between the Main Bushveld Complex and that of the northern limb, with an inferred correlation between the Platreef and the Merensky Reef (White, 1994). Note that the variable rock types constitute the Transvaal floor in the northern limb. Kinnaird et al. (2002) shows that the Platreef may be separated by country rock from the Lower Zone or basement rocks. 27
Figure 3. 2: (A) Ternary diagram for the classification of mafic rocks. (B) Ternary diagram for the classification of gabbroic rocks (Le Bas and Streckeisen, 1991). 30
Figure 3. 3: Photographs of different lithologies in core sampled: (A) Serpentinised harzburgite from the 923 metres below base. The poikilitic texture consists of orthopyroxene oikocrysts, which encloses remnants of olivine grains. Most orthopyroxene grains have not been serpentinised. Most probably secondary olivine formed through fluids, possibly associated with a xenolith, although no evidence for a xenolith was preserved. (B) Sharp contact between the 'UG2-like' chromitite and a pyroxenite. Chromite and host pyroxenite appear to be primarily magmatic, thus good candidates for further mineral chemistry studies. (C) Hybrid of a spotted and mottled anorthosite, at 1558m. Notice the dark-green clinopyroxene 'mottles', and cores of brown orthopyroxene. (D) Orthopyroxenite in hole UMT 335 consists of cumulus orthopyroxene grains, along with intercumulus plagioclase (5%) and minor clinopyroxene. (E) Gabbronorite with small chromite-stringer at 1570 m in UMT 366 comprises of green, anhedral clinopyroxene, with more euhedral, brown orthopyroxene grains. The presence of the chromite grains is rather rare within such lithologies. (F) Feldspathic pyroxenite in UMT 377. Notice interstitial plagioclase and sulphides, with cumulus, sometimes rounded orthopyroxene grains..... 32
Figure 3. 4: Photographs of different lithologies in core sampled (A) Dolomite xenolith in hole UMT335, displaying well-defined, thin layering. (B) Hornfels xenolith with sedimentary layers still evident. It is difficult to determine the protolith, but in terms of its fine-grain size and the layering, it may well have been part of the Duitschland formation shales. (C) Parapyroxenite with some garnets and olivine, UMT336. The dominant pyroxene is diopside (dark green), along with sugary olivine

grains (light sea-green). The brown minerals are garnets, possibly grossular garnet. (D) Pegmatoidal feldspathic pyroxenite. Although there is a significant amount of plagioclase present, some of which is cumulus, by convention it is called a feldspathic pyroxenite rather than a norite. (E) Chromite-rich horizon at 1520 m in ZF-116. Notice the large cumulus orthopyroxene grain, around which the chromite has crystallised. This may indicate a secondary process for chromite crystallisation. (F) Between the two dotted red and yellow lines is a hybrid rock, at a gradational contact between the banded dolomite xenolith shown in Figure 3.3.A, and a serpentinised, probably metamorphic harzburgite. Notice towards the right is a rock similar in appearance to 3.3A, and in between, there is a complete mixture of magmatic and sedimentary rocks occurring. 33
Figure 3. 5: A typical norite cycle progressing from mafic-poor to mafic-rich lithologies, as seen in the upper to middle parts of the Platreef succession. 35
Figure 3. 6: Position and locality of the boreholes studied on the Turfspruit property (A) Locality of the holes logged and presented in Figure 3.7. The A-B delineates the direction in which Figure 3.7 is orientated. (B) A map of the northern limb, with the Turfspruit property highlighted in red (Adapted from Van der Merwe, 1978). 36
Figure 3. 7: Stratigraphic columns of holes UMT377, 336, 335 and 366. Some of the chromite-horizons, such as the 'UG2-like' chromite was vertically exaggerated in order to identify their position more clearly. The scales are in metres below surface. 37
Figure 3. 8: Position of the study area in relation to the general stratigraphy. The study area is highlighted in yellow, and occurs within the proposed underground mining project of Ivanhoe, although in the footwall of the selective high-grade zone (Ivanplats, 2013). 38
Figure 3. 9: Stratigraphic column of hole ZF 116, part of the Akanani project on the farm Zwartfontein 814LR (Figure 2.2). 43

Figure 4. 1: Photomicrographs of various rock types from Turfspruit under a transmitted light microscope. (A) Single vein of serpentine cross-cutting a feldspathic pyroxenite and a chromite striger in UMT 377 at 1033 m. Notice that the serpentine vein has not affected the surrounding minerals in any way. (CPL) (B) Lath-shaped orthopyroxene grains that exhibit foliation which is defined by subparallel alignment of these elongated grains. UMT 377 at 1007 m (CPL). (C) Tricuspidate-shaped plagioclase inclusion within an orthopyroxene grain. Notice the concave-inward boundaries of the inclusion, resembling intercumulus plagioclase within feldspathic pyroxenites. UMT-335 at 1717 m (PPL) (D) Large, intercumulus clinopyroxene grains that encloses older orthopyroxene and olivine grains. UMT 366 at 1585 m (CPL) (E) 1.6 cm, cumulus orthopyroxene oikocryst, occurring within a chromitiferous zone in UMT 366 at 1586.2 m (PPL). CPL=Crossed polarised light. PPL=Plane polarised light. 51
Figure 4. 2: Photomicrographs of various rock types from Zwartfontein and Turfspruit under a transmitted light microscope. (A) Serpentine vein running across a norite, including a number of clinopyroxene grains and Cr spinels. The surrounding minerals appear to be unaltered though. UMT 366 at 1561.4 m. (CPL) (B) Rare plagioclase grain in a chromite-rich pyroxenite showing Carlsbad twinning, from 1538.6 m in hole ZF 116. (CPL) (C) Highly serpentinised rock with the only recognisable minerals grains being skeletal, intercumulus clinopyroxene grains. UMT 366 at 1586.2 m. (CPL) (D) Paraharzburgite consisting out of an interlocking framework of olivine grains. UMT 377 at 922 m. (CPL) (E) Olivine grain highly serpentinised by what appears to be chrysotile.UMT 366 at 1595.5 m. (CPL) (F) Hornfels xenolith with what appears to be a norite patch. UMT377 at 973 m. (PPL) 52
Figure 4. 3: Photomicrographs of different rock types from Turfspruit under a transmitted light microscope. (A) and (B) Both these photos are typical examples of the poikilitic texture displayed by

olivine chadacrysts in orthopyroxene oikocrysts. The olivine in these photos were formed earlier and corroded later by the orthopyroxene oikocryst. During serpentinisation more water is absorbed into the crystal structure of these grains, leading to volume expansion and the 'cracked' feature seen in the olivines. (A) is from UMT366 at 1595.5 and (B) from UMT366 at 1585.4. Both photos were taken under CPL (C) Granular harzburgites which consists of lesser olivine and more opx, and are texturally comparable to olivine orthopyroxenites. This sample is from UMT366, within the hanging wall of the so-called UG2 on Turfspruit. (PPL). 53
Figure 4. 4: Photomicrographs of the different features present in parapyroxenite from Turfspruit and Zwartfontein. (A) Parapyroxenite in the footwall of the UG2 on Turfspruit in UMT 335 at 1720 m that is dominated by clinopyroxene. (CPL). (B) Highly altered parapyroxenite that shows the presence of carbonate minerals inherited from a dolomitic xenolith in UMT 335 at 1720 m. (CPL). (C) Parapyroxenite from the Zwartfontein property, showing a distinctive clinopyroxene morphology, indicative of metamorphic behaviour. (CPL). (D) Chromitiferous pegmatoidal feldspathic pyroxenite that contains elongated laths of clinopyroxene and more than 15% interstitial plagioclase. Situated in the hanging wall of the Lower chromite zone in ZF116 at 1538 m. (PPL). (E) Sulphides in a parapyroxenite, in UMT 377 at 998 m, that have been replaced due to extensive alteration. Taken under PPL in reflected light. 54
Figure 4. 5: Hybrid rock from UMT335 at 1720 that contains orthopyroxene grains orientated with the layering of the original dolomite protolith. 58
Figure 4. 6: Photomicrographs of different chromite morphologies. (A) Chain-textured chromites occurring within plagioclase, within the boundaries of pyroxenes. UMT366 at 1579.3 m. (CPL). (B) Annealed massive chromite grains showing 120° triple junctions where grains meet. These triple junctions are indicative of the sintering process in chromites. UMT 366 at 1584 m. (Reflected light) (C) Chain-textured chromite cross-cutting all minerals. UMT 377 at 1035 m. (PPL) (D) Massive chromites with small interstitial sulphides. Massive chromites show considerably larger grain sizes than those that are disseminated, due to the annealing and sintering of grains. ZF116 at 1538 m. (Reflected light) (E) A chain-textured chromite stringer cross-cutting silicate minerals (Modified from Cawthorn and Boerst, 2006; Reproduction of a diagram from Wagner, 1929). 61
Figure 4. 7: Photomicrographs of atoll-type and chain-textured chromites. (A) Atoll-type chromite with orthopyroxene inclusion, which is optically continuous with opx outside the chromite grain. UMT 366 at 1595 m. (CPL) (B) Atoll-type chromite with chalcopyrite inclusion. ZF116 at 1538 m. (Reflected light) (C) Atoll- and mantle- type chromite within a highly serpentinised area. UMT 366 at 1561 m. (CPL) (D) Chain-textured and atoll-type chromites. UMT 377 at 984.1 m. (CPL) (E) Atoll and mantle-type chromites, showing olivine inclusions. (CPL) (F) Highly serpentinised olivine grain that is mantled by chromite. ZF116 at 1538 m. (PPL). 62
Figure 4. 8: Different morphologies and compositions of sulphide minerals in various rock types, taken under reflected light. (A) Intercumulus sulphide grains that mantle rounded pyroxenes in UMT366 at 1595.5 m. (B) Intercumulus sulphides occurring within the boundaries of pyroxenes. ZF116 at 1520 m. (C) Complex sulphide from UMT 366 at 1586 m, consisting out of a core of pyrrhotite, pentlandite exsolution, and rimmed by chalcopyrite. ZF 116 at 1537.15 m. (D) Multiphase sulphide grain that mantles a chromite grain. (Pyrh=Pyrrhotite; Pn=Pentlandite; Cpy=Chalcopyrite). ZF116 at 1537.15 m. (E) Angular grain of pyrrhotite with very little chalcopyrite and flames of pentlandite. Early magmatic sulphide as explained by Kinnaird (2005). ZF116 at 1538.3 m. (F) Isolated, large, disseminated sulphides (predominantly chalcopyrite) in a parapyroxenite in ZF116 at 1520 m. 65

Figure 5. 1: Binary diagram of Cr vs Ti and Cr vs Al for different parts of the Bushveld Complex, including ZF (Zwartfontein), UG2-W (Waterval mine), UG1-U and UG2-U (Union section) and LZ (Lower Zone of the eastern limb). Chemical data and references are shown in Table 1 and 2 in the appendix..... 77
Figure 5. 2: Binary diagrams of both Ti and Mn vs Mg# for different lithologies in the study area. The abbreviations in the legend are as follows: TU (Turfspruit), ZF (Zwartfontein), Para-HZB (Paraharzburgite), LZ-FHZB (Lower Zone feldspathic harzburgite), DUN (Dunite), FPYX (Feldspathic pyroxenite), HZB (Harzburgite). Chemical data is shown in Table 2 and Table 4. 80
Figure 5. 3: Binary diagrams of Ni, Ti and Mn vs Mg# of different areas around the Bushveld Complex. 81
Figure 5. 4: Back-scattered electron images of the positions and morphologies of base metal sulphides and Platinum group minerals. Table 5.1 on the next page lists the chemical composition of the points shown on the figures above. (A) A multiphase sulphide consisting of pentlandite and pyrite, with a grain of Pd-sulphide on the edge. (TMT 870). (B) Cubic chalcopyrite grain. (C) Extremely small grain of a gold-mercury alloy. (D) Pd-dominated bismuthotelluride, occurring on the flanks of pentlandite and an arsenic-sulphide. (E) Small grain of Pd-Pt sulphide. (F) A strange Pt-sulphide mineral, with high amounts of Cu, Rh and Fe. 83
Figure 5. 5: A stratigraphic column of hole UMT336, with the associated chemistry of the economic elements. 86
Figure 5. 6: Binary diagrams with different elemental plots, highlighting chemical differences between various lithologies in hole UMT366 on Turfspruit. The graphs show the relationship between PGE's and S and base metals, as well as the relationship between Pt and Pd. The abbreviations in the legend are as follows: AN (Anorthosite), CR (Chromite), CRT (Chromitite), CS (Calc-silicate), DN (Dunite), FHA (Feldspathic harzburgite), FPX (Feldspathic pyroxenite), GRV (Granite vein), HA (Harzburgite), HFN (Hornfels), N (Norite), NC (Norite cycle), OLOPX (Olivine orthopyroxenite), OLPX (Olivine pyroxenite), OPX (Orthopyroxenite), PAPX (Parapyroxenite), PX (Pyroxenite), QZ (Quartz vein). 88

List of Tables

Table 1: EMPA on chromite from holes ZF116 and ZF48 on the Zwartfontein property……..105

Table 2: EMPA on olivine grains from hole UMT6 on Turfspruit……106

Table 3: EMPA on chromite from the main Bushveld Complex. *UG2-W* was done by Opoubou-Lando (2010) at the Waterval Mine. UG1-U and UG2-U was done by Eales and Reynolds (1986) in the Union section. The LZ (Lower Zone) was analysed by Cameron (1978). UMT377 and TMT 870 was analysed by EDS at the University of the Witwatersrand……117

Table 4: EMPA on olivine grains from hole ZF116 on Zwartfontein……118

Table 5.1: Mineral chemistry of different grains shown in figure……84

Chapter 1

General Geology of the Bushveld Igneous Complex

1.1 Background Geology of the Bushveld Complex

The Bushveld Igneous Complex in South Africa was emplaced into the Kaapvaal Craton at 2055-2060 Ma (Walvaren et al. 1990, Scoates and Friedman 2008), although recent zirconology results from Zeh et al. (2015) indicate that the whole Complex may have intruded in as little as 1 million years. It is the largest known layered igneous intrusion, covering an area of roughly 65 000 km^2 (Tankard et al., 1982; Grunewaldt et al. 1985, Cawthorn 1999), with recent research suggesting 90 000 km^2 (Finn et al., 2015) and an estimated volume of 370 000 – 600 000 km^2 (Eales and Cawthorn, 1996; Cawthorn and Walvaren, 1998). The pre-Bushveld tectonic setting is a contentious topic and a number of models have been proposed in the past for the shape and distribution of the complex (example: Willemse, 1969, Hunter, 1975). Concepts vary from a stable cratonic setting (Crockett, 1969, Hunter 1975), to large-scale orogenies (Van Biljon, 1976, De Wit, 1987) as well as an extensive system of major mafic complexes (which includes the Great Dyke and Trompsburg Complex) that are linked to a proposed 'primeval' fracture zone (Cousins, 1959), later termed the 'Bushveld line of intrusion' (Darracott, 1975). Today, it seems the most favourable model is that of a stabilised craton (Groves et al., 1987; Maier and Groves, 2011).

Generally, the Complex was intruded into the Transvaal Supergroup, which comprises a very thick package of volcanic and intracratonic chemical and clastic sedimentary rocks (Hall, 1932; van der Merwe, 1976; Eriksson and Reckzo 1995), ranging in age from 2551 to 2204 Ma (Walvaren et al. 1990; Barton et al. 1994). Although in the northern limb, north of Mokopane, the contact transgresses downwards such that ultimately the mafic rocks abut against Archaean granitic gneiss (White 1994). The Bushveld complex comprises of four exposed sectors, these include the eastern limb, the western limb, the far western limb, the northern limb (Du Plessis and Walvaren 1990, Cawthorn and Walvaren 1998), and the south-eastern Bethal limb, obscured by younger sediments (Figure 1.1) (Kinnaird et al. 2005).

A number of different definitions of the Bushveld Complex and the suites of rocks encompassed by the Bushveld event have been suggested. The South African Committee of Stratigraphy (1980) proposed a three-fold subdivision into the mafic rocks of the Rustenburg Layered Suite (RLS), the Lebowa Granite Suite and the Rashoop Granophyre Suite, while more recently the felsic volcanic rocks of the Rooiberg Group have also been included (Hatton and Schweitzer, 1995).

The economically significant Rustenburg layered suite, which has an average thickness of 6km (Ashwal et al. 2005), is divided into five major zones (Hall, 1923), namely the Marginal, Lower, Critical, Main and Upper Zones (Figure 1.2) (SACS 1980), although their exact boundaries have been a topic of much debate (Kruger 1990). Three major PGE-mineralised horizons occur within the RLS, they include the Merensky Reef and the Upper Group 2 (UG2) chromitite layer, which can be traced over 150km along strike and are mirrored in both the eastern and western limbs (Cawthorn and Eales, 1996), and the Platreef, which is unique to the Northern Limb. Combined, these three layers contain most of the world's platinum and palladium resources (Vermaak, 1995; Cawthorn, 1999; Vermaak and van der Merwe, 2002).

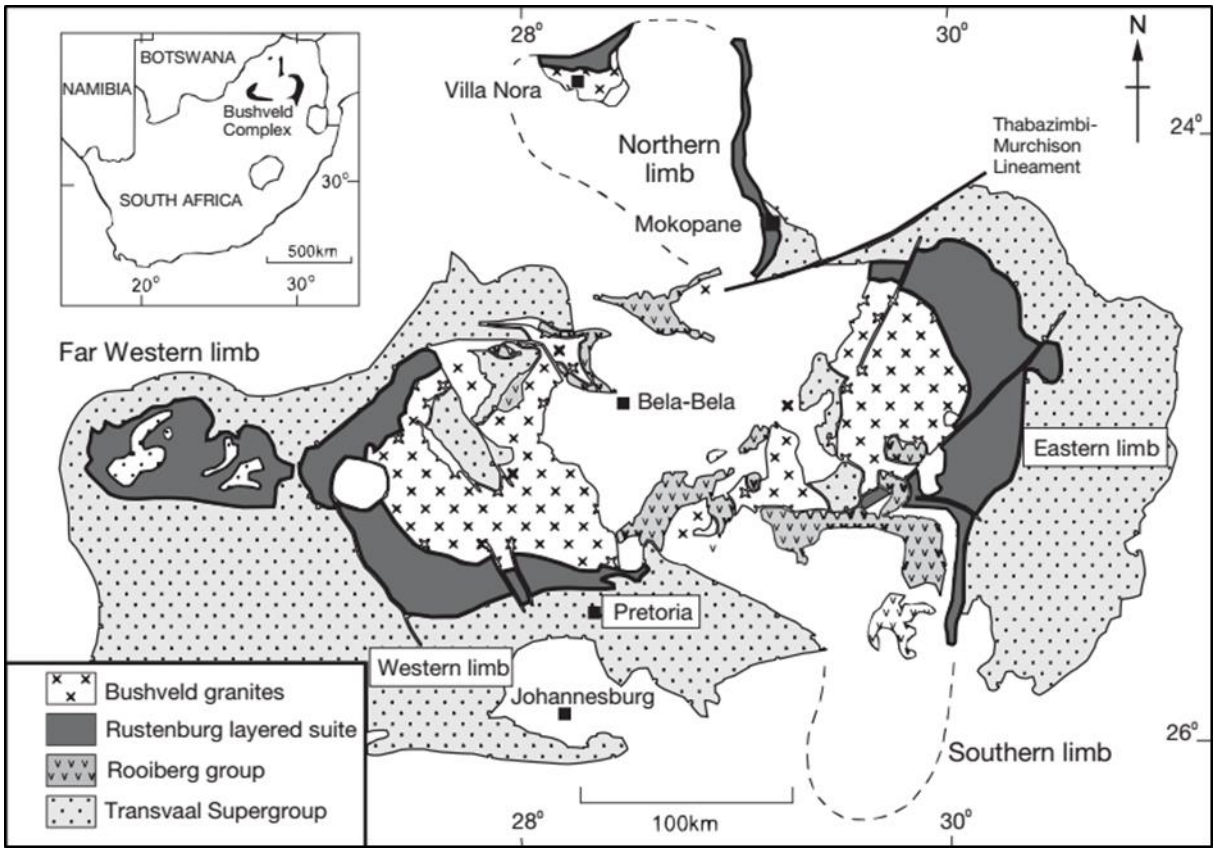


Figure 1. 1: Map of the Bushveld Igneous Complex, showing the position of the various limbs, lithologies and major structures (Reczko et al. 1995; Cawthorn and Lee, 1998). The dotted lines outlining the Southern and Northern limbs are interpreted from aeromagnetic and gravity data.

1.2 The Rustenburg layered suite

In the international literature, the term 'Bushveld' is generally used to describe the mafic and ultramafic layered rocks of the Bushveld Complex, however, the South African Commission for Stratigraphy (1980) named this package of rocks the Rustenburg Layered Suite (RLS). The RLS forms the world's largest layered intrusion (400km by 300km in area and up to 8km thick), although based on the preserved thermal metamorphic aureole, the original extent of the area was much greater (Reichhardt, 1994). In the western and eastern limbs, the RLS shows a similar stratigraphy, whereas

it is generally thinner and less developed within the northern limb. The RLS consists of a wide range of rock types from dunite and pyroxenite through norite, gabbro, anorthosite to magnetite-rich diorite, and thus exhibits a complete differentiation sequence for a basic magma (Cawthorn and Boerst, 2006; Cawthorn, 2007a). The RLS is divided into five zones based on the lithostratigraphy and the order of appearance and disappearance of cumulus minerals, such as olivine, orthopyroxene, magnetite etc. due to changes from magmatic differentiation (Kruger, 1994; Kinnaird 2002).

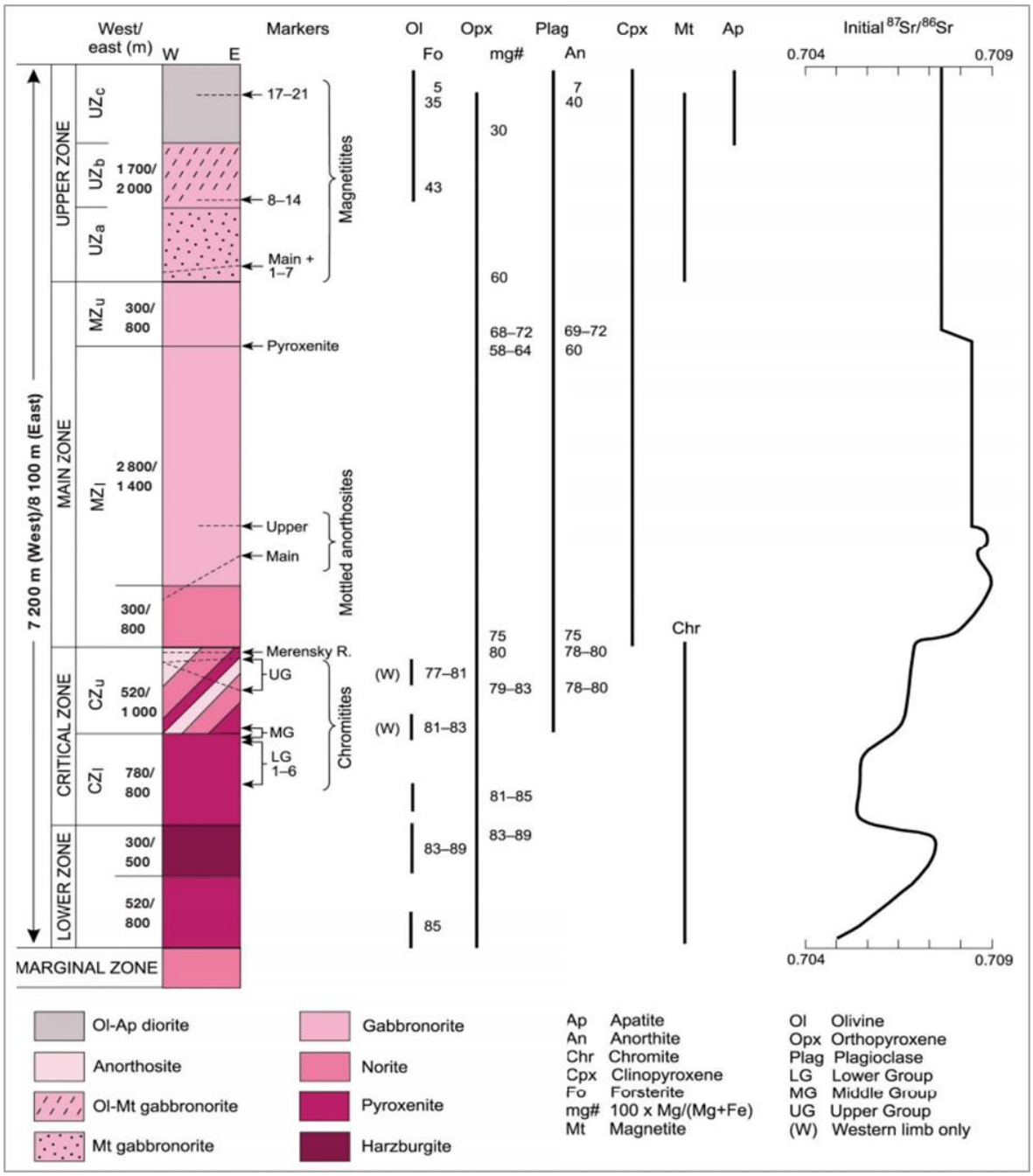


Figure 1. 2: Stratigraphic column of the Bushveld Complex, with a summary of mineral compositions and initial Sr isotopic ratio through the complex (Cawthorn, 2015).

The subdivisions include the basal Marginal Zone (MaZ), consisting of 0-800 m of norites, which is overlain by the Lower Zone (LZ) 800-1300 m of cyclic units of harzburgites and pyroxenites, the Critical Zone (CZ),1300-1800 m of cyclic units of chromitite, pyroxenite, and norites, the Main Zone (MZ), 3000-3400 m of norites, gabbronorites and anorthosites, and the Upper Zone (UZ), 2000-2800 m of magnetites, gabbronorites, anorthosites, and diorites (Figure 1.2). According to Kruger (1994), the RLS formed from new influxes of magma, indicated by the change in strontium isotopes that mark major boundaries, therefore resulting in a large layered igneous intrusion.

1.3 Marginal Zone (MaZ)

The Marginal Zone rocks, which are not always present, comprises up to 880 m of heterogeneous, medium-grained noritic rocks that form the basal contact of the complex (Harmer and Sharpe, 1985). Evidence for country rock assimilation is indicated by the presence of a variable quartz and biotite content (Cawthorn *et al*., 2006). According to Cawthorn (2015), the sequence represents the relatively rapid crystallisation of magmas which are variably contaminated and differentiated relative to the subsequent, more voluminous injections of magma that produced the RLS.

1.4 Lower Zone (LZ)

The Lower Zone sequence is subdivided into the Lower Pyroxenite subzone, the Harzburgite subzone, and the Upper Pyroxenite subzone (Cameron, 1978; SACS 1980). It consists of alternating layers of bronzite, dunite, and harzburgite (Von Gruenewaldt *et al*., 1985), with the thickest sections developed in the central sector of the eastern limb, near the union section in the western limb, in the far western limb, south of Mokopane (Hulbert and von Gruenewaldt, 1985), and beneath the Platreef on the Turfspruit property in the northern limb (Yudovskaya et al. 2013). The upper boundary of the Lower Zone is poorly defined. Cameron (1978) defined the boundary based on the increase in intercumulus plagioclase from 2 to 6 %, Teigler and Eales (1996) proposed putting the boundary at the top of the uppermost harzburgitic layer, while Cawthorn et al., (2006) defined the boundary by the first occurrence of cumulus chromitite. All the proposed boundaries have some weakness. Firstly, a variable amount of plagioclase occurs at different stratigraphic levels of the Lower and Lower Critical zones, and the change is not sufficiently characteristic to define a boundary (Yudovskaya *et al*., 2013). Secondly, even though the Grasvally area south of Mokopane in the Northern limb is not readily correlated with the stratigraphy elsewhere, large chromitite seams do occur within the Lower Zone of this area (Hulbert and Von Gruenewaldt 1985), therefore this would not make a fitting boundary. This suggests that the position of the uppermost harzburgite is the most reliable marker, although that would mean that the overlying pyroxenitic layer (which presumably is part of the same cycle), and the whole pyroxenitic package beneath the lowermost LG1 chromitite layer should be attributed to the Lower Critical Zone (Yudovskaya *et al*., 2013).

1.5 Critical Zone (CZ)

The Critical Zone hosts the world's largest platinum-bearing ore bodies (Upper group 2 chromitite and the Merensky Reef) and vast reserves of chromite within the Lower (LG), Middle (MG) and Upper (UG) group chromitite layers (Figure 1.3) (Eales, 1987; Scoon and Teigler, 1994; Schürmann *et al*., 1998). It is subdivided into a lower subzone (lCZ), which consists of a ~700-800 m thick package of predominantly orthopyroxenitic cumulates (89%: Teigler and Eales 1996) and an upper subzone (uCZ) comprising packages of chromite, harzburgite, pyroxenite, through norite to anorthosite (Teigler and Eales, 1996; Kinnaird *et al.*, 2002). The base of the uCZ is defined by the first appearance of cumulus plagioclase, which usually occurs in the middle of a cluster of four chromite layers, referred to as the Middle Group (MG1-MG4; Figure 1.3) (Cawthorn et al., 2006). In the western and eastern limbs, this is shown by a laterally continuous, 1-3 m thick anorthosite layer, which forms a sharp contact marked by a 1-2 mm chromite stringer with underlying orthopyroxenite (Maier et al., 2013). However, in the Northern limb, fine-grained uCZ rocks overlie thick harzburgites of what is believed to be LZ, implying that the LCZ might be absent (Hulbert, 1983; Maier et al., 2008a).

A feature that is particularly characteristic of the uCZ is the occurrence of cyclic units (Cameron, 1982; Eales et al., 1986, 1990). The base of the units typically consists of ultramafic rocks (such as chromite and/or harzburgite) that are overlain by progressively more feldspathic rocks (i.e. first pyroxenite and then norite followed by anorthosite). PGE-mineralisation tends to be concentrated in the basal ultramafic portions of the larger units, particularly in the case of the economically important Merensky Reef and UG2 chromitite (Maier et al., 2013). The base of each unit is sharp, but internal contacts may be gradational (Cawthorn, 2015).

There are 13 major chromitite seams in the CZ (Figure 1.3), Lower group (LG) seams 1-7 and Middle group (MG) seams 1-4, and UG 1-2, of which LG6 hosts the largest chromite reserve on Earth (Crowson, 2001). Some of the chromitite layers can be traced for over 100 km in strike in both the eastern and western limbs (Hatton and Von Gruenewaldt 1987; Schürmann *et al*., 1998).

1.6 Main Zone (MZ)

Most authors place the boundary between the MZ and the CZ at the top of the Giant Mottled Anorthosite, a distinctive layer characterised by large oikocrysts of pyroxene at the top of the Bastard Cyclic unit (eg. de Klerk 1992), although based on mineralogical criteria it is difficult to define an unambiguous boundary (Eales and Cawthorn, 1996). Kruger and Marsh (1982), however, drew the boundary between the CZ and MZ at the base of the Merensky unit, due to a significant break in Sr isotopic ratios (Figure 1.2).

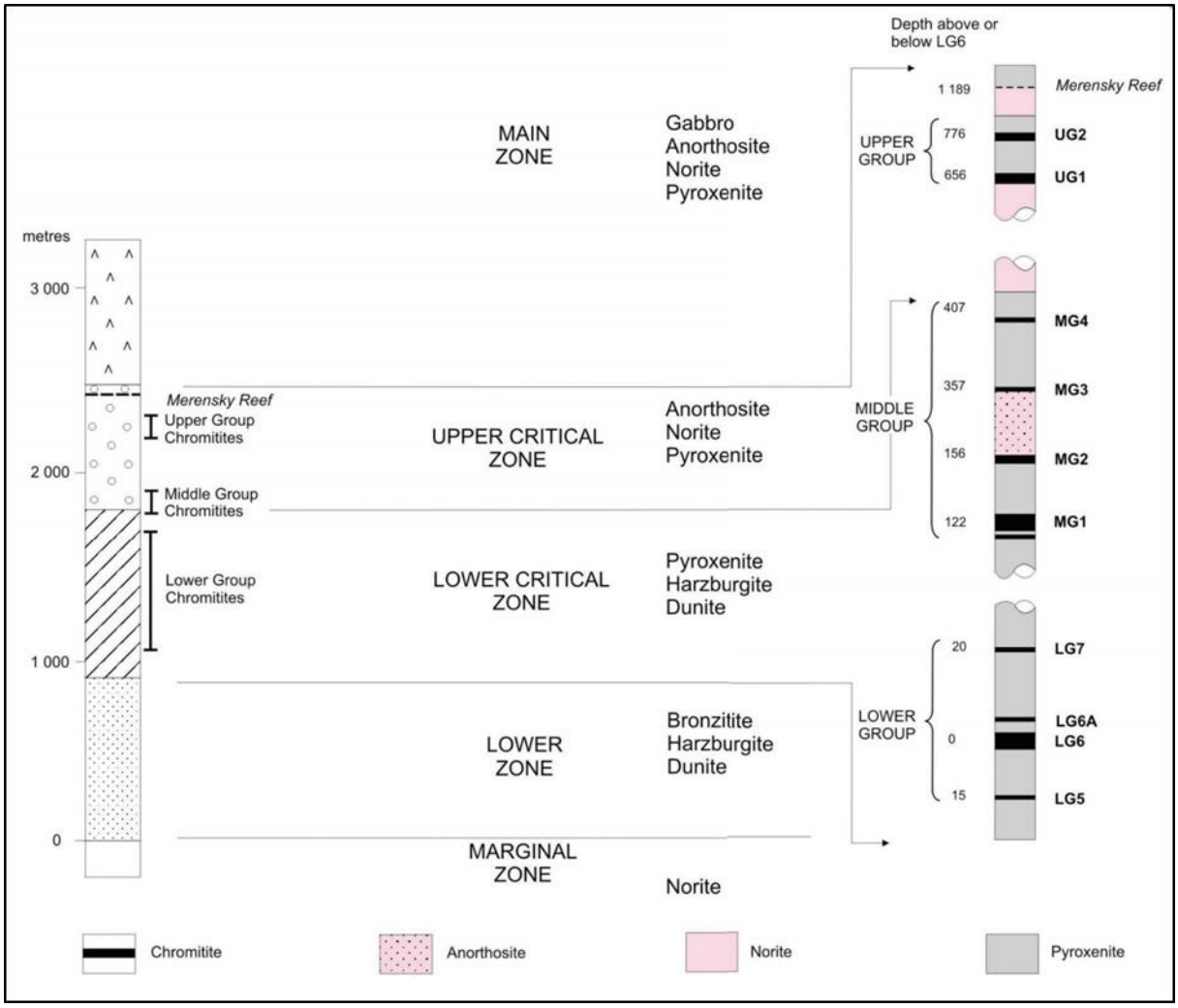


Figure 1. 3: Stratigraphy through the Critical Zone, showing the position of chromitite layers and the cyclic nature of the rocks (Schürmann et al., 1998).

The MZ is the thickest zone of the layered suite (ca 3500 m), comprising predominantly norites and gabbronorites, that are devoid of olivine and chromite, while anorthosites are rare (Kinnaird et al., 2002). In general, the MZ lacks the fine-scale layering of the CZ and its extreme lithological diversity (Eales and Cawthorn, 1996), although discrete packages of modally layered rocks can be identified (Mitchell, 1993). Augite (300 m above the base of the MZ) and then pigeonite sequentially become cumulus phases. At 2200 m in the western limb (Mitchell, 1990), and 3100 m in the eastern limb (Von Gruenewaldt, 1973) above the base of the MZ, pigeonite is replaced by orthopyroxene (Nex et al., 2002). The reappearance of orthopyroxene marks the base of a distinct melanocratic termed the Pyroxenite Marker (Figure 1.2). This marks a significant compositional reversal and contains some PGE mineralisation (Maier et al. 2001; Maier and Barnes, 2010).

1.7 Upper Zone (UZ)

The mineralogical base of the UZ is defined as the first appearance of cumulus magnetite (SACS 1980), although Kruger (1990) redefined it at the Pyroxenite Marker, a hundred or more metres below, on the basis of an abrupt break in Sr isotope ratios at another major unconformity (Sharpe, 1985). The UZ is the most laterally extensive zone (Kruger, 2005) and has traditionally been subdivided into three subzones based on cumulate mineralogy (Figure 1.2) (SACS 1980). Subzone A contains cumulus plagioclase, low Ca-pyroxene and magnetite. In subzone B, olivine becomes an additional cumulus phase. Subzone C is defined by the appearance of apatite.

Chapter 2

Location and aim of study

2.1 General Geology of the Northern Limb

The northern limb, previously known as the Potgietersrus limb (Van der Merwe 1976), extends from south of Mokopane at the Zebediela fault, northwards for about 110 km until it reaches the Melinda fault (part of the Palala Shear Zone) where it is covered by younger Waterberg sediments (Figure 2.1.A) (Buchanan et al. 1981). Geophysical data suggests that the exposed northern limb only forms part of a much larger 'basin', which is mostly covered by Waterberg sediments and has an actual extent of ~160 x ~125km, with modelled thicknesses that are not well constrained but vary from <1000 m to >12000 m, averaging ~4000 m (Finn et al., 2015). Unique to the northern limb is the economically significant body known as the Platreef, which contains world-class magmatic PGE and Ni-Cu deposit hosted by a feldspathic pyroxenite-norite succession (Kinnaird and Nex, 2015). The Platreef is a heterogeneous magmatic sequence that contains both reef-style and disseminated contact-style mineralisation that has been correlated, by some authors, with some of the economic horizons in the Main Bushveld Complex.

The Bushveld Complex in the northern limb intruded Transvaal Supergroup metasediments and Archaean basement at ~ 2060 – 2054 Ma (Walvaren, 1987; Walvaren et al., 1990; Harmer and Armstrong, 2000). Following Merensky (1925), the Platreef can be subdivided into three sectors, according to the footwall lithology (Figure 2.1.B), a classification that was further developed by Kinnaird et al., 2005. The northern sector has a footwall of Archaean granite on farms Overysel, Drenthe, Witrivier and northwards. The central sector is characterised by a dolomitic footwall of the Malmani Subgroup and occurs on farms Zwartfontein, Sandsloot, Vaalkop and Tweefontein. The southern sector of the Platreef has a footwall composed of Transvaal Supergroup shales, banded ironstones, calc-silicates, mudstones and siltstones and extends from Townlands in the south to Tweefontein in the north (Kinnaird et al., 2005).

Structurally, the northern limb is separated from the rest of the complex by a major tectonic boundary, known as the Thabazimbi-Murchison Lineament (TML), which formed by the collision of the Pietersburg and Kaapvaal terranes at around 2.7 Ga (Truter, 1947; Good and De Wit, 1997; Griffin et al., 2004). The stratigraphy of the northern limb does not correlate strictly to the stratigraphy in the other limbs across the Thabazimbi-Murchison Lineament, and there are several differing opinions on whether the Platreef can be correlated with the Critical Zone, or whether the Critical Zone is even present in the Northern Limb (eg. Van der Merwe, 1976; Buchanan et al., 1981;

Cawthorn et al., 1985, Hulbert and von Gruenewaldt 1985; Eales and Cawthorn, 1996; Yudovskaya and Kinnaird 2010).

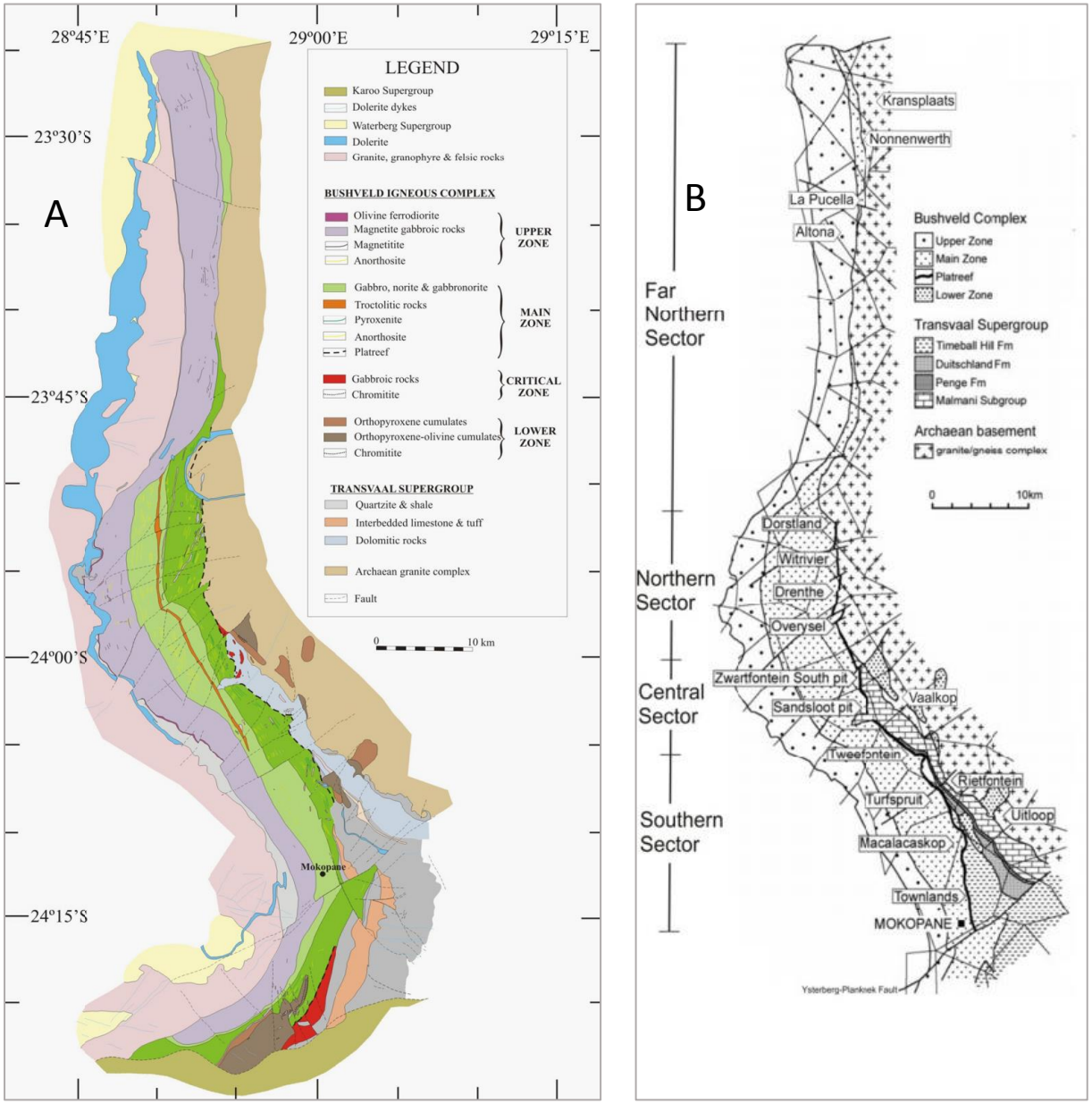


Figure 2. 1: Schematic illustration of the geology of the northern limb of the Bushveld Complex. (A) The complete northern limb indicating all the lithologies and major structures (Van der Merwe, 1978; Ashwal et al., 2005). (B) Geological map of the northern limb with the position of the farms indicated as well (Viljoen and Schürmann, 1998) and the four sectors (Kinnaird et al., 2005).

One of the fundamental questions still disputed and unanswered relates to the parental magma of the northern limb. The details on whether there was any connection between the northern limb and the main complex remains unclear, although it is highly probable that the TML had some control over the structure and injection of the magma (Kinnaird et al., 2005). Kruger (2005) believes that the TML was a zone of uplift against which early Bushveld magma was dammed, preventing it from flowing northwards, and only during Main Zone times did Bushveld magma begin to flow north,

therefore allowing the northern limb to evolve separately from the main complex (McDonald et al., 2005). A gravity high to the west of Mokopane led Van der Merwe (1978) to believe that a possible feeder zone may be present, which was responsible for the formation of the northern limb. Others suggested the TML may have acted as a dyke-like feeder for Bushveld magmas (Friese and Chunnett, 2004), which occurred under transpression as suggested by positive flower structures (Kinnaird et al. 2005).

The Platreef package, a dominantly pyroxenitic unit, is generally the lowest unit of the Rustenburg Layered Suite in the northern limb, except for isolated occurrences of Lower Zone rocks (Yudovskaya et al., 2013), and the composite structure of the Platreef indicates multiple discrete magmatic influxes (Kinnaird et al., 2005). Although the Platreef does not show typical Bushveld-type layered cyclicity and contains only two discontinuous chromitite horizons, it is considered to be analogous to the Critical Zone of the eastern and western limbs by many authors, both in terms of its stratigraphic position below the Main Zone and the silicate geochemistry (Wagner, 1929; Willemse, 1969, van der Merwe, 1978; Kruger 2005). However, this is disputed, and some authors claim that the origin and nature of platinum mineralisation within the Platreef differs completely from that in the Merensky Reef and the UG2 chromitite, even though rock types within the Platreef are similar to those encountered in the Upper Critical Zone elsewhere (Gain and Mostert, 1982; McDonald et al., 2005). Comparisons and contrasts of the Platreef with the Main Complex will be more carefully examined in a later chapter.

2.2 Location

The study areas are in the Limpopo province of South Africa, near the town of Mokopane, and form part of the Northern Limb of the Bushveld Igneous Complex. Samples were obtained from two separate companies operating in the area, namely Ivanhoe mining at the Turfspruit property and Lonmin's Akanani project on the Zwartfontein property (Figure 2.2 and 2.3). In 2007 Lonmin purchased a 74% interest in the Akanani PGM deposit (Incwala Resources owns the remaining 26% of the project). Drilling continues at the property to extend resources and Lonmin is currently undertaking pre-feasibility work (Lonmin 2014). Diamond drillcore was obtained from the Akanani exploration project, which is located on the farm Zwartfontein 814 LR, approximately 35 km north-west from Mokopane. The Akanani project is downdip from the adjacent open-cast workings of Anglo American's Mogalakwena operations, which is situated on the farms Sandsloot 236 KR, Vaalkop 819 LR, Zwartfontein 818 LR and Overysel 815 LR.

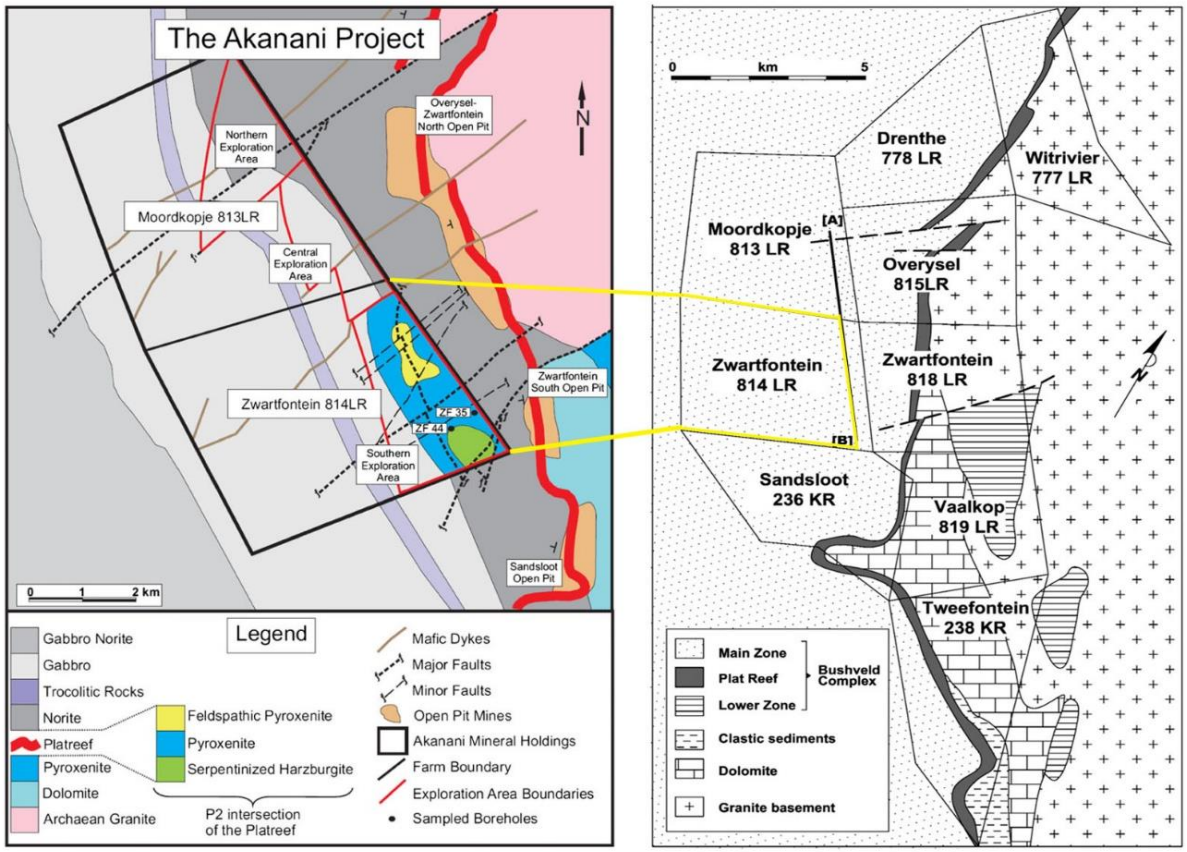


Figure 2. 2: Location of the Akanani project on the farm Zwartfontein 814 LR. Open cast mining is currently taking place up dip on the farms Sandsloot 236KR, Vaalkop 819 LR, Zwartfontein, 818 LR and Overysel 815 LR. (Van der Merwe et al., 2012; Mitchell and Scoon, 2012).

The second locality is on the farm Turfspruit 241 KR (Figure 2.3), which forms part of the Underground Mining Project operated by Ivanhoe mining company. Initial exploration efforts during the early 2000's focussed on mineralisation that could support open-pit mining, although, from 2007 to 2012, Ivanplats started with a deep drilling program to investigate whether there is a continuity and grade in an area targeted as having underground mining potential. This study makes use of drill core from the Underground Mining Turfspruit (UMT holes) drilling program on the farm Turfspruit (Figure 2.3). The samples occur in the footwall of what Ivanhoe has termed as the 'Flatreef' area, and are positioned well below the proposed mining horizon. The Flatreef, according to Ivanplats, is amenable to highly mechanised, underground mining methods.

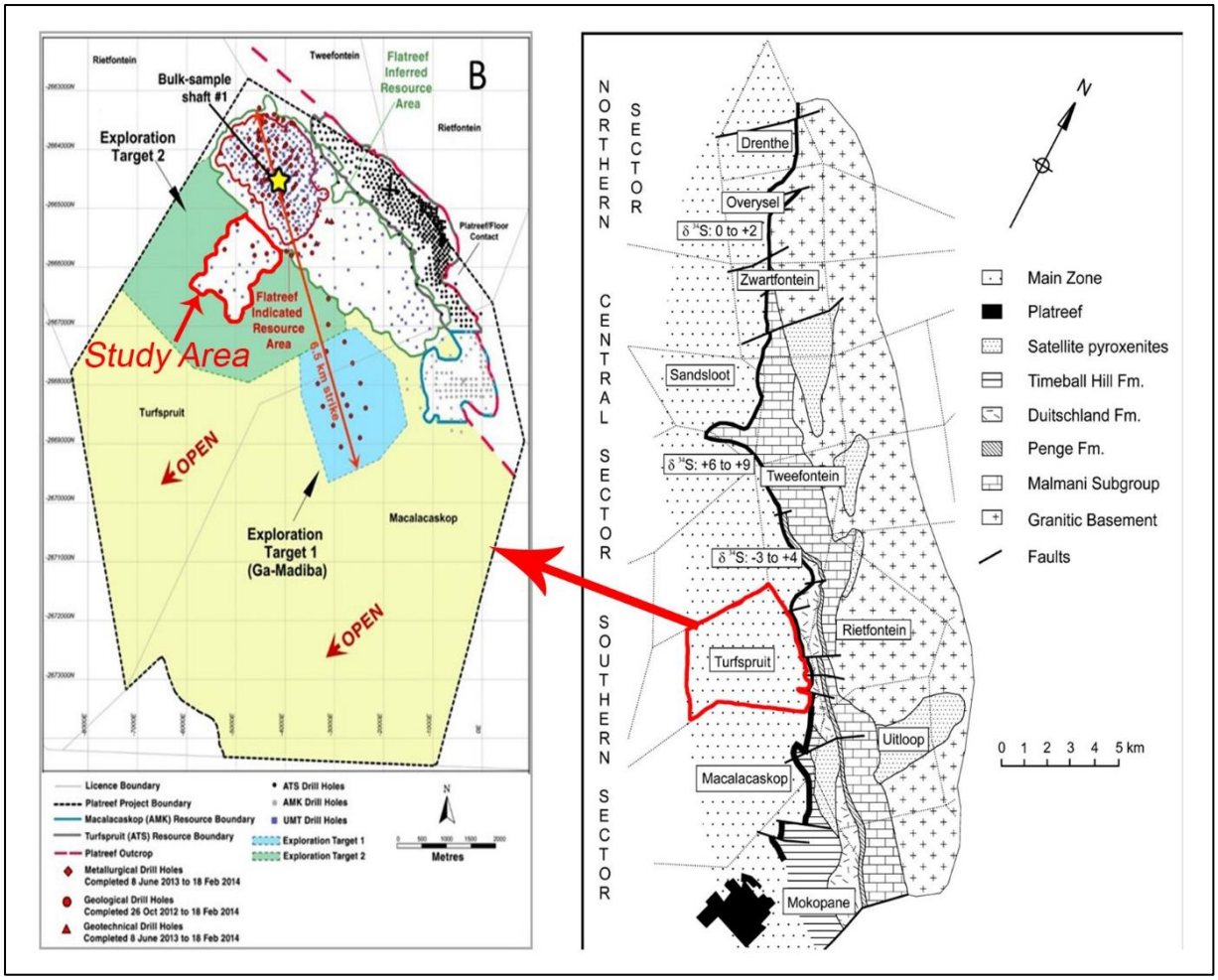


Figure 2. 3: Location of the Ivanplats Underground Mining project on Turfspruit. The areas highlighted in red delineate the location of the boreholes used in this study (Van der Merwe, 1978; Ivanplats, 2013).

2.3 Aim

There is presently no consensus as to whether the northern limb can be correlated with that of the eastern and western limbs of the Bushveld Igneous Complex. The Ni-Cu-PGE-bearing reefs within the Platreef show a number of similarities and differences with that of the Merensky Reef, and the same can be said for the UG2 and the chromitite layers within the Platreef. Initial strontium isotope ratios of the Platreef are too disturbed to be correlated with the initial ratios of the different zones in the Bushveld Complex presented by Kruger (1994) and Kinnaird et al. (2002), and therefore any correlation must be made by using lithological packages, mineral- and whole-rock chemistry. The first aim of this study is to gather stratigraphical, mineralogical and chemical data, which would be compared to previous work done on both the Platreef and the main Bushveld Complex, thereafter providing evidence on whether the limbs can be correlated or not.

The focus of the study is based on chromitiferous horizons and their host rocks, which occur in the Platreef on the Turfspruit and Zwartfontein properties. A detailed investigation into the key features of these layers was conducted, making use of their morphology, petrography, and chemistry. The stratigraphic position of the chromite-layers, along with their compositions can shed some light on the magma involved, as well as the crystallisation history. Any vertical or lateral trends of chromite chemistry could provide evidence on how the magma evolved, and what led to chromite crystallisation. At the end of each chapter the results obtained will be compared to previous literature, and thereafter a comparisons and contrasts section with the main Bushveld Complex will follow.

2.4 Objectives

- One of the difficulties of working in the northern limb is the irregular and sometimes poorly developed stratigraphy, and therefore efforts to place the samples in a stratigraphic context will be made through core logging.
- Determine whether there are any lateral variations in the characteristics of chromitites that occur at the same stratigraphic level from the different holes sampled on the Turfspruit and Zwartfontein property.
- Identify major chemical and/or physical comparisons and contrasts between chromitites from Turfspruit and Zwartfontein, and relate those to the main Bushveld complex.
- Apart from the chromitites, the mineralogy and textures of the host rocks will also be investigated. The major minerals occurring in the area include varying proportions of orthopyroxene (almost ubiquitous), plagioclase, clinopyroxene, and olivine. For interest sake, some exotic minerals such as anhydrite and other alteration minerals that formed through contact metamorphism were sampled and studied as well.
- Identify and outline major geochemical trends, if there are any, along the length of the stratigraphy. What were the controlling factors and does it coincide with existing knowledge? Whole-rock geochemical data from Ivanplats will aid in identifying and delineating trends.
- Determine whether chrome-rich layers are true chromitites, or actually chrome-spinels that formed as a reaction product through contact metamorphism. Identify the type of spinels, and what controlled their chemistry.
- Did the chromitite form purely through magmatic processes, or was their crystallisation induced by contact metamorphism with country rock? Assimilation-driven chromitite precipitation is quite common in the northern limb. Is there any evidence for postcumulus fluid interactions, and what effect did this have on the mineralogy and textures?

- How does the chemistry and textures of metamorphic and magmatic chromitite differ?
- What influence did the host rocks have on the characteristics of chromitite?
- What influence did the presence of xenoliths have on the chromite composition and morphology?
- Is there a correlation between the amount and type of sulphides present and the chromite or host rock chemistry? How are the sulphides hosted and where do they occur?
- Search for Ni-Cu-PGE grains using the Scanning Electron Microscope to determine where they occur, how they are hosted, their chemistry etc.
- After the completion of all the analyses, the results will be compared to previous work done on the chromitites of the area, and elsewhere in the Bushveld to establish what similarities and/or differences exist.

Chapter 3

Field observations

3.1 Introduction

In order to undertake an investigation into chromite layers and chromitiferous zones, in parts of the Platreef, a field progamme of core logging was undertaken to log cores, collect appropriate samples and to determine the stratigraphic position of the chromitiferous horizons. On a local scale, the aim of the project was to determine whether there are any lateral variations in the characteristics of chromitites that occur at the same stratigraphic level from the different holes sampled on the Turfspruit and Zwartfontein property. In addition, samples were analysed to confirm whether they were true chromitites, or chrome-spinels that may have formed during metamorphism. Geologists at Ivanplats recognise a chromitiferous unit in the Flatreef at depth, which they equate to be the UG2. On a more regional scale therefore, the data obtained in this study can be compared with the UG2 in the eastern and western limbs of the Complex to evaluate this potential correlation.

3.2 Stratigraphy of the area

The stratigraphy of the northern lobe is dramatically different to those of the eastern and western limbs. It is very similar to the part of the Complex south of the Planknek-Ysterberg fault, where the conventional subdivision of an Upper-, Main-, Critical- and Lower Zone is applied, although north of this fault, the Platreef occurs between the Main and the Lower Zone. Figure 3.1 illustrates the evolution of our understanding of the relationship between the northern limb stratigraphy with that of the rest of the complex. The first detailed description of the Platreef was done by van der Merwe (1976), who followed Wagners' (1929) interpretation and considered the Platreef to be part of the Critical Zone (CZ), that has only been poorly developed south of Mokopane. Today it is clear that the stratigraphy south of the Thabazimbi-Murchison lineament (TML), which has been studied by many authors over the years (Barret et al., 1978; Hulbert and Von Gruenewaldt, 1982 and Hulbert, 1983), can directly be correlated with that of the eastern and western limbs of the Bushveld Complex. Evidence for this includes the recognition by Hulbert (1983) of the Grasvally norite-pyroxenite-anorthosite (GNPA) member, which can be correlated with the Critical Zone, as well as the Moorddrift-Drummondlea-Volkspruit chromitiferous harzburgites that can be equated with the Lower Zone elsewhere in the Bushveld Complex. However, north of the Planknek-Ysterberg fault, the mineralised Platreef, which is a moderate to steeply dipping, 100 to 400 m thick, composite mafic-ultramafic intrusion was emplaced into Transvaal Supergroup metasedimentary rocks, and to the north into Archaen granite-gneiss (Kinnaird et al., 2005) occurs and its relationship with the Critical Zone is still debatable (McDonald et al., 2005).

The Lower Zone rocks are best developed in the Grasvally area, south of Mokopane (Hulbert and von Gruenewaldt, 1983), and a thick 800m sequence of Lower Zone rocks underlies the Platreef on the Turfspruit property (Yudovskaya et al., 2013). North of Mokopane there are a number of small satellite bodies of Lower Zone rocks that outcrop, such as the Uitloop body, which occurs to the southeast of Turfspruit. Kruger (1990) also ascribes a thick zone of serpentinised peridotite and pyroxenite on Macalacaskop to the Lower Zone. Lower Zone lithologies commonly occur as sills between the Platreef and footwall lithologies, and on Turfspruit, it may be separated from the Platreef by Transvaal metasediments.

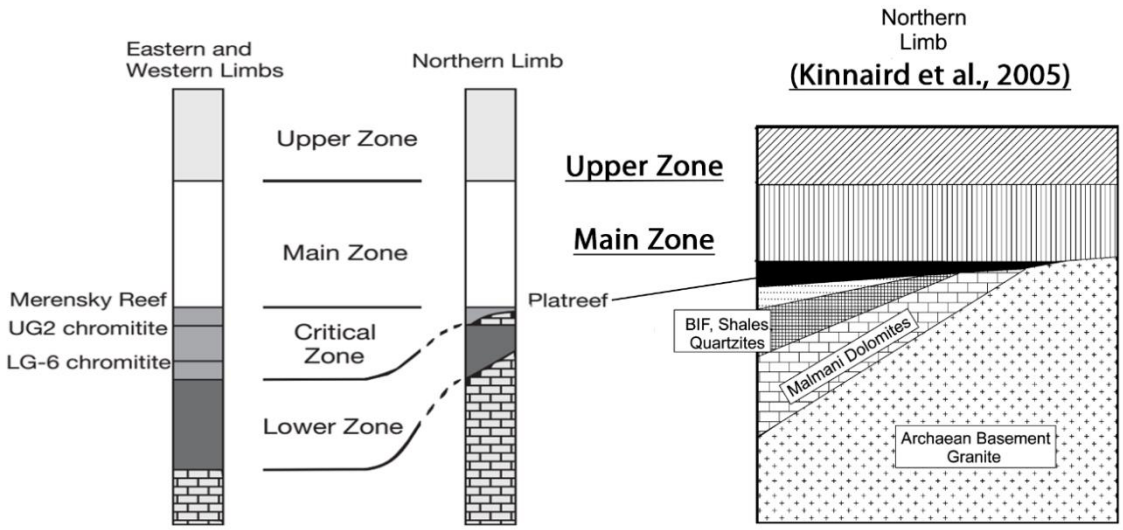


Figure 3. 1: Traditional correlation of stratigraphic columns between the Main Bushveld Complex and that of the northern limb, with an inferred correlation between the Platreef and the Merensky Reef (White, 1994). Note that the variable rock types constitute the Transvaal floor in the northern limb. Kinnaird et al. (2002) shows that the Platreef may be separated by country rock from the Lower Zone or basement rocks.

In terms of its stratigraphical position between the Lower- and Main Zone, the Platreef is analogous to the Critical Zone. However, apart from the position, there are several contrasting stratigraphic characteristics that the Platreef displays. For example, it lacks the well-developed and extensive layering of the Main Complex, with only two main chromite-rich zones within the succession that were highlighted by Yudovskaya and Kinnaird (2010), compared to around ten prominent and persistent chromitite horizons in the Critical Zone of the eastern and western Bushveld Complex (Figure 1.3).

The contact between the Main Zone and the Platreef generally follows the topography of the footwall of the Platreef with the Lower Zone or Transvaal rocks. It is generally a sharp contact that is represented by a mottled anorthosite at the base of the Main Zone. On Turfspruit it appears as though the lithologies of the Main Zone and the Platreef are interfingered, with fine-grained

gabbronorites, characteristic of the Main Zone, occurring within the Platreef succession. Main Zone gabbronorite often hosts hornfels xenoliths, and this has been suggested as evidence for the Main Zone predating the Platreef, as these are considered fragments of the Transvaal floor that were caught up by Main Zone magma. However, commonly near the base of the Main Zone, there exists a 'disturbed' zone above the contact with layers of norite, pyroxenite, anorthosite and xenoliths. The chemistry of these pyroxenes within the disturbed Main Zone are similar to that of Platreef pyroxenite, and rather different to the host Main Zone, which suggests that these are fragments of Platreef pyroxenes caught up in the Main Zone. This suggests that the Platreef predates the Main Zone, and Holwell et al. (2005) suggested that the Transvaal metasediments may have originally formed a roof to the Platreef, and as the Main Zone magma intruded it incorporated xenoliths of hornfels from the roof, as well as Platreef pyroxenite. However, Ivanplats' geologists claim that such pyroxenites form part of the Bastard cyclic unit and therefore part of the Upper Critical Zone (Grobler, 2017, personal communication).

The internal stratigraphy of the Platreef has been very difficult to correlate between different properties throughout the northern limb, although, Kinnaird et al. (2005) gave an excellent description of the crude internal stratigraphy of the Platreef. The lower part of the succession usually consists of a heterogeneous and moderately mineralised zone of variable lithologies, including pyroxenite, norite, gabbronorite, harzburgite and xenoliths of variably digested and metamorphosed Transvaal Supergroup rocks. Overlying this is a well-mineralised zone comprised mainly of pyroxenite and locally harzburgite, such as at Akanani, and finally, an upper, generally poorly mineralised pyroxenite.

3.3 Methodology

This study utilised diamond drill cores from both the Turfspruit and Zwartfontein properties, which includes the following boreholes on the Turfspruit property: UMT 335, UMT 336, UMT 366 and UMT 377, as well as hole ZF116 on the Zwartfontein farm. The cores obtained from the Turfspruit property are part of the Ivanplats underground mining project, while the Zwartfontein cores form part of the Akanani exploration project of Lonmin. Confidential whole-rock geochemical data was received for all the Turfspruit boreholes, and although this data is not be included in the report, it was used to create geochemical plots that accompanies the stratigraphic logs.

UMT 336 was logged by Dr Marina Yudovskaya and her data was utilised in order to construct a stratigraphic column. The core logging was crucial in identifying various rock types (which is complicated by the contaminated nature of the northern limb), orientating oneself with the stratigraphy, as well as attempting to identify any cycles. Entries within the logs include the following

features: rock type; an approximate modal mineralogy; nature of the contacts; grain sizes, shapes, textures, colours, and the presence and percentage of sulphides.

Most importantly the position, size, texture, host rock, and morphology of the chrome-rich layers were logged, as it is the key focus of this project. The nature of the chromitiferous contacts (sharp or gradational), as well as the lithologies that occur both above and below, was taken special note of. Sampling of core took place after all logs were finalised, and in this manner, the exact position of the samples was known, and they could be viewed in stratigraphic context. Samples were cut into quarter cores, bagged and labelled. Thereafter, the samples were sent in to be cut into polished thin sections at the University of the Witwatersrand.

3.2 Lithologies of the Study area

The diversity of rock types found in the northern limb of the Bushveld Complex is considerably greater than that of the other limbs. This can be attributed to the large variation of the footwall lithologies, as well as the interaction of the magma with these lithologies, leading to significant contamination of the magma. All the primary magmatic rocks that occur within the Platreef contain the following minerals in varying proportions: orthopyroxene, clinopyroxene and plagioclase. However, there are a number of metamorphic and hybrid lithologies that do not conform to this rule. Rocks are classified according to several standards that can be seen on the ternary diagrams in Figure 3.2.

The basis for classifying the igneous rocks in the study area is the subcomission on the systematics of igneous rocks by the International Union of Geological Sciences (IUGS) (Le Bas and Streckeisen, 1991). Firstly, rocks are classified according to their number of mafic minerals, where rocks with more than 90% mafic minerals are termed ultramafic, etc. In the Platreef, the most frequently used ternary diagrams includes one for ultramafic rocks (Figure 3.1 A), which contains olivine, orthopyroxene, and clinopyroxene on the three apexes, as well as one for mafic rocks which contain plagioclase, ortho- and clinopyroxene (Figure 3.2 B). Rocks are then categorised by the proportions of these minerals. Therefore, in order to categorise mafic and ultramafic rocks, a keen distinction between ortho- and clinopyroxene is required, which may be difficult to the inexperienced eye.

It is crucially important in the Bushveld Complex to distinguish between cumulus and intercumulus minerals in order to correctly identify rock types. This usually refers to the presence of intercumulus or cumulus feldspar, which is mainly plagioclase in the case of the Platreef. The most common application of identifying cumulus or intercumulus plagioclase in this study was to distinguish between norites and feldspathic pyroxenites. Norite may contain between 35-65 % cumulus plagioclase, and 35-65% cumulus orthpopyroxene, and typically contains more plagioclase than

orthopyroxene (Figure 3.3 E). The prefixes leuco-, and melanorite is used in order to indicate the proportion of plagioclase to orthopyroxene, especially if the percentages were to fall outside the field of norite. Leuconorite has more plagioclase than orthopyroxene, with 65-90% plagioclase and 10-35% orthopyroxene, while melanorite is darker coloured with between 10-35% plagioclase and 65-90% orthopyroxene. Norite is one of the predominant rock types in the holes that were logged during the study, commonly occurring as part of norite cycles, usually in the upper parts of the holes.

Pyroxenite may contain up to 10% cumulus plagioclase before being termed a norite according to the IUGS classification scheme. Whereas feldsphatic pyroxenite (Figure 3.3 F), which is an informal term used by Bushveld geologists', can contain an unlimited amount of plagioclase, given that it is intercumulus. Usually feldspathic pyroxenites contain between 8 – 25 % plagioclase in the study areas. It is vital to accurately distinguish between norites and feldspathic pyroxenites, as the latter is one of the most mineralised rocks in the Bushveld Complex. In some cases, rocks may be logged as feldspathic pyroxenite due to their economic grades and intercumulus plagioclase content, whereas according to the IUGS classification, they are technically norites.

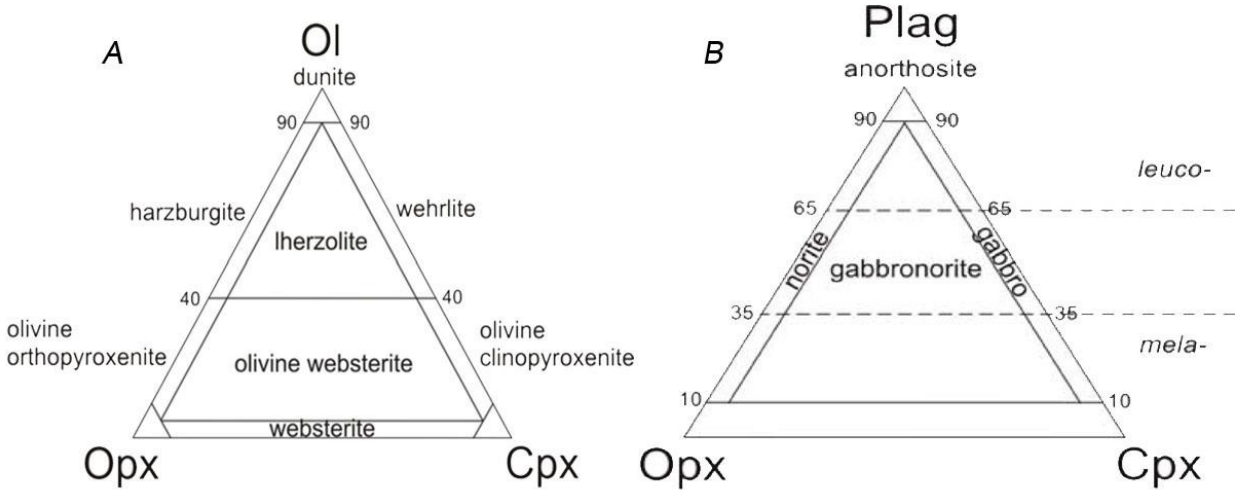


Figure 3. 2: (A) Ternary diagram for the classification of mafic rocks. (B) Ternary diagram for the classification of gabbroic rocks (Le Bas and Streckeisen, 1991).

Pyroxenite may be further subdivided into clino- or orthopyroxenite, depending on the dominant pyroxene mineral. In this study orthopyroxene is without question the more dominant of the two, with clinopyroxene usually occurring as an accessory phase. They usually consist of larger, cumulus orthopyroxene, with variable amounts of plagioclase. Grain sizes are commonly between fine and medium, although in some cases where there was significant fluid ingress or signs of contamination, they may become pegmatoidal.

The most ultramafic rock type present in the study area is harzburgite, which is present in the Lower Zone rocks on Turfspruit, and occurs within the Platreef on Zwartfontein. Although, in UMT 336,

which was logged by Dr Yudovskaya, dunite is present at the bottom of the borehole core. In the Platreef, harzburgite may contain accessory intercumulus feldspar and clinopyroxene, especially where contamination from country rocks is significant. Where intercumulus plagioclase exceeds around 5%, these rocks are termed as feldspathic harzburgites. Not all the harzburgite encountered are of purely magmatic origin, and some formed through metamorphic processes, in which case they are termed paraharzburgite. Parapyroxenites formed in a similar manner and is a common lithology in the Platreef.

Parapyroxenite is a term first used by Wagner (1926) when describing the metamorphic rocks of the northern limb that formed through contact metamorphism, commonly containing granoblastic clinopyroxene (Holwell et al, 2005). Close to the contact of xenoliths, magmatic pyroxenites were transformed into a mixture of massive diopside clinopyroxenite (which gives parapyroxenites their green colour), locally rich in metamorphic olivine that has been variably serpentinised, and in some cases, contains garnet (Figure 3.3-C). When there is a significant amount of metamorphic olivine present it may be referred to as a paraharzburgite. Some metamorphic rocks show both primary magmatic, as well as original sedimentary features of the country rock protolith, in which case they have been termed as hybrids (Figure 3.3-F). The metamorphic textures present in these rocks are very distinctive, and instead of seeing distinct minerals in cumulus rocks, parapyroxenites have interlocking mineral grains. Textures such as these, along with considerably larger grain sizes, indicate the presence of fluids during metamorphism. Parapyroxenites commonly have a number of alteration minerals associated with them, such as anhydrite, gypsum and chlorite.

Four different types of xenoliths were identified within the study area, namely calc-silicates, banded iron formations (BIF's), dolomites (usually banded) and hornfels (Figure 3.3). Calc-silicate is formed through contact metamorphism of carbonate rocks, which are dolomites in the case of this study, and they consist of mainly calcium-bearing silicates such as diopside and wollastonite (Wenk and Bulakh, 2004). On Turfspruit and Zwartfontein, the calc-silicates vary from a creamy white to green colour, depending on the metamorphic grade, and which Ca-bearing silicate is dominant between wollastonite (white) and diopside (green). Hornfels is a metamorphic facies that consist of fine-grained rocks with equidimensional grains without any preferred orientation and is usually the product of contact metamorphism of pelites or psammites (Bates and Jackson, 1987). There was only one occurrence of hornfels in the study area (Figure 3.3.B), and the xenolith still retained some original sedimentary layering. It was difficult to determine the protolith due to an extensive overprint of secondary alteration minerals.

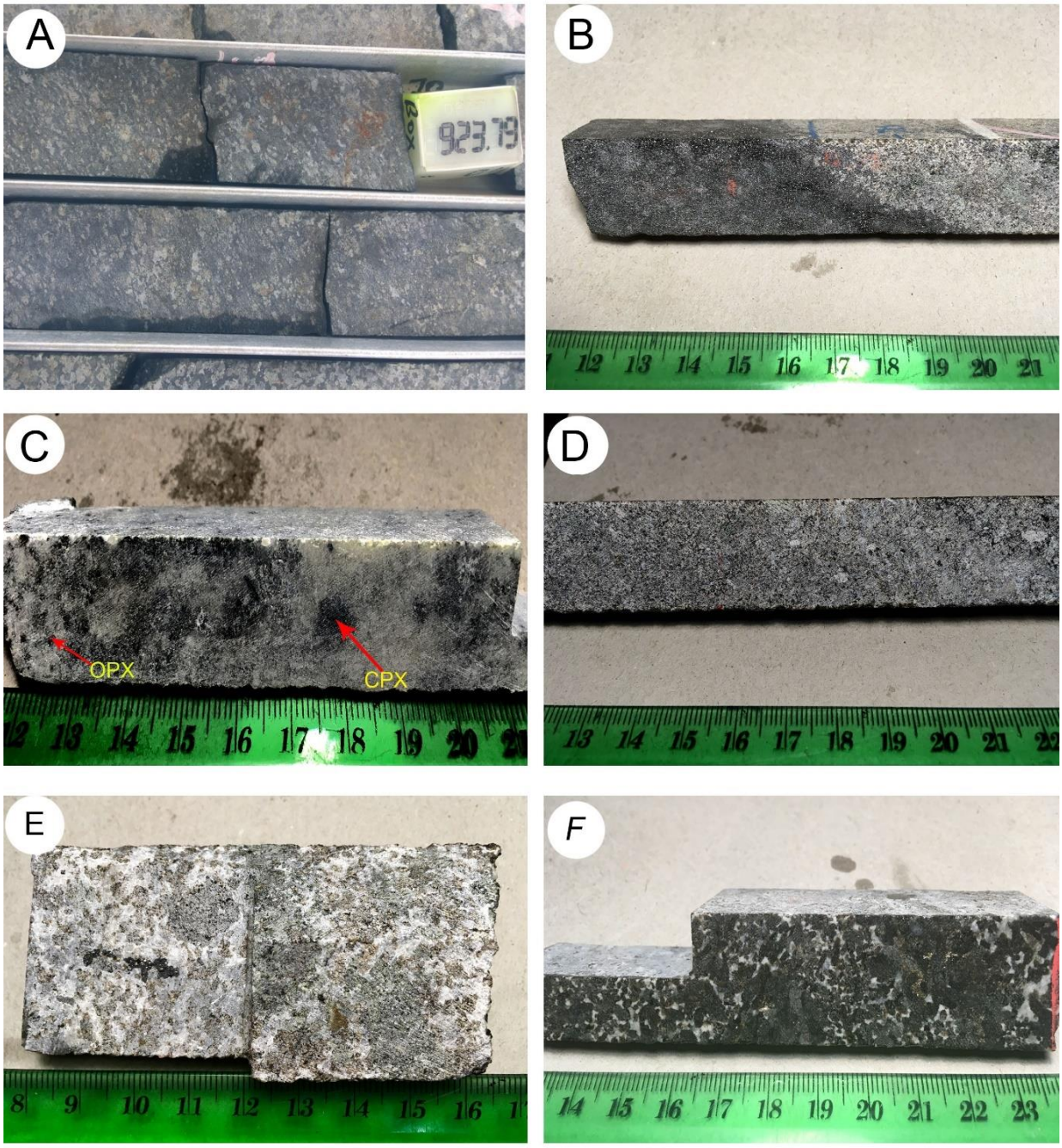


Figure 3. 3: Photographs of different lithologies in core sampled: (A) Serpentinised harzburgite from 923 metres below base. The poikilitic texture consists of orthopyroxene oikocrysts, which encloses remnants of olivine grains. Most orthopyroxene grains have not been serpentinised. Most probably secondary olivine formed through fluids, possibly associated with a xenolith, although no evidence for a xenolith was preserved. (B) Sharp contact between the 'UG2-like' chromitite and a pyroxenite. Chromite and host pyroxenite appear to be primarily magmatic, thus good candidates for further mineral chemistry studies. (C) Hybrid of a spotted and mottled anorthosite, at 1558m. Notice the dark-green clinopyroxene 'mottles', and cores of brown orthopyroxene. (D) Orthopyroxenite in hole UMT 335 consists of cumulus orthopyroxene grains, along with intercumulus plagioclase (5%) and minor clinopyroxene. (E) Gabbronorite with small chromite-stringer at 1570 m in UMT 366 comprises of green, anhedral clinopyroxene, with more euhedral, brown orthopyroxene grains. The presence of the chromite grains is rather rare within such lithologies. (F) Feldspathic pyroxenite in UMT 377. Notice interstitial plagioclase and sulphides, with cumulus, sometimes rounded orthopyroxene grains.

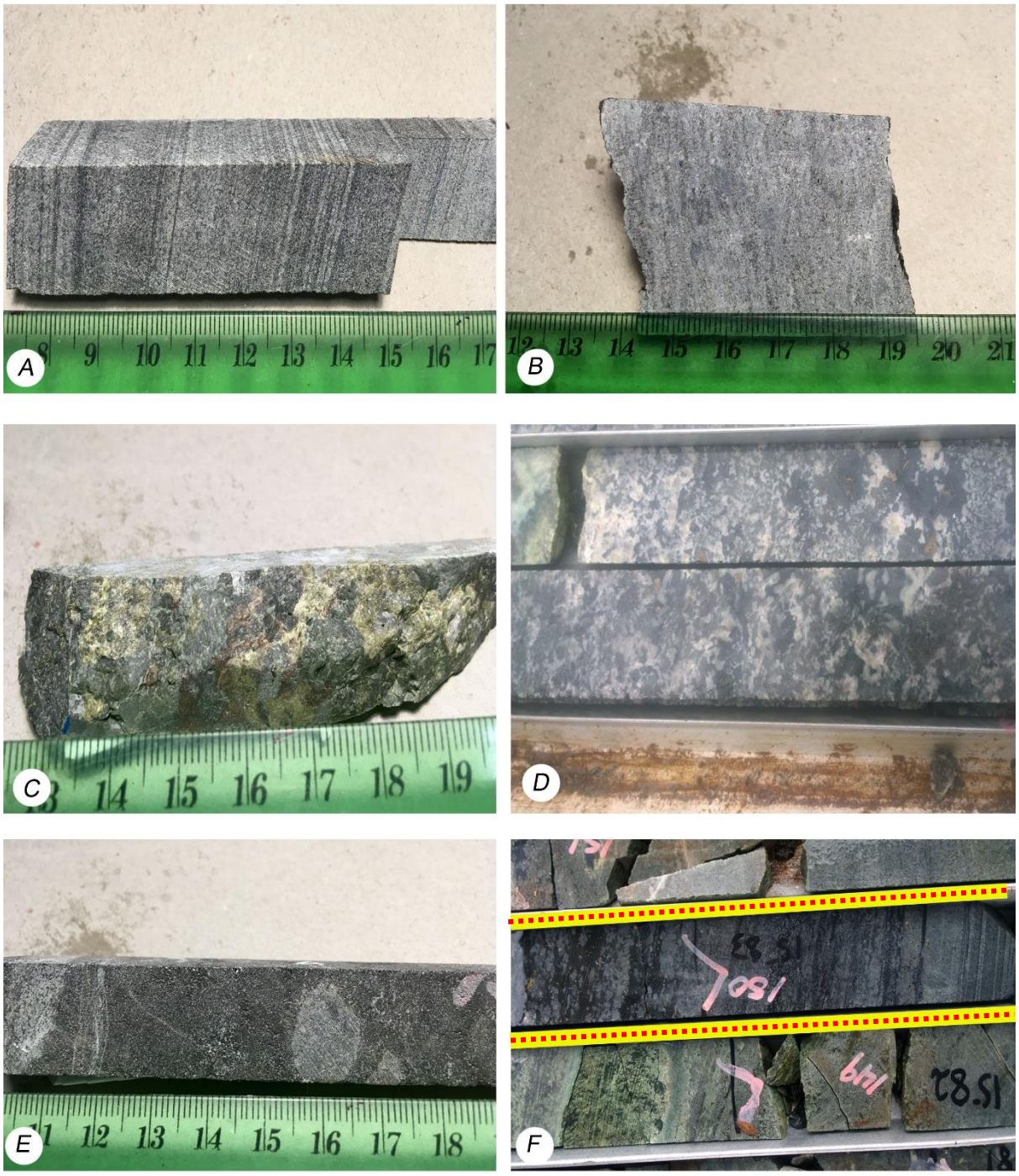


Figure 3. 4: Photographs of different lithologies in core sampled (A) Dolomite xenolith in hole UMT335, displaying well-defined, thin layering. (B) Hornfels xenolith with sedimentary layers still evident. It is difficult to determine the protolith, but in terms of its fine-grain size and the layering, it may well be part of the Duitschland formation shales. (C) Parapyroxenite with some garnets and olivine, UMT336. The dominant pyroxene is diopside (dark green), along with sugary olivine grains (light sea-green). The brown minerals are garnets, possibly grossular garnet. (D) Pegmatoidal feldspathic pyroxenite. Although there is a significant amount of plagioclase present, some of which is cumulus, by convention it is called a feldspathic pyroxenite rather than a norite. (E) Chromite-rich horizon at 1520 m in ZF-116. Notice the large cumulus orthopyroxene grain, around which the chromite has crystallised. This may indicate a secondary process for chromite crystallisation. (F) Between the two dotted red and yellow lines is a hybrid rock, at a gradational contact between the banded dolomite xenolith shown in Figure 3.3.A, and a serpentinised, probably metamorphic harzburgite. Notice towards the right is a rock similar in appearance to 3.3A, and in between, there is a complete mixture of magmatic and sedimentary rocks occurring.

3.4 Stratigraphy of the Turfspruit area

Turfspruit is situated in the southern sector of the northern limb (Figure 3.6), which is lithologically heterogeneous and significantly more variable than other sectors further north (Kinnaird et al., 2005). Only four holes were logged, which makes it impossible to portray the geology of the area due to the high variability, even on a local scale. However, Figure 3.7 attempts to put all the logged holes in context with one another. The overall geometry of the studied area is mainly controlled by that of the floor rock topography, and when looking at Figure 3.7, it is clear that the floor is not horizontal. The Platreef on Turfspruit strikes northwest and dips at around 40° to the southwest. The stratigraphic columns are arranged from the northeast to the southwest when looking at Figure 3.6, and thus the stratigraphy dips steeply towards the southwest.

The UMT drill holes intersect a part of the stratigraphy that has been described by Ivanplats' geologists as the Flatreef, in which the Platreef flattens out over a distance, as opposed to the steep dip of the rest of the Platreef. The subhorizontal position of this portion of the Platreef appears to be broadly controlled by faults that were active after intrusion of the Platreef, which may have been reactivated by older faults (Ivanplats, 2013).

Ivanplats geologists introduced a new subdivision and nomenclature termed the Turfspruit Cyclic Unit (TCU) for the upper Platreef on Turfspruit (Grobler and Nielsen, 2012). They claim to have recognised a magmatic sequence within the project area that has been subdivided into five cyclic units and correlate these units with the Upper Critical Zone elsewhere in the Bushveld Complex (Grobler et al., 2012). The units include from top to bottom: Norite Cycles 1 (NC1), which is the hanging wall to the TCU and contains the 'Giant Mottled Anorthosite' (GMA) at the top of the cycle. A typical and complete norite cycle is illustrated in Figure 3.5. Below this cycle occurs the most mineralised unit, known as the Turfspruit Cyclic Unit (TCU), which Ivanplats suggests is analogous to the Merensky Cyclic Unit elsewhere in the Bushveld Complex.

A large part of the studied core occurs in the footwall of the TCU, which is termed the Norite Cycles 2 (NC2) by Ivanplats geologists. The NC2 is usually separated from the overlying TCU by a small anorthosite layer, which is represented at the top of hole UMT366 and 336 (Figure 3.7). UMT-336 gives an excellent example of three norite cycles that are very well developed in the upper part of the succession. Not all the cycles identified are complete, with many of them being poorly developed and lacking some of the lithologies of a perfect cycle. According to Kinnaird et al. (2005), incomplete cycles may indicate an interruption to normal steady-state fractionation processes.

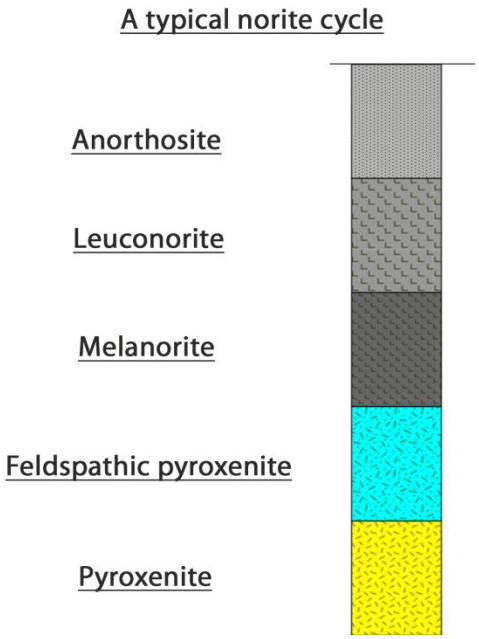


Figure 3. 5: A typical norite cycle progressing from mafic-poor to mafic-rich lithologies, as seen in the upper to middle parts of the Platreef succession.

Well developed, large-scale norite cycles can be seen in UMT 366 and 335 (Figure 3.7), in which the base is made up of a thick package of pyroxenite, followed by feldspathic pyroxenite, and finally norite at the top. The norite cycles usually occur in the upper parts of the successions, and most of the logged core was made up out of pyroxenites situated at the base. Norite cycles are common in the southern sector of the Platreef (Kinnaird et al., 2005). Some cycles, such as holes UMT 366, contain gabbroic material within them, which has been attributed to fingers of Main Zone that have cut down into the Platreef, due to hot Main Zone magma intruding when the Platreef magma had already cooled (Holwell et al., 2005). This theory has been challenged, however, and Ivanplats geologists attribute the gabbroic appearance of rocks to Ca-assimilation that formed clinopyroxene (Grobler, 2017, personal communication). Chromite layers are generally rare in gabbronorite, although a very small chrome-rich stringer is present in UMT 366, shown in Figure 3.2.E.

There is a discrete gabbronorite package of about 6 meters in thickness, approximately 150 m from the contact of the Platreef with the Main Zone, which begs the question of whether it is an interfingering part of the Main Zone or part of the Platreef magma. Several authors have described the disturbed contact between the Main Zone and the Platreef, that is represented by an interlayered sequence gabbronorites and pyroxenite (White, 1994), although at 150 m this package might be too far to fit this explanation.

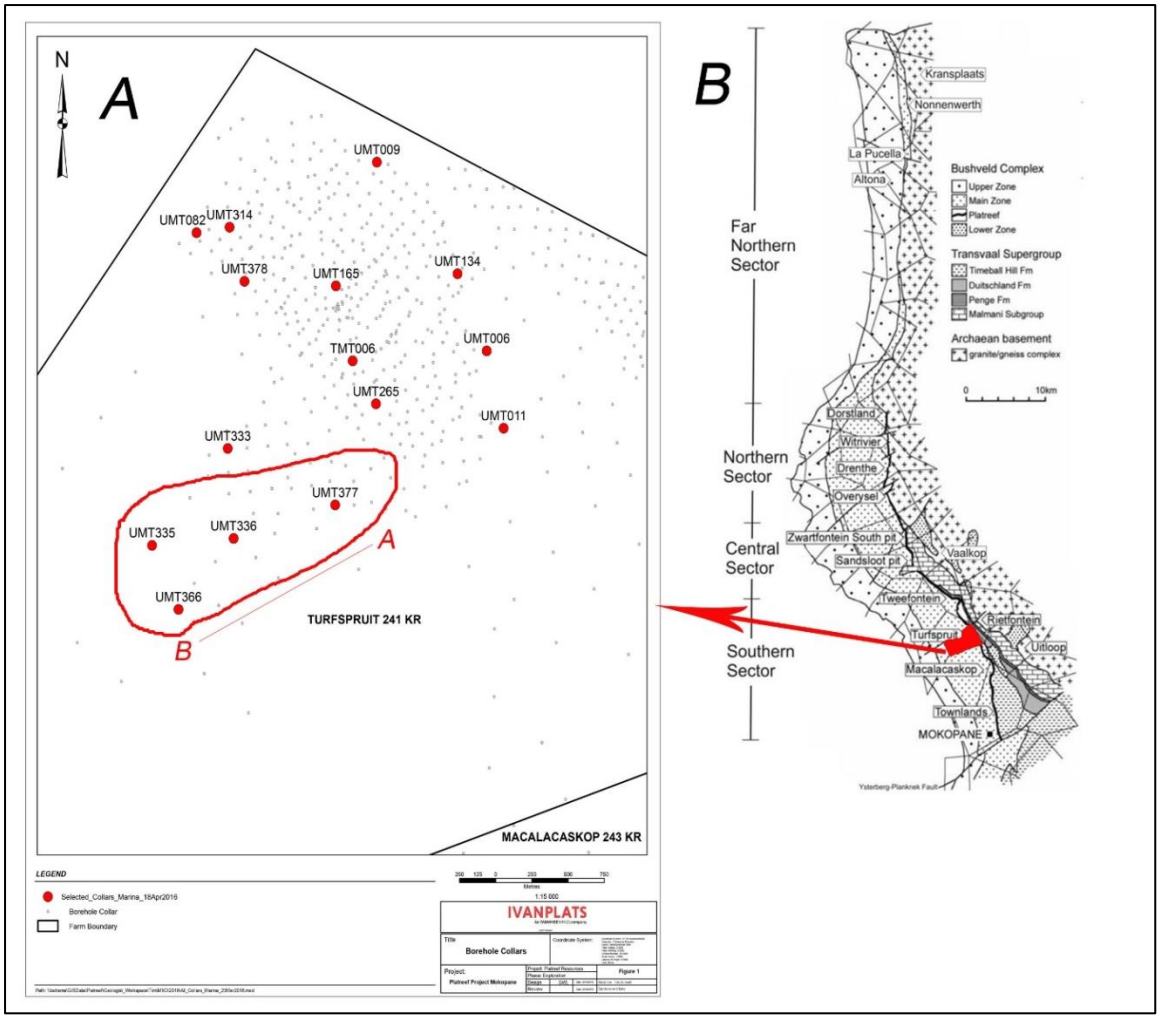


Figure 3. 6: Position and locality of the boreholes studied on the Turfspruit property (A) Locality of the holes logged and presented in Figure 3.7. The A-B delineates the direction in which Figure 3.7 is orientated. (B) A map of the northern limb, with the Turfspruit property highlighted in red (Adapted from Van der Merwe, 1978).

Well-developed chromite-rich zones occur in UMT 336, 335 and 366, and has been identified as the 'UG2'-like chromitite by the Ivanplats geologists. The so-called 'UG2' chromitite is not a well-defined, monomineralic chromitite horizon, as is the case of the UG2 in the main Complex, but rather a very chromite-rich zone in which the largest single, undisturbed chromitite layer may be around 30cm. The position of these chromite-rich zones is illustrated in Figure 3.7. This suggestion is according to the position of these layers, which occur in a cyclic magmatic sequence recognised on the property by Grobler et al. (2012), which they have correlated with the Upper Critical Zone south of the Thabazimbi Murchison Lineament. Lower Zone rocks are present in UMT 336 and 366, and in both instances, are separated from the Platreef by Transvaal Supergroup sediments. There appears to be a steady increase in plagioclase content moving upwards in the stratigraphy, with the more magnesian rocks of the Lower Zone at the base, and anorthosites at the top. Apart from the norite cycles identified in two of the holes, it is difficult to recognise any continuity between the holes, and a bigger area would need to be covered if any correlation were to be found.

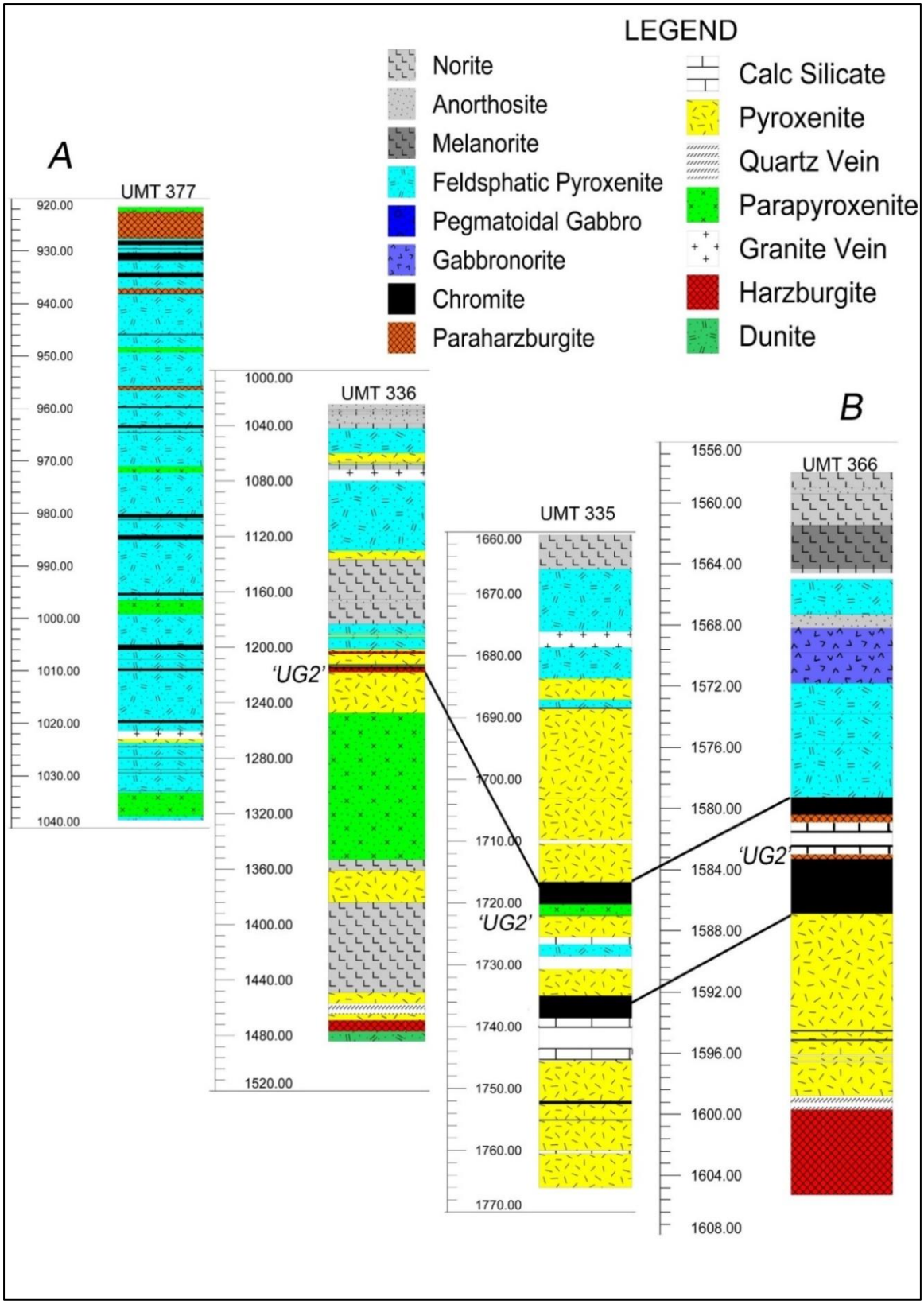


Figure 3. 7: Stratigraphic columns of holes UMT377, 336, 335 and 366. Some of the chromite-horizons, such as the 'UG2-like' chromite is vertically exaggerated in order to illustrate their position more clearly. The scales are in metres below surface.

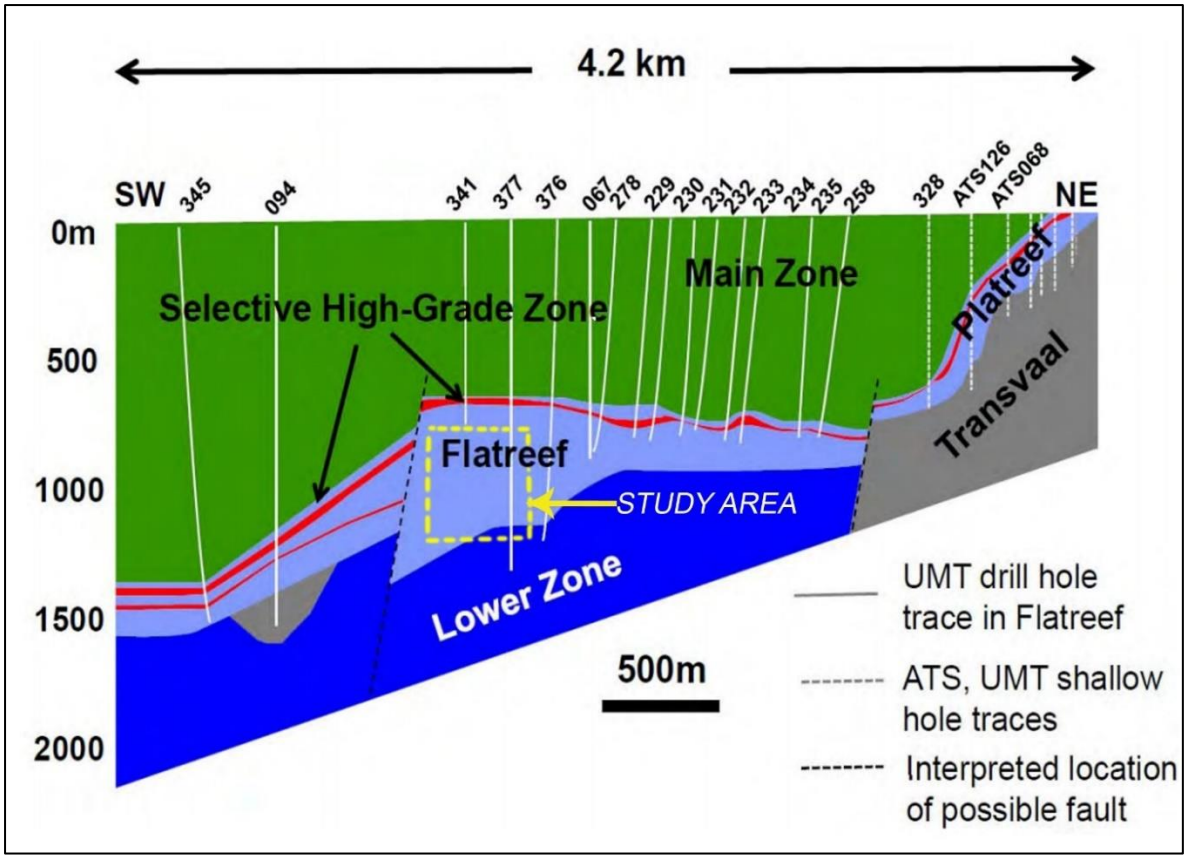


Figure 3. 8: Position of the study area in relation to the general stratigraphy. The study area is highlighted in yellow, and occurs within the proposed underground mining project of Ivanhoe, although in the footwall of the selective high-grade zone (Ivanplats, 2013).

3.5 Lithologies of the Turfspruit Area

The boreholes described are shown in Figure 3.7. UMT 366 has Lower Zone harzburgite at the base of the hole, with an example demonstrated in Figure 3.2 A. The rock consists of about 80% orthopyroxene and 20% olivine, although it is sometimes difficult to determine the proportions because of the extensive serpentinisation. Texturally, the harzburgite is poikilitic, with oikocrysts of rounded orthopyroxene abundant, and varying amounts of intercumulus plagioclase, but not more than 5%. Serpentinisation of the harzburgite has resulted in the formation of magnetite, which imparts a dark colouration to the rocks that are intensely altered. There is a progressive increase in the plagioclase content upwards, where a gradational contact exists with a cross-cutting quartz vein.

Immediately above this quartz vein is a fine-grained orthopyroxenite, with around 8% sulphides at and near the contact, while the average sulphide content for the rest of the package was around 2%. Two, thin, centimetre-sized chromite stringers occur at 4 and 4.5m from the quartz vein contact. They appear to have formed at a late-stage, as the stringer forms around an orthopyroxene oikocryst, similar to the example in Figure 3.3 E, although significantly smaller. This pyroxenite package slowly increases in gran size upwards, and becomes a medium-grained pyroxenite at around

1590 m. Small, disseminated grains of chromite appear from 1588 m, and a fairly sharp contact with the so-called 'UG2-like chromite occurs at 1587 m.

The section between 1587 and 1583.5 m has been logged as chromite in Figure 3.7 to highlight their position, although in reality it is more of a very chrome-rich 'zone'. The largest massive chromite layers occur at 1586.4-1586.6 m and 1584.1-1584.2 m, while the rest of this area is dominated by disseminated chromite of 40-60% occurring within a similar pyroxenite as the one described previously. The pyroxenite gradually increases in olivine content, and eventually forms a thin layer of paraharzburgite at the contact with a calc-silicate. The calc-silicate contact is gradational, with hybrid rocks (Figure 3.3 F) occurring at the edges and a banded dolomite occurring at 1582.9 m. Although the xenolith is highly assimilated, the dolomite retained some of its original sedimentary layering (Figure 3.3 A). The contact above is essentially a mirrored image of the lithologies below, in that paraharzburgites rim the xenolith, followed by an increase in chromite content, and a massive chromite layer at 1580.3 m. The coarsest chromite grains usually occur clustered, and up to 3 mm in size, while the finest grains are not discernible with the naked eye.

A transitional zone exists above this chromite, where coarse, sulphide-rich (5%), feldspathic pyroxenite occurs for 2.5 m, becoming progressively finer grained upwards. Sulphides include mainly chalcopyrite and pyrite as disseminated, intercumulus grains. Clinopyroxene oikocrysts of up to 1 cm are present, becoming less abundant as the rock becomes less feldspathic and finer grained. A medium to coarse-grained feldspathic pyroxenite is logged at 1576.3 m which contains no visible sulphides. From here on upwards, the rock again becomes increasingly clinopyroxene-rich, with a gradational contact to gabbronorite. At 1571.8 m, it is logged as a pegmatoidal gabbronorite, with big feldspar laths and large sulphide blebs of, especially chalcopyrite that reach up to 2 cm in size. There is a sharp contact at 1568.2 m with spotted anorthosite, which consists of small cores of 0.2 to 1 cm cores of clinopyroxene, 1-2 cm oikocrysts of orthopyroxenes, while the majority of the rock (70%) consists of cumulus plagioclase. There is a transition from spotted to mottled anorthosite, which is shown in Figure 3.2 C.

A very plagioclase-rich (20%), medium-grained feldspathic pyroxenite occurs as a sharp contact with underlying anorthosite at 1567.3 m, with very little (1-2%) visible sulphides. Continuing upwards there is a loss of core from 1564.6 to 1564.8 m below surface. The package between 1564.3 to 15564.6 m represents a thin transitional zone of leuconorite with no sulphides, which is followed by a thick homogeneous package of coarser, darker, melanorite, from 1564.3 to 1561.5 m. At the top of this package there is a steady decrease in the pyroxene content, with an extremely small Cr stringer present in this transitional zone, shown in Figure 3.2 E. At 1559 m, a thin and similar anorthosite

layer occurs for half a meter, and is followed by a medium-grained norite, with about 30% plagioclase and some 3% visible sulphides.

The end-of-hole in UMT 335 does not have Lower Zone harzburgite, but is represented by a plagioclase-free, medium-grained pyroxenite, with lath-shaped orthopyroxene grains, similar to those present in Lower Zone or Lower Critical Zone rocks elsewhere. Moving upwards there are two intervals of parapyroxenite, with no indication of a xenolith, but an increase in grain size and a green colour due to clinopyroxene and epidote content. This is followed by a similar pyroxenite, which contains 2 disseminated chromite-zones of 3 and 2 cm at 1752 and 1755 m respectively. From 1748 m upwards, there is an increase in the grain size and plagioclase content of the pyroxenite, with a gradational contact with a calc-silicate xenolith at 1745.6.

The xenolith consists of a coarse to pegmatoidal dolomitic rock, in which the plagioclase present has been altered through sericitisation and chloritisation. Large augite crystals of 3 cm are present with sulphides at 4%. Moving upwards the rock becomes more hybrid, with an anhydrite, epidote, garnet and chlorite assemblage. The contact with fresher orthopyroxenite is marked by a 30 cm chromitiferous zone, which has been vertically exaggerated in Figure 3.7 to highlight its presence. There is a loss of core from 1730.7 to 1728.9 m. This is followed by a fine-grained feldspathic pyroxenite with 2% sulphides, which increase in grain size up the hole and forms a contact with a calc-silicate at 1726.7 m. This calc-silicate has a pegmatoidal overprint with clinopyroxene crystals up to 2 cm, 2-3 % anhydrite and big garnet crystals of 1 cm.

There is a rather sharp contact at 1725.5 m with a fine-grained orthopyroxenite, which contain elongated orthopyroxene grains, 2% plagioclase and around 5% clinopyroxene. At 1722 m there is an unobvious contact with a pyroxene-plagioclase-phlogopite-hornfels rock, which has been logged as a parapyroxenite. This is followed by the so-called ‘UG2’ chromite, which is represented by a large number of Cr seams and stringers of 2-3 cm thick, and moving upwards become disseminated within a pyroxenite. At 1716 m, there is a gradational decrease in chromite content, and contact with a orthopyroxenite similar to those describe below, which contained lath-shaped orthopyroxene grains. At 1709.8 to 1710.4 m there is quartz vein cross-cutting the pyroxenite.

Above this vein is a new package of orthopyroxenite characterised by clinopyroxene and plagioclase segregation, with 1 % plagioclase and 5% clinopyroxene. This is followed at 1703 m by a new orthopyroxenite, which is chromite-rich in places, and sporadic coarse-grained plagioclase-clinopyroxene segregation, representing pods of pegmatoidal veins with an increase in plagioclase. Veins such as these have a marked increase in sulphides of up to 10%. The upper, sharp contact with a coarse to pegmatoidal feldspathic pyroxenite is represented by a disseminated Cr seam of 10 cm.

Thereafter, there is a new contact at 1678.1 m with a similar medium-grained orthopyroxenite, with yet another package of pegmatoidal feldspathic pyroxenite at 1683.7 m.

At 1678.7 m, there is a sharp contact with a granophyric granite, with a high quartz and plagioclase content. A sharp top contact with a medium-grained feldspathic pyroxenite follows, which has 10-15% plagioclase, small amounts of sulphide, and 0.3 – 0.5 mm oikocrysts of clinopyroxene. At 1666 m is a similar norite package as those at the top of hole UMT 366.

UMT 336 was logged by Dr. Marina Yudovskaya, but show a very similar stratigraphy to the two holes described previously, with the exception of dunite occurring at the end-of-hole. Again, the Lower Zone rocks are separated from the Platreef succession by a cross cutting quartz vein, as seen in UMT 366. In this case, however, the 'UG2' chromite is hosted by a contaminated paraharzburgite. The lithologies on Turfspruit can broadly be traced laterally across the stratigraphy, with most of the differences being local, and due to xenolithic material.

3.6 Stratigraphy of Zwartfontein

The stratigraphy of the Zwartfontein property is based on the logging of hole ZF 116 (Figure 3.9), which is part of the Akanani exploration project of Lonmin. ZF 116 is situated on the farm Zwartfontein 814 LR (Figure 2.2), which is situated a few km down dip from the Zwartfontein south open pit to the east, part of the Mogalakwena operation of Anglo American. It is near impossible to gain an understanding of the stratigraphy of Zwartfontein relying on the logging of one hole, and apart from that it could lead to misleading representations, and therefore previous work on Akanani was utilised in combination with this study in trying to construct a more informed representation.

The bottom of ZF116 is represented by a package of fine-grained granofels that appears to represent a chill margin. A sharp contact with an overlying melanorite occurs at 1616 m below surface. This melanorite consists of 45 % plagioclase, and could be classified as a feldspathic pyroxenite if it were not for the presence of some cumulus plagioclase. There are areas where the plagioclase content disappears, in which case it is logged as pyroxenite, such as at 1608 m. At 1605 m a similar melanorite starts increasing in plagioclase content upwards, and with this increase in plagioclase is an increase in sulphide content.

A thin feldspathic pyroxenite occurs at 1584 m, which is extremely plagioclase-rich (25%), with up to 6% sulphides. This is followed by a sharp contact with a fine-grained pyroxenite. A 2m thick, medium-grained harzburgite, which is extensively serpentinised occurs at 1571.8 m. There is a repetition of similar mela- and leuconorites occurring above this harzburgite.

The first prominent chromite-rich horizon at 1527,1 m is hosted by a medium-grained feldspathic pyroxenite and could potentially represent the Lower Chromitite Zone described by Yudovskaya and Kinnaird (2010). It has an irregular and gradational bottom contact, while the top contact is sharp with a sulphide-rich pyroxenite. The horizon consists out of two well-developed chromite-rich zones (15 and 13 cm respectfully), which has several stringers of between 0.5 – 3 cm in thickness below them. They contain tiny orthopyroxene oikocrysts (Figure 3.3 E) in places and have rather sharp contacts, and locally extremely fine-grained sulphides. The hanging wall pyroxenite of the chromite layer becomes pegmatoidal from 1526 m to 1523 m, in which extremely large blebs of chalcopyrite occur as interstitial grains.

Two thick packages of parapyroxenites, separated by feldspathic pyroxenite, occur between 1523 m 1500 m. They are extremely coarse-grained, with some diopside crystals reaching 1.5 cm in size. Above these rocks is a similar sequence of norites and feldspathic pyroxenites. This is followed by a sharp contact at 1460 m with a calc-silicate, which appears extremely assimilated, such that the original protolith is difficult to recognise, although assumed to be dolomitic. The next 180 m is represented by a layered sequence of calc-silicate xenoliths, followed by highly altered pyroxenite, then magmatic pyroxenite, and thereafter another xenolith. A number of the more altered pyroxenite were termed parapyroxenite, and in some cases these rocks contain anhydrite and other alteration products.

The extremely contaminated sequence ends at 1280 m where a more magmatic pyroxenite with very little plagioclase occurs, although zones of serpentinisation continue to occur locally within all rocks upwards in the stratigraphy, as far as the anorthosite layer, which represents the top of the hole. At 1235 m the economic PGE reef occurs, which is termed the Main Mineralised Unit (MMU). It is represented by an intensely serpentinised harzburgite, which has a poikilitic texture with olivine grains and orthopyroxene oikocrysts, of which only the olivine has been serpentinised. There is a significant amount of intercumulus base metal sulphides within the reef (4-10%), with some grains reaching up to 2 cm in diameter. A small chromitite layer of about 2 cm is located within the harzburgitic reef. According to Yudovskaya et al. (2011) the PGE reef on Akanani is located at the same stratigraphic level as the one mined towards the east at Mogalakwena, however, the Akanani reef is hosted by more primitive rocks, with olivine and pyroxene being richer in Mg and Ni.

The top of the succession is represented by a mottled anorthosite, which is the boundary between the Main Zone and the Platreef (personal communication with Lonmin geologist).

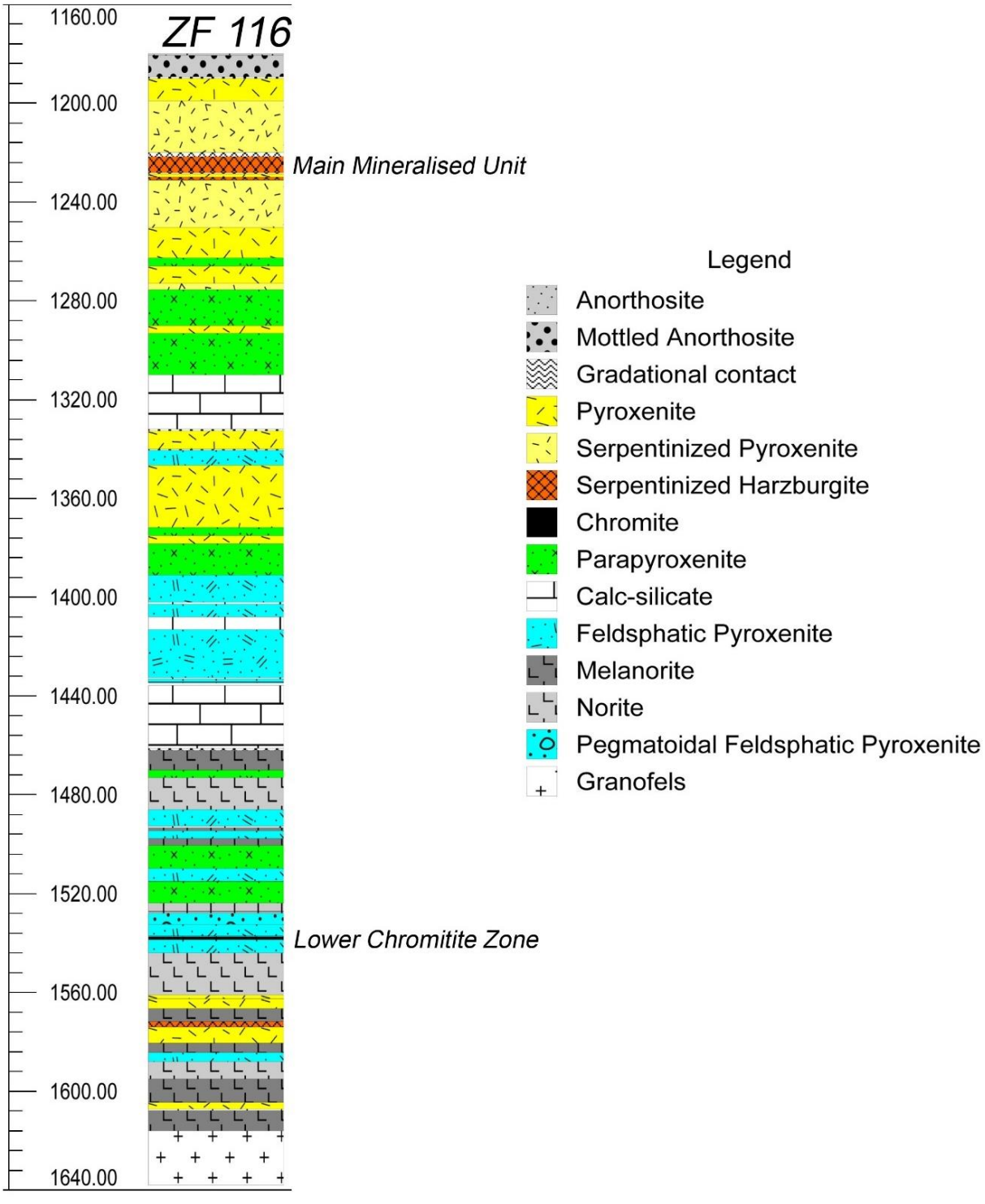


Figure 3. 9: Stratigraphic column of hole ZF 116, part of the Akanani project on the farm Zwartfontein 814LR (Figure 2.2).

3.7 Discussion

The presence of harzburgite is generally restricted to the lower portions of the Platreef succession, and in some cases harzburgites of the recognised Lower Zone is present. Some of the harzburgite encountered on Turfspruit may be xenoliths of Lower Zone material that were incorporated into the more pyroxenitic Platreef. According to Yudovskaya et al. (2013), Lower Zone sequences of up to 800 m thick are present on the Turfspruit property, where it is separated from the overlying Platreef by an interval of country rocks. This may be the case in UMT 366 and 336, where harzburgite and dunite occur at the base of the holes, and in both cases, they are separated from the overlying rocks by sedimentary layers. The separation of the Lower Zone from the Platreef may be explained by the proposed hiatus that took place between the emplacement of the Lower Zone and the Platreef. This hiatus is based on the following observations made by Van der Merwe (1978): (i) The Lower Zone has been intruded by the Platreef, (ii) The Platreef transgresses the Lower Zone to the north, (iii) The Lower Zone has been metamorphosed by the Platreef and (iv) there exists an angular unconformity between the Lower Zone pyroxenite and the Platreef.

All the harzburgites encountered were heavily serpentinised, which generally gave these rocks a darker appearance. Some of the harzburgite identified was magnetic, and this dark colour could be attributed to the formation of magnetite. This is due to a reaction that takes place during serpentinisation between olivine and water, which leads to the production of magnetite.

Fresh olivine grains are extremely rare (apart from the dunite in hole UMT 336) and most are serpentinised, while oikocrysts of orthopyroxene may be preserved depending on the extent of alteration. In other cases, such as at the top of UMT 377, unaltered olivine grains occur within highly serpentinised rocks, and this may indicate a magnesian rich fluid ingress, and therefore the olivine remained in equilibrium

Pyroxenite is by far the most common lithology logged at Turfspruit, and it occurs in several varieties, with differing grain sizes, textures, sulphide content, and it is difficult to make generalisations on the rock type. It varies from fine-grained to pegmatoidal, predominantly contains cumulus orthopyroxene, with lesser plagioclase and clinopyroxene. The majority of chromitiferous zones were hosted by pyroxenite, and quite often the boundaries between different types of pyroxenite would be marked by the presence of a chromite stringer. The sulphide content varies widely, ranging from 0-12%, and typically the larger the grain size the higher the visual sulphide percentage.

Pyroxenites that occurs in UMT 366 and 336, are characterised by laminated and lath-shaped orthopyroxene grains. There may be two reasons for this occurrence, firstly, these grains may be

deformed through compaction of overlying melt and crystal mush, or there may have been a quiescent period during which they were flattened. Lath-shaped orthopyroxene grains were all orientated parallel to one another, possibly indicating the flow direction of the magma. Different packages of pyroxenite are commonly separated from one another by the presence of either calc-silicate or hornfels xenoliths or by discrete chromite horizons. This may refer to pyroxenite sills that Kinnaird (2005) described in the southern sector of the Platreef.

As mentioned in Chapter 2, Yudovskaya and Kinnaird (2010) outlined two main chromite-bearing zones in the Platreef that they identified in two-thirds of about 20 boreholes studied. The upper chromitite zone occurs near the top of the Platreef succession, around twenty or so meters from the Main Zone contact, hosted by pegmatoidal pyroxenite or at the boundaries between major lithologies. On Turfspruit, the 'UG2-like' chromitite represents a thick zone of chromite-rich lithologies, occurring some distance below the "Merensky" pyroxenite. The Lower chromititie zone, however, occurs near the base of the Platreef, as a number of seams which are hosted by a wide array of lithologies, ranging from pyroxenite, norite, paraharzburgite, calc-silicate and parapyroxenite.

Chromite horizons encountered on Turfspruit were not confined to a specific host rock. One of the more striking observations made is the fact that many of the prominent chromite-rich layers occur at the major contacts between different rock types. For example, in UMT366, the major chromitite horizon occurs at the contact between a large feldspathic pyroxenite package and an orthopyroxenite package, which is represented by a calc-silicate raft and some paraharzburgite. This is supported by Ivanplats geologists that have identified a clear unconformity within the footwall to the UG2-like chromite-zone, especially in the flatreef area (Grobler 2017, personal communication).

On Turfspruit, norites are usually medium- to coarse-grained, with orthopyroxene having more euhedral and larger grains than the anhedral greenish clinopyroxenes. Most of the norites logged formed part of norite cycles (Figure 3.5). Cycles such as these, that progress from mafic-rich to mafic-poor lithologies, are unique to the Turfspruit area (Kinnaird *et al.,* 2010), and have not been recorded elsewhere in the northern limb. Some norites are considered to be interfingering Main Zone rocks that cut down into the Platreef succession, and some may have formed as a result of mixing Main Zone and Platreef magmas (Kinnaird and Nex, 2015).

A number of different xenoliths, or rafts, are found on the Turfspruit property, ranging from dolomites, BIF's, and cross cutting granitic rock. Adjacent rocks are usually highly altered and contaminated, particularly with more reactive xenoliths, such as calc-silicates and dolomites. Usually, there is an increase in the grain size of the surrounding rocks, indicating the presence of

fluids that passed through. The most striking characteristic of rocks that have undergone assimilation is the change in colour to either creamy white (when the metamorphism is limited), to dark yellow-green (increased metamorphism).

In UMT 366 and 336, both mottled and spotted anorthosite layers occur at the top of the succession, which indicates the start of a new norite cycle. Mottled anorthosite usually has around 10% mottles that consist of oikocrysts of clinopyroxene, and spotted anorthosite consists of brown cores of orthopyroxene. Figure 3.2 indicates that there is a continuum between mottled and spotted anorthosites, which contains euhedral grains of brown orthopyroxene with skeletal overgrowths, as well as oikocrysts of green clinopyroxene.

There are several authors who claim the Platreef must have formed from a separate Critical Zone magma than those in the eastern and western limbs (McDonald et al., 2005), while others believe the Platreef to be a part of the Upper Critical Zone (Von Gruenewaldt et al., 1989; White, 1994). In a stratigraphic context, the modern research stems from van der Merwe (1976), who agreed and built upon the work of Wagner (1929), who correlated the mineralised portions of the Platreef with the Merensky Reef. Von Gruenewaldt (1989) suggested that the Platreef could be correlated with the GNPA member to the south of Mokopane, due to the layering of some of the units and the presence of cumulus chromite and development of a chromitite layer. All of these features are characteristic of the Critical Zone of the eastern and western limbs.

3.7.1 Comparison between Akanani and Turfspruit

The end-of-hole on Zwartfontein is represented by a thick, fine-grained granofels, rather than the Lower Zone rocks encountered on Turfspruit. It may be possible that the granofels layer on Zwartfontein represents the separation of the Platreef with the Lower Zone, although this is simply speculation. The quartz veins that separated the Lower Zone rocks from the Platreef in both UMT 336 and 366 was absent on Zwartfontein, although these are only localised features that were controlled by structures. The thick norite package occurring in the lower parts of ZF116, was very similar to that encountered in UMT 336.

The general increase in plagioclase content upwards through the succession was not as obvious on Zwartfontein, with plagioclase-free lithologies occurring in the top of the hole, while magmatic olivine-rich rocks are limited on Turfspruit. Gabbronorites, thought to represent interfingering Main Zone rocks, are only present in UMT 366, and were not noted anywhere else.

Turfspruit holes were generally more Cr-rich, with random stringers occurring throughout the Platreef. Also, the Cr-rich zones were better developed on Turfspruit, with the so-called ‘UG2’ layer

reaching 30-40 cm of chromitite in places. Although, the Lower chromite zone appears to be better developed in ZF116, as well as being more sulphide-rich than any chromite zone encountered on Turfspruit. According to Yudovskaya et al. (2011) and Mitchell and Scoon (2013), the finer grained chromitite in the lower parts of the Platreef generally have lower PGE grades than those in the upper parts of the succession.

The hole on Zwartfontein generally has more primitive rock types, and the presence of serpentinisation was far more prevalent. For example, serpentinisation on Turfspruit was spatially associated with the presence of xenoliths, which was not the case in ZF116. The reason for this could be the abundance of olivine-bearing rocks on Zwartfontein.

3.7.2 Comparison with the Main Bushveld Complex

One of the main aims of this study is to investigate whether the northern limb of the Bushveld can be correlated with that of the Main Complex. This is a highly contentious topic that has puzzled many authors over the last two decades and continues to do so. Due to the limited amount of material, as well as time available for this study, the focus will be on the southern sector of the Platreef and specifically on chromite-rich zones. This will provide more detailed results, which may not be representative for the entire northern limb, but might deliver some answers to the debate at hand.

Stratigraphic similarities between the Northern limb and the Main Complex

The stratigraphy of the Northern Limb is not as well developed as that of the Western and Eastern limbs (Figure 3.5). Nevertheless, many authors, as well as industry geologists have claimed that the Platreef is the northern equivalent of the Critical Zone. In terms of the position of the Platreef, situated between the Lower and Main Zone, it is analogous to the Critical Zone, which is why early authors such as Wagner (1929) and Willemse (1969) linked the economic horizons within the Platreef with that of the Merensky Reef.

The economic portion of the Platreef on Turfspruit is situated near the top of the unit, similar to the Merensky in the Upper Critical Zone in the rest of the Bushveld. Both units are dominated by orthopyroxene cumulates, with lesser amounts of clinopyroxene along with plagioclase (McDonald et al., 2005). The occurrence of chromitite layers are almost entirely restricted to the Critical Zone in the Main Complex, if one follows the boundary of the Lower Zone set by Teigler and Eales (1996), in which the top contact of the Lower Zone is represented by the uppermost olivine-rich (harzburgite) interval. Apart from the chromite horizons in the Grasvally area south of Mokopane, chromitite occurs almost exclusively within the Platreef as well, although not nearly as well developed as in the

eastern and western limbs. The highest PGE concentrations in the Merensky Reef is usually defined by two to four thin chromite stringers, where the highest grades are usually near the upper stringer (Lee, 1996). According to Viljoen and Schurmann (1998), PGE grades are highest in a pyroxenite immediately beneath a chromite developed on the farm Tweefontein, and they suggest that at this locality the Platreef bears the greatest similarity to that of the Upper Critical Zone.

In the NI 43-101 report released by Ivanplats [LTD] (2013), they correlate a succession termed the Turfspruit Cyclic Unit (TCU) directly with that of the Merensky Cyclic Unit. The TCU consists of a harzburgite at the base, followed by an orthopyroxenite, then the mineralised zone, a feldspathic pyroxenite and then a mottled anorthosite layer at the top. Directly below the TCU a harzburgite has been correlated with the Pseudo Reef, and thereafter the UG2. The study area occurs at a much lower stratigraphic position than that of the mineralised area on Turfspruit, and as a result no deductions will be made on these areas.

Stratigraphic differences between the eastern and western limbs and the Platreef

The stratigraphic differences that could be identified in the study area were as follows: (i) Absence of well-developed chromitite horizons. The Critical Zone hosts enormous reserves of chromium within the Lower (LG), Middle (MG) and Upper (UG) chromitite layers, which can be traced over the eastern and western limbs of the Bushveld for hundreds of kilometres (Hatton and Von Gruenewaldt, 1987). Most of the chromitite horizons encountered on Turfspruit and Zwartfontein is difficult to correlate laterally. Each hole on Turfspruit had one well developed zone of chromitite, which Ivanplats claimed to be the equivalent of the UG2, and which Yudovskaya and Kinnaird (2010) termed the Lower Chromitite Zone. This is opposed to the 13 recognised chromitite horizons in an ideal stratigraphic column of the main Bushveld Complex. Ivanplats states that they have correlated the chromite stringers laterally in their geological model (Grobler ,2017, personal communication).

Although the Turfspruit Cyclic Unit and Main Mineralised Zone on Akanani could be regarded as an equivalent to the Merensky Reef, the chromite distribution is sporadic in comparison to the thin, but persistent chromitite stringers associated with the Merensky Reef (Kinnaird, 2002). The two zones highlighted by Yudovskaya and Kinnaird (2010) were only present in two thirds of the boreholes studied, which questions the persistence and extensiveness of these zones.

(ii) Lack of typical cycles that are found in the Critical Zone. The Upper Critical Zone consists of partial or complete sequences of harzburgite, or chromitite, at the base of the cycle, followed by pyroxenite to norite, and norite to anorthosite (eg. Scoon and Teigler, 1994). The Lower Critical Zone does not display such cycles, both in terms mineral assemblages and compositions (Cameron, 1980).

According to the Ivanplats geologists', the studied area takes place from the Upper to the Lower Critical Zone, if one had to compare it to the eastern and western limbs. There is a broad trend within these three holes that show a decrease in the amount of plagioclase downhole, and if examined closely, small incomplete cycles can be identified of norite, to feldspathic pyroxenite, through to pyroxenite. This is a unique feature to the Platreef, and has been termed norite cycles However, it simply cannot be likened to the superb layering, and sharp contacts of the Main Complex.

(iii) The presence of clinopyroxene in the Platreef. According to Maier and Barnes (1998), clinpyroxene is not an important component in the Upper Critical Zone and is never present as a cumulus association with chromite. Although most probably induced through means of contact metamorphism and assimilation with xenoliths, clinopyroxene is present as a cumulus phase with chromite in some of the chromite-bearing parapyroxenites outlined in the study. Clinpyroxene grains are also very common in a number of pyroxenite, feldspathic pyroxenite and noritic packages. This may be explained by the different crystallisation sequence within the Platreef. In the Merensky Reef, the sequence is orthopyroxene-plagioclase-clinopyroxene (Cawthorn, 2002), whereas in the Platreef clinopyroxene either follows orthopyroxene, or crystallises concurrently, either way it precedes plagioclase which is generally intercumulus (McDonald et al., 2005).

The Platreef stratigraphy is characterised by the presence of numerous xenoliths, reflecting the fact that in the southern sector the immediate footwall of the Platreef is Transvaal sediments. The increased thickness of the Platreef is ascribed to intercalated metasediments, that occurs in the study areas as hornfels, calc-silicate and BIF xenoliths. In the Main Complex the presence of such material is minor.

In terms of the stratigraphic position of the Platreef, occurring between the Main- and Lower Zone, it is analogues to the Critical Zone of the Main Complex. The footwall of the Platreef is represented by a Lower Zone package on Turfspruit, while on Zwartfontein the footwall is a fine-grained granofels. The great diversity of rock types identified on the study areas has been attributed to the variety in footwall, as well as the interference of footwall/country rock with the Platreef magma. Due to the extensive contamination which these rocks experience, any sophisticated layering that may have been present is difficult to identify. Ivanplats geologists have done detailed work and claim to have identified the different Critical Zone layers, even in areas with significant contamination.

Chapter 4

Petrography

Petrographic studies on thin sections were carried out using both reflected and transmitted light. Around 80% of the core sampled consisted of chromitiferous horizons, or stringers, as this is the primary focus of the study. The rest of the samples either contained primary magmatic silicate rocks, to gain insight into the features of the Platreef magma, highly mineralised rocks, or extremely contaminated rock types to provide evidence as to what the effects were of assimilation of country rock. A special note on the positions of samples was made, which makes it possible to identify the presence of any large-scale trends.

4.1 Introduction

White (1994) introduced a very simplified terminology for the Platreef, now defunct, which categorised the Platreef into three principal rock types, namely the A, B and C reef. The A reef is at the base of the proposed sequence, and consists of pegmatoidal feldspathic pyroxenite and carries erratic base metal sulphides. The principle PGE-mineralised reef, termed the B reef, is situated above and is composed of a coarse-grained pyroxenite with approximately 50-90% orthopyroxene, the presence of chromitite in the B reef is limited. Following Ivanplats' stratigraphic units, this would coincide with their TCU (Turfspruit Cyclic Unit). Lastly, the top of the sequence is a fine-grained feldspathic pyroxenite that contains considerable amounts of clinopyroxene and is termed the C reef. None of these proposed 'reefs' conforms to the standards set out by the IUGS classifications, and they do not allow for sufficient distinction between units and promotes pigeonholing of rock types (McDonald et al., 2005). Therefore, petrographical descriptions in this study will refer to internationally-accepted classification schemes, based on the modal percentages of minerals, and the cumulus and intercumulus phases.

4.1.1 Pyroxenite

Pyroxenite is the dominant rock type on Turfspruit and these rocks show great textural and compositional variability. They most commonly range from medium (2-5 mm) to fine-grained (< 2 mm) phaneritic rocks, while coarse to pegmatoidal varieties (> 5 mm) are limited to feldspathic pyroxenite, which will be discussed separately. A typical magmatic Platreef pyroxenite consists of 80 to 95 % of cumulus orthopyroxene, and therefore the more appropriate term would be an

orthopyroxenite, although for practical reasons it is referred to as simply a pyroxenite in this study.

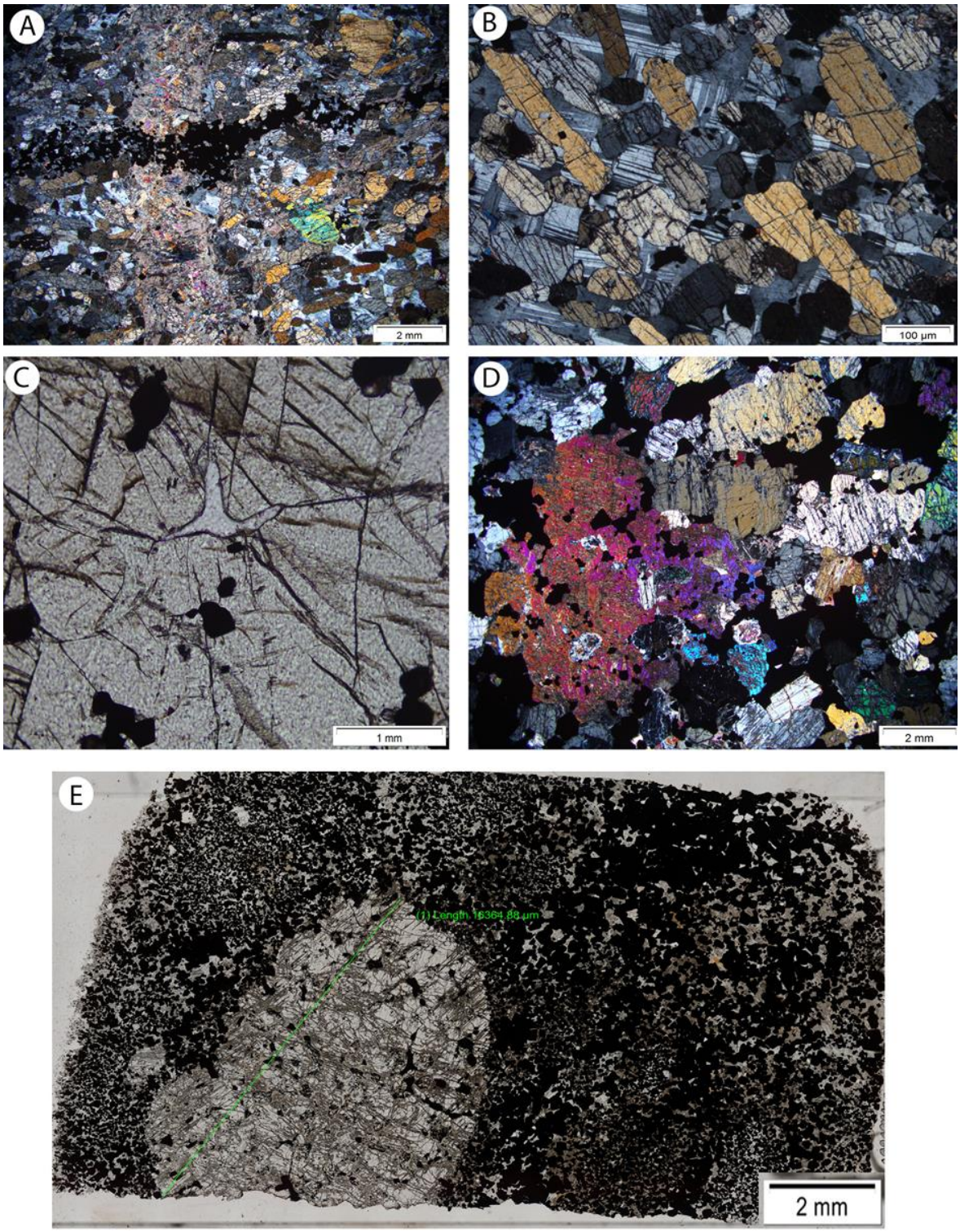


Figure 4. 1: Photomicrographs of various rock types from Turfspruit under a transmitted light microscope. (A) Single vein of serpentine cross-cutting a feldspathic pyroxenite and a chromite stringer in UMT 377 at 1033 m. Notice that the serpentine vein has not affected the surrounding minerals in any way. (CPL) (B) Lath-shaped orthopyroxene grains that exhibit foliation which is defined by subparallel alignment of these elongated grains. UMT 377 at 1007 m (CPL). (C) Tricuspidate-shaped plagioclase inclusion within an orthopyroxene grain. Notice the concave-inward boundaries of the inclusion, resembling intercumulus plagioclase within feldspathic pyroxenites. UMT-335 at 1717 m (PPL) (D) Large, intercumulus clinopyroxene grains that encloses older orthopyroxene and olivine grains. UMT 366 at 1585 m (CPL) (E) 1.6 cm, cumulus orthopyroxene oikocryst, occurring within a chromitiferous zone in UMT 366 at 1586.2 m (PPL). CPL=Crossed polarised light. PPL=Plane polarised light.

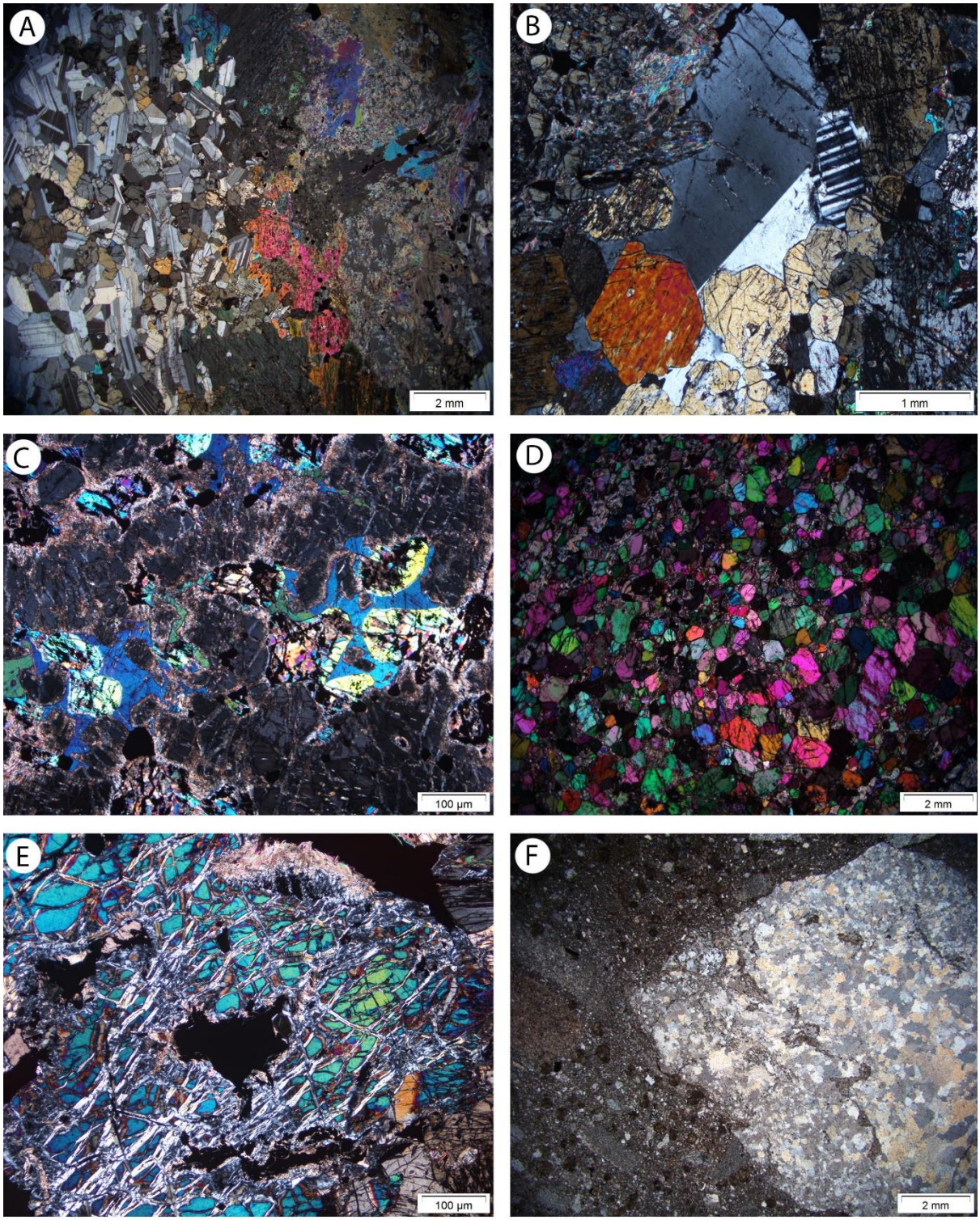


Figure 4. 2: Photomicrographs of various rock types from Zwartfontein and Turfspruit under a transmitted light microscope. (A) Serpentine vein running across a norite, including a number of clinopyroxene grains and Cr spinels. The surrounding minerals appear to be unaltered though. UMT 366 at 1561.4 m. (CPL) (B) Rare plagioclase grain in a chromite-rich pyroxenite showing Carlsbad twinning, from 1538.6 m in hole ZF 116. (CPL) (C) Highly serpentinised rock with the only recognisable minerals grains being skeletal, intercumulus clinopyroxene grains. UMT 366 at 1586.2 m. (CPL) (D) Paraharzburgite consisting out of an interlocking framework of olivine grains. UMT 377 at 922 m. (CPL) (E) Olivine grain highly serpentinised by what appears to be chrysotile.UMT 366 at 1595.5 m. (CPL) (F) Hornfels xenolith with what appears to be a norite patch. UMT377 at 973 m. (PPL)

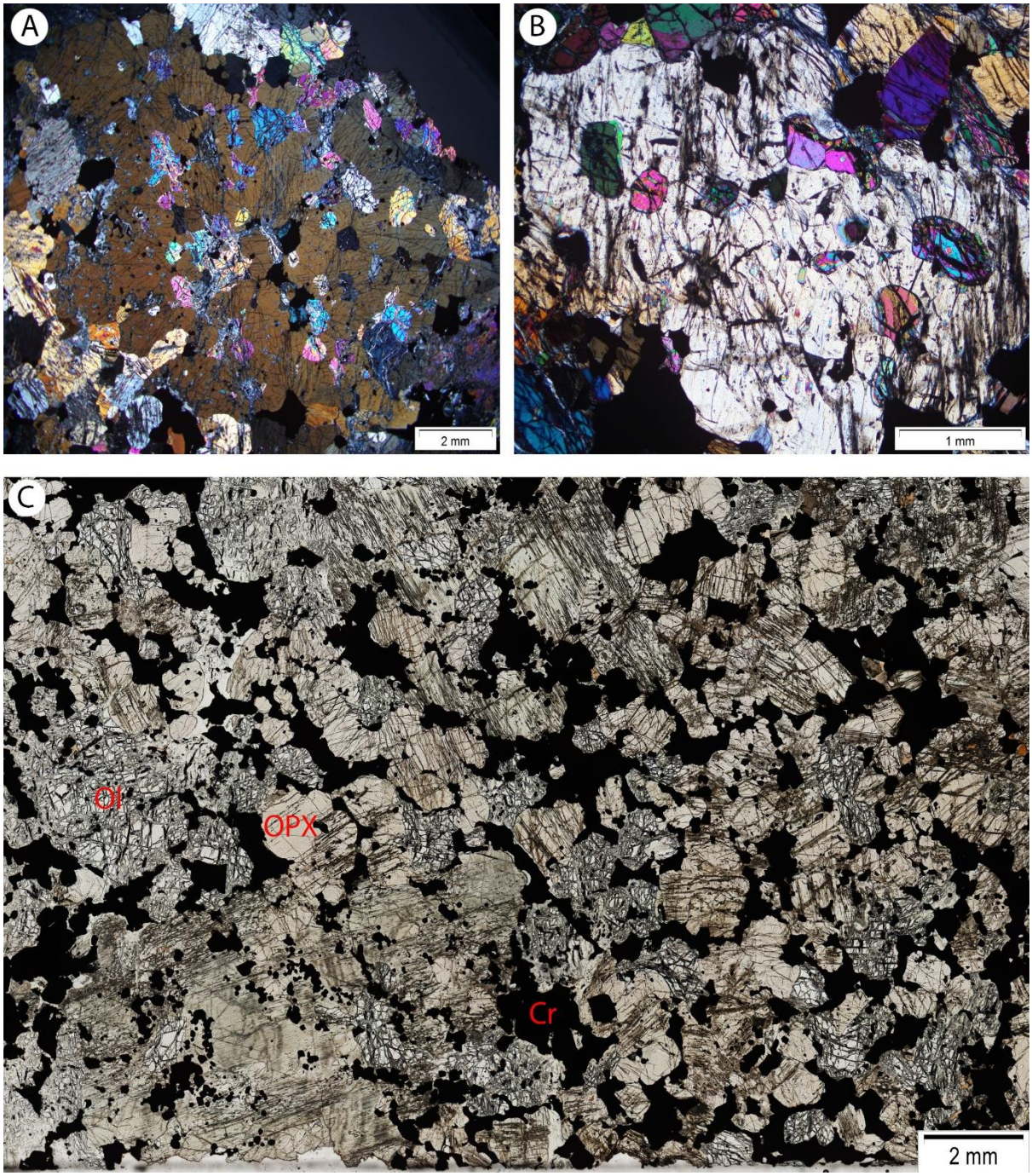


Figure 4. 3: Photomicrographs of different rock types from Turfspruit under a transmitted light microscope. (A) and (B) Both these photos are typical examples of the poikilitic texture displayed by olivine chadacrysts in orthopyroxene oikocrysts. The olivine in these photos were formed earlier and corroded later by the orthopyroxene oikocryst. During serpentinisation more water is absorbed into the crystal structure of these grains, leading to volume expansion and the 'cracked' feature seen in the olivines. (A) is from UMT366 at 1595.5 and (B) from UMT366 at 1585.4. Both photos were taken under CPL (C) Granular harzburgites which consists of lesser olivine and more opx, and are texturally comparable to olivine orthopyroxenites. This sample is from UMT366, within the hanging wall of the so-called UG2 on Turfspruit. (PPL).

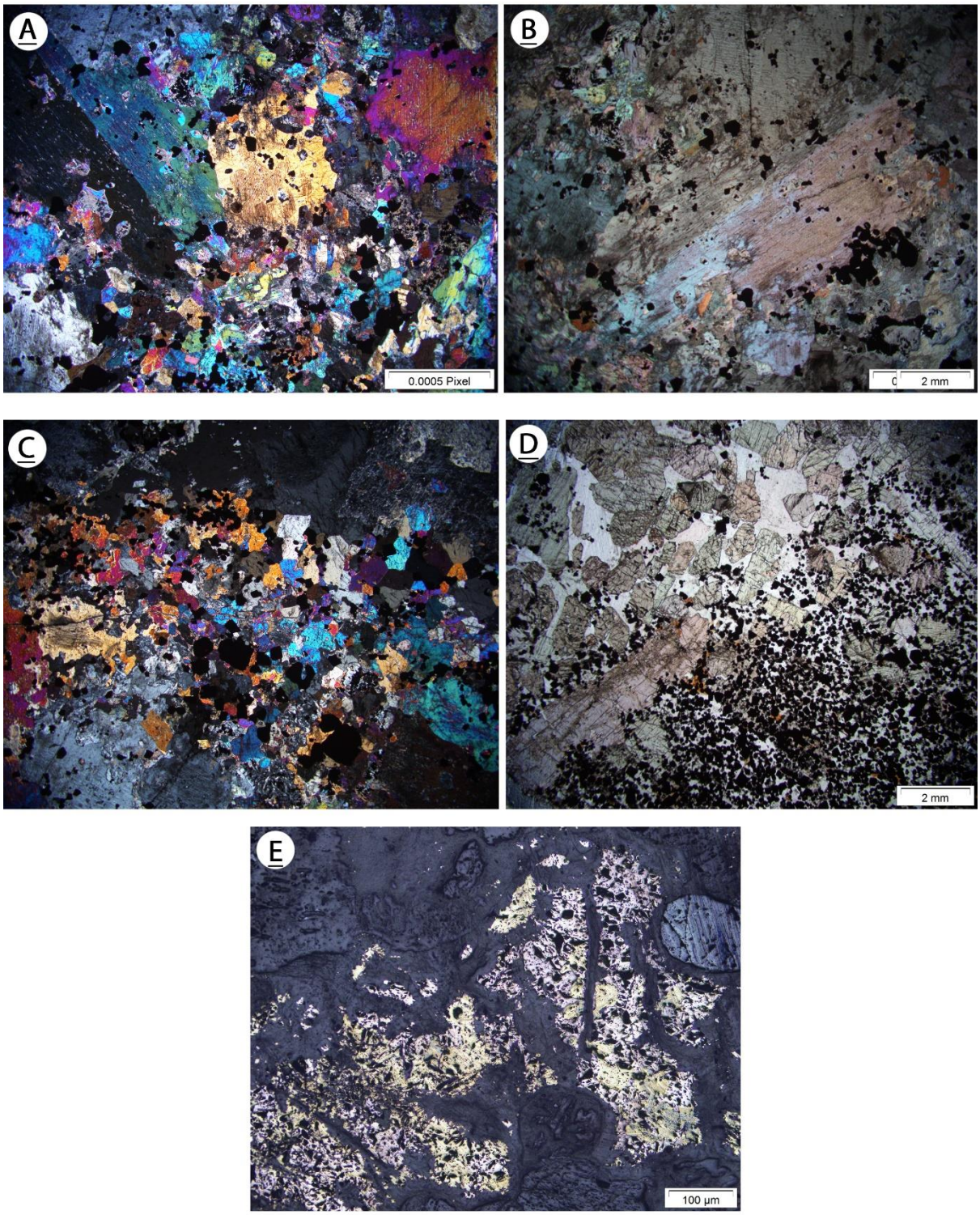


Figure 4. 4: Photomicrographs of the different features present in parapyroxenite from Turfspruit and Zwartfontein. (A) Parapyroxenite in the footwall of the UG2 on Turfspruit in UMT 335 at 1720 m that is dominated by clinopyroxene. (CPL). (B) Highly altered parapyroxenite that shows the presence of carbonate minerals inherited from a dolomitic xenolith in UMT 335 at 1720 m. (CPL). (C) Parapyroxenite from the Zwartfontein property, showing a distinctive clinopyroxene morphology, indicative of metamorphic behaviour. (CPL). (D) Chromitiferous pegmatoidal feldspathic pyroxenite that contains elongated laths of clinopyroxene and more than 15% interstitial plagioclase. Situated in the hanging wall of the Lower chromite zone in ZF116 at 1538 m. (PPL). (E) Sulphides in a parapyroxenite, in UMT 377 at 998 m, that have been replaced due to extensive alteration. Taken under PPL in reflected light.

Other common constituents include plagioclase, which is almost ubiquitous, as well as accessory olivine and clinopyroxene. Orthopyroxene grains can occur as a range of grain sizes, but are typically equigranular in a specific rock type, displaying sub- to euhedral shapes. There are two main shapes in which orthopyroxene grains occur, either as rounded to sub-rounded grains (which is by the far the more common morphology), or as elongated, lath-shaped grains (Figure 4.2 B). The rounded edges present in a lot of cumulus orthopyroxene is indicative of thermal, mechanical or chemical erosion (Kinnaird et al., 2005).

In some pyroxenite, such as the olivine-rich variety in UMT 366 at 1585 m (Figure 3.1 D), there is almost a complete absence of plagioclase in the rock, although this is an exception and generally the majority of Platreef pyroxenite has some plagioclase present, with most having at least around 2% interstitial plagioclase. In these rocks, plagioclase appears as anhedral grains of varying size, and are always intercumulus. Olivine is generally smaller in grain size (< 4 mm) when present in pyroxenitic rocks as compared to olivine-dominant lithologies, such as those on Akanani. Olivine occurs mostly as rounded to semi-rounded grains in pyroxenite (Figure 3.1 D), and are frequently serpentinised.

Rocks that experienced significant alteration, such as the samples taken in ZF116 at 1586,2 m shown in Figure 4.2 B, generally have increased calcium content and thus, the plagioclase in these rocks become more calcic. In such cases either anorthite or labradorite is the dominant mineral. Polysynthetic twinning in intercumulus plagioclase within pyroxenite is widespread (Figure 4.2 A for example). Carlsbad twins are generally associated with K-feldspars, but there are a few occasions in this study where plagioclase feldspar displays this type of twinning. An example is shown in Figure 4.2 B, and it was confirmed through SEM analyses that the grains were in fact plagioclase.

Clinopyroxene is a common accessory mineral in most pyroxenite rocks, occurring as large (up to 1 cm) intercumulus grains. In UMT 366 a chromitiferous pyroxenite, occurring in the lower parts of the ‘UG2’ chromite zone, show large intercumulus clinopyroxene blebs that enclose earlier formed and smaller orthopyroxene grains (Figure 4.1 D). The presence of clinopyroxene could be correlated with the extent to which rocks had been altered as well, and generally where there is an increase in serpentinisation there would be an increase in the modal percentage of clinopyroxene.

In Figure 4.2 C, which is a highly serpentinised olivine-rich pyroxenite from UMT 366 at 1586.2 m, a groundmass of fine-grained serpentine is contrasted by unaltered, clearly intercumulus clinopyroxene grains. Although serpentinisation is mostly confined to olivine-dominant lithologies such as harzburgite, some pyroxenites experienced this alteration, especially olivine-bearing pyroxenite. In many cases, serpentinisation may be limited to olivine grains, while pyroxenes and feldspars are left unaltered. Figure 4.1 A depicts a ‘vein-like’ zone of serpentine that cross-cuts a

pyroxenite in UMT377 at 1033 m, with small grains of clinopyroxene present in the vein. It is difficult to determine what type of serpentine is present in most cases, but where the serpentine is coarse-grained it generally looks like chrysotile, with grains that are fibrous, elongated and parallel to the crystallographic axis (Figure 4.3.E).

Veinlets of serpentine is also common in the more harzburgitic rocks at the Zwartfontein site, although not limited to these lithologies. A strange observation is the occurrence of thin veins of serpentine that cross-cut the length of both a pyroxenite in UMT377 at 1033 m (Figure 4.1 A) and norite in UMT366 at 1561.4 m (Figure 4.2 A), without affecting the surrounding minerals in any way. The serpentine veins are not aligned to the orientation of other grains, and simply cross-cut other mineral grains. This is a common occurrence in the thin sections studied from Turfspruit.

4.1.2 Feldspathic Pyroxenite

Generally, this rock is very similar to the pyroxenites in the study areas, except for a higher interstitial modal plagioclase content. This informal term has been used by Bushveld Complex geologists to describe an orthopyroxenite with significant intercumulus plagioclase, and it is important to distinguish it from a norite. As mentioned in Chapter 3, the term carries economic significance as it is one of the most common PGE-bearing lithologies, and should, therefore, be classified appropriately. Compositionally, feldspathic pyroxenite has a higher feldspar content, commonly ranging between 10-20 %, but may reach up to 40% feldspar locally. Orthopyroxene occur as cumulus grains and constitute 70 – 90 % of the rock.

Pegmatoidal varieties of feldspathic pyroxenite were present on both Turfspruit and Zwartfontein and were spatially associated with xenoliths. On Turfspruit, extremely feldspar-rich (40%) pegmatoidal feldspathic pyroxenite occurs in UMT 335 at 1729 m, and is illustrated in Figure 3.4 D. Orthopyroxene grains reach up to 3 cm in size in this package, with euhedral to polygonal shapes, constituting from around 60 – 90% of the modal mineralogy. Interstitial minerals include clinopyroxene, biotite, quartz and sulphides. Sulphides are considerably larger in size within pegmatoidal rocks, and consisted mainly of chalcopyrite.

Zwartfontein has one isolated occurrence of pegmatoidal feldspathic pyroxenite in ZF116 situated in the hanging wall of the Lower chromitite zone. This rock is characterised by a high chromite content due to its proximity to the chromitiferous zone, as well as large (1 cm), elongated laths of clinopyroxene (Figure 4.4 D). Orthopyroxene grains has rounded edges and ranged between 2 mm to 4 mm in size, with around 20 % interstitial plagioclase, and large zones of disseminated chromite.

The feldspathic pyroxenite in UMT 335 at 1717 m has one distinctive petrographic aspect that involves plagioclase inclusions within orthopyroxene that display a very characteristic texture. The plagioclase inclusion has a tricuspidate shape, with concave-inward boundaries (Figure 4.2 C) that resemble interstitial plagioclase grains occurring in pyroxenite. When looking at some of the orthopyroxene grains that host the plagioclase inclusion, it appears that it may have consisted of several orthopyroxene grains with interstitial plagioclase, but now occur as a single grain.

4.1.3 Parapyroxenite

Parapyroxenite is petrographically characterised by a distinct metamorphic texture of interlocking mineral grains (For example in Figure 4.2 D) (Yudovskaya and Kinnaird, 2010). Parapyroxenite samples collected on Turfspruit, such as the package in the footwall of the UG2 in UMT 335 at 1720 m, were dominated by diopside and is illustrated in Figure 4.4 A. Compositionally the rock consists of about 70 % clinopyroxene, 10 % orthopyroxene, 10 % chromite and accessory biotite, sulphides and chromite. This rock appears to have experienced significant alteration as shown by the mineral assemblage and textures. Figure 4.4 B shows the presence of carbonate minerals, which was inherited from a dolomite xenolith (indicated by remnants of the original protolith in Figure 4.5), biotite, as well as secondary chromite grains that mantle orthopyroxene. In UMT 336, an extremely thick package of parapyroxenite occurs between 1355 m and 1245 m. These rocks are dominated by clinopyroxene, locally very rich in olivine, and in some cases, grossular garnet is also present (Figure 3.3 C). Unfortunately, no thin sections were made available for this hole.

On Zwartfontein, a lot of the rocks sampled are highly serpentinised, which makes it extremely difficult to distinguish between those that formed solely through magmatic processes and those that are metamorphic-dominated. Petrographically, the clinopyroxene grains encountered in parapyroxenite on Zwartfontein could be distinguished by having a quite different morphology than the isolated grains found in magmatic pyroxenite. They are typically much smaller in size, ranging from 0.1 to 4 mm in diameter, and their shapes range from rounded to completely anhedral (Figure 4.4 C).

The sulphide content in parapyroxenite varies greatly, but a consistent characteristic is that the sulphides occur as considerably larger grains than in most other rock types. On Zwartfontein the serpentinised lithologies generally has a higher sulphide percentage. Parapyroxenite typically has more chalcopyrite present, and less pentlandite and pyrrhotite. The parapyroxenite in ZF116 at 1520 m was typified by vein-like sulphide grains occurring within the boundaries of pyroxenite grains (Figure 4.6 B). In other cases, where rocks had experienced considerable alteration, such as in UMT 377 at 998 m, sulphides appears to have been replaced and display a remnant texture (Figure 4.4 E).

Although, for the most part, sulphides within parapyroxenite grains occur as large (> 0.5 cm), disseminated grains.

The degree of assimilation of xenolith rafts varies considerably on both properties, and in some cases the original material is completely obliterated, and the only evidence available that there was once a xenolith may be the presence of clinopyroxenes and alteration minerals. This is the case on Zwartfontein, where no original protoliths were encountered. In contrast, when there has been minimal assimilation, the original morphologies of the parental rocks, such as layering in dolomites (Figure 4.1), may still be present, as seen on Turfspruit in UMT 335 at 1720 m. In this rock, there is a complete mix of both original sedimentary material, as well as magmatic pyroxenes that are orientated parallel to the original layering (Figure 4.6), and these rocks have been termed as 'hybrids' (Nex et al., 2006).

In addition to dolomite, there is one extremely fine-grained hornfels xenolith that occurred in UMT 366 at 1595 m rock on Turfspruit (Figure 4.2 F). This xenolith also exhibited hybrid qualities in which there were both sedimentary, as well as magmatic properties. Looking at Figure 4.2 F there are centimetre-sized inclusions of what appears to have been a norite within a matrix of extremely fine-grained hornfels rock.



Figure 4. 5: Hybrid rock from UMT335 at 1720 that contains orthopyroxene grains orientated with the layering of the original dolomite protolith.

4.1.4 Harzburgite

Olivine-bearing lithologies is much more prevalent in the Zwartfontein hole, than at Turfspruit where they are restricted to the Lower Zone rocks, as well as two packages of metamorphic olivine-bearing rocks. As mentioned earlier, it is difficult to distinguish whether olivines are of a primary magmatic or metamorphic origin, and those olivine-dominant rocks that are clearly metamorphic has been given the informal term, 'paraharzburgite'.

The granular harzburgite in the Lower Zone rocks in UMT 366 on Turfspruit are quite rich in orthopyroxenes, between 40-70%, and is comparable to olivine orthopyroxenite (Figure 4.3 C). Olivine grains commonly display a 'broken' or cracked texture (Figure 4.3 A and B), which can be attributed to volume expansion of the grains due to water being absorbed into the rock during serpentinisation. In some cases, olivine is enclosed by orthopyroxene grains, in which case the volume expansion experienced during alteration would 'crack' the host pyroxenes as well. Olivine occurs as small (1-2 mm), isolated and rounded grains within granular harzburgite.

There is a close spatial relationship between zones of serpentinisation and the presence of dolomite and hornfels xenoliths on Turfspruit, such as in UMT335 at 1720 m, whereas on the Zwartfontein property the presence of serpentinisation appears to be present in the whole stratigraphy, with no obvious association to xenoliths. In UMT 377 at 922 m, a metamorphic olivine-bearing rock is logged as a paraharzburgite. The xenolith responsible for the alteration is assumed to be above the extent of the core logged, as indicated by a parapyroxenite at the top of the hole. This paraharzburgite shows recrystallisation textures, such as granoblastic textures in places, and is composed of several small polygonal grains of olivine, and lesser pyroxene and plagioclase (Figure 4.2 D). This rock experienced limited serpentinisation (<10 %).

The degree of serpentinisation is far more extensive on the Zwartfontein property, and in ZF116 at 1570 m, where alteration is very extensive, almost none of the original primary magmatic minerals are recognisable in section. Some of the minerals that occur within these serpentinised assemblages include talc, calcite, tremolite, chlorite, biotite and magnetite. Sulphides are commonly replaced by magnetite and display so-called relict structures (as shown in the parapyroxenite in Figure 4.4 E). In cases where alteration was not as extensive on Zwartfontein the rocks typically contain large orthopyroxene oikocrysts of up to 6 mm in size, occurring in a groundmass of serpentine with relict, at times unaltered, rounded olivine grains.

4.2 Petrography of Chromitiferous horizons

Introduction

Chromite-rich zones were sampled from the three boreholes on Turfspruit and one on Zwartfontein, which is described in the previous chapter. Stratigraphically, the areas in which these zones occur could not be correlated laterally across the different borehole intersections. During this section, an attempt will be made to determine whether certain textures of chromite can be related to certain settings in which the chromite occurs in.

The factors that control the shape of crystals that grow from a melt are rather complex. Crystal growth has been described in terms of three processes, which include transport, capillarity and interface kinetics (Sekerka, 1993). One of the most important processes that control the size and shape of chromian spinel is the very high distribution coefficient of Cr between chromian spinel and the melt. Three main morphologies could be identified in the chromite layers, namely coalescent, sub-coalescent (both disseminated) and annealed, which is also termed massive chromite (Figure 4.6 B). The difference between coalescent and sub-coalescent chromite grains is the amount of pore space between grains, where sub-coalescent grains have slightly more pore space than the former. There is also a difference in the shape of grains and in general the bigger the pore space between grains the more rounded they are, and the more coalesced the more angular the grains are. The rounded nature associated with the grains that have larger pore space could be due to chemical and mechanical erosion in these grains.

Coalescent chromites commonly form chain-textured chromite grains, that may either form along the boundaries of silicates (Figure 4.6 A), or cross-cut them with no preferred orientation (Figure 4.6 C). Zones of annealed chromite grains, also called massive chromite (Figures 4.6 B and D), are rather common in the study area and is thought to represent recrystallisation of these grains. While disseminated grains are most likely a product of in situ crystallisation, and are supposed to equilibrate with other cumulus minerals, massive chromite might be in disequilibrium with the surrounding grains (Cameron, 1975). However, it has been shown by Hulbert and von Gruenewaldt (1985) that interaction with interstitial fluids can result in significant chemical changes of disseminated chromite compared to those in a massive layer.

The occurrence of massive chromite grains has been a problem highlighted by many authors in the past. Densely packed massive chromite grains is mostly restricted to pyroxenite in the study areas, while massive chromite in harzburgitic rocks are less common, and where present, occur as isolated disseminated grains or stringers. A common observation made in massive chromite zones hosted by pyroxenite is the presence of very large (up to 1,5 cm) cumulus orthopyroxene oikocrysts,

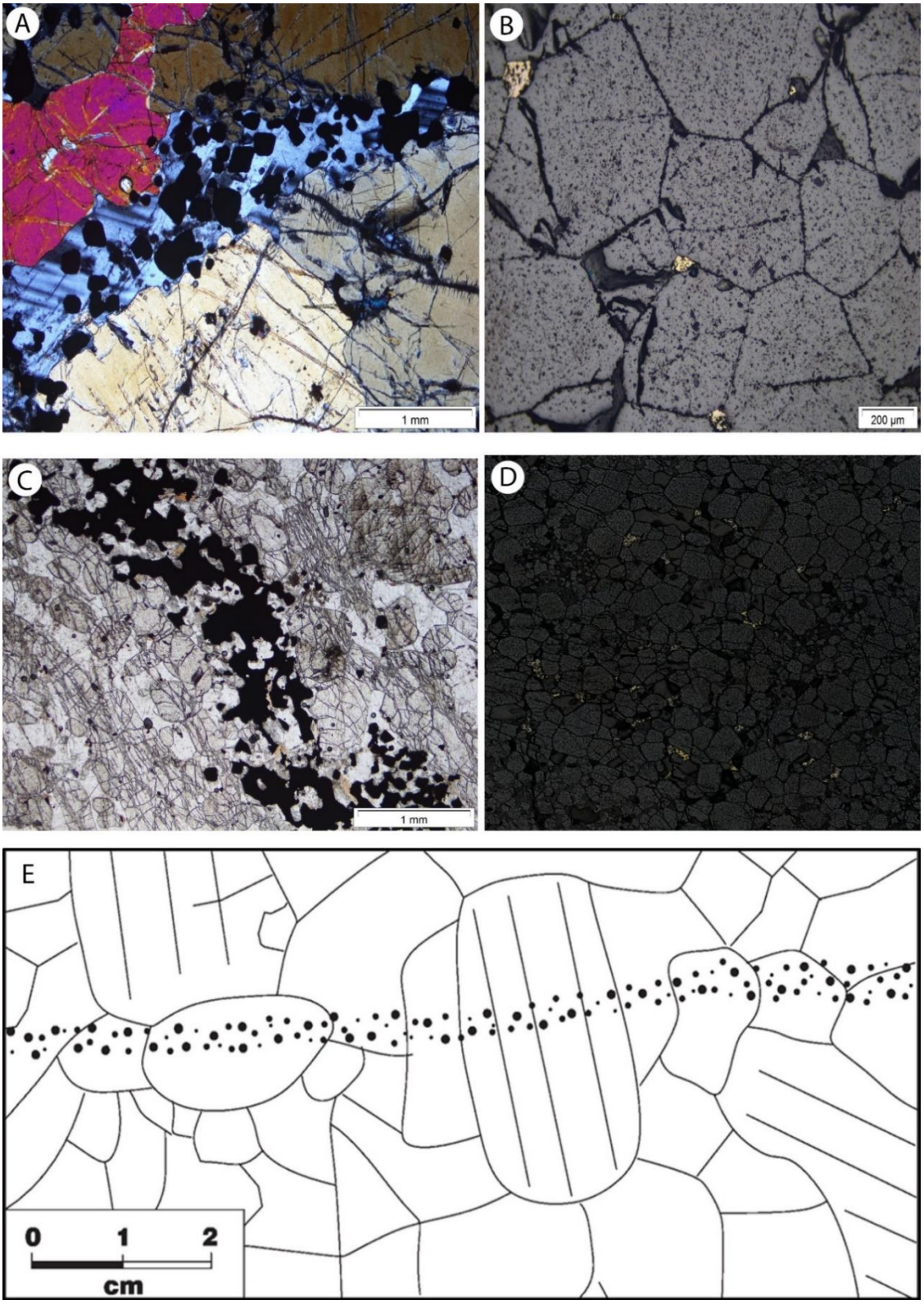


Figure 4. 6: Photomicrographs of different chromite morphologies. (A) Chain-textured chromites occurring within plagioclase, within the boundaries of pyroxenes. UMT366 at 1579.3 m. (CPL). (B) Annealed massive chromite grains showing 120° triple junctions where grains meet. These triple junctions are indicative of the sintering process in chromites. UMT 366 at 1584 m. (Reflected light) (C) Chain-textured chromite cross-cutting all minerals. UMT 377 at 1035 m. (PPL) (D) Massive chromites with small interstitial sulphides. Massive chromites show considerably larger grain sizes than those that are disseminated, due to the annealing and sintering of grains. ZF116 at 1538 m. (Reflected light) (E) A chain-textured chromite stringer cross-cutting silicate minerals (Modified from Cawthorn and Boerst, 2006; Reproduction of a diagram from Wagner, 1929).

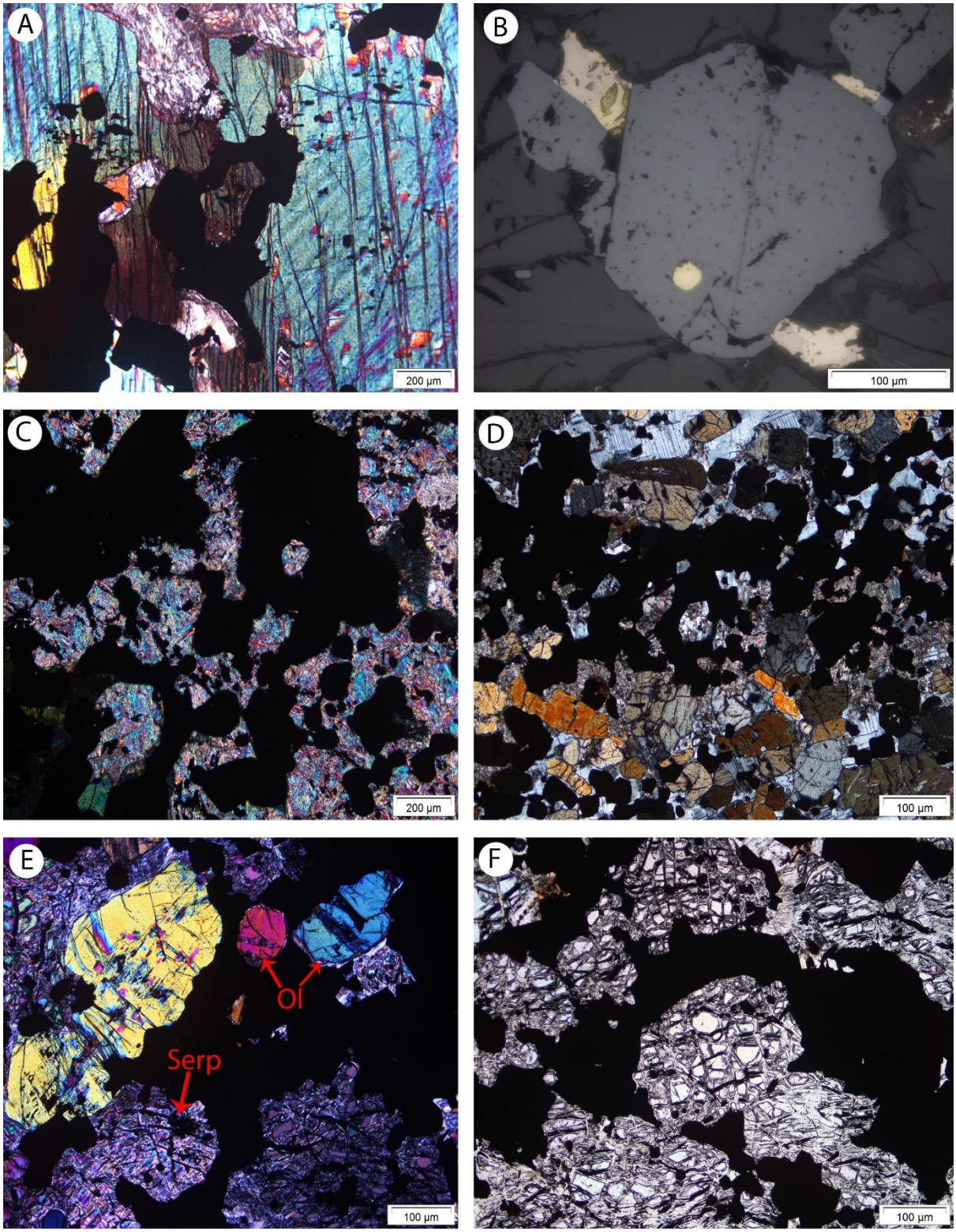


Figure 4. 7: Photomicrographs of atoll-type and chain-textured chromites. (A) Atoll-type chromite with orthopyroxene inclusion, which is optically continuous with opx outside the chromite grain. UMT 366 at 1595 m. (CPL) (B) Atoll-type chromite with chalcopyrite inclusion. ZF116 at 1538 m. (Reflected light) (C) Atoll- and mantle- type chromite within a highly serpentinised area. UMT 366 at 1561 m. (CPL) (D) Chain-textured and atoll-type chromites. UMT 377 at 984.1 m. (CPL) (E) Atoll and mantle-type chromites, showing olivine inclusions. (CPL) (F) Highly serpentinised olivine grain that is mantled by chromite. ZF116 at 1538 m. (PPL)

around which chromites have crystallised (Figure 4.1 E). Most of the zones where chromite grains have been annealed occurred as a localised patch within disseminated grains. There is a question whether this occurs due to postcumulus recrystallisation, or postcumulus enlargement of chromite grains.

4.2.1 Atoll-type chromites

A variety of minerals can be enclosed by atoll-like chromites (Figure 4.7 A to F), most commonly it is plagioclase, followed by sulphides such as pyrrhotite and chalcopyrite, olivines and in rare cases there may be platinum group minerals present in the inclusion, although in this study PGE's mostly occurred on the edges of chromite grains (Chapter 5). In some instances, especially where olivine grains are present, chromite only partially encloses mineral grains, and this is termed a mantle-chromite (Figure 4.7 E & F). Atoll- and mantle-type chromites are absent in larger chromitiferous zones, and were restricted to areas of disseminated chromite or small Cr stringers.

The inclusions within and mantled by chromite grains are optically continuous, which proves that these silicate spheres are due to postcumulus growth processes. Most of the inclusions usually consist of intercumulus minerals, such as plagioclase, clinopyroxene and sulphides, and only very rarely, such as in small chromite stringers in UMT 366 at 1595 m do cumulus minerals such as orthopyroxene occur as an inclusion (Figure 4.7 A). Such chromite stringers occur within magmatic rocks and are extremely fine-grained (<500 μm).

Chromites occurring within the olivine-bearing rocks of the Zwartfontein property, commonly had chromites mantling olivine grains. Figure 4.7 F shows an extremely serpentinised olivine grain from ZF116 at 1538 m, mantled by chromite. Figure 4.7 E (from the UG2-like chromite in UMT 366) shows an extremely serpentinised lithology mantled by chromite, while fresh and unaltered orthopyroxene grains occur as atolls.

4.2.2 Chain-textured

Chain-textured chromite grains, that commonly contain inclusions as well, occur either as cross-cutting stringers (Figure 4.6 C) or along the boundaries of cumulus silicates (Figure 4.6 A) on Turfspruit. This chromite morphology was absent from the chromitiferous samples collected on the Zwartfontein property. Chain-textured chromites occur in most of the chrome-rich zones on Turfspruit. For example, the hanging wall of the UG2-like chromite in UMT 366 has several chain-textured chromites occurring along the boundaries of cumulus pyroxenes. There appears to be two stages of chromite growth in this rock, as there is cumulus disseminated chromite grains within the same rock that occur within cumulus pyroxene.

A common feature among these chromite zones is the development of serpentinisation that is restricted to the chromite zone and does not affect the surrounding silicate rocks. In the upper parts of UMT 366, at 1561 m, an atoll-type, chain-textured chromite is hosted by a melanorite. When the rock was logged there were no signs of alteration, only a thin chromite stringer. In Figure 4.7 C, this rock is shown with the presence of alteration evident in the partings between chromite grains, which probably formed due to postcumulus reactions. It was unusual, in that the alteration was restricted to the chromite zone, while the rest of the rock remained unaltered.

4.3 Petrography of sulphide minerals

Introduction

In comparison to the Critical Zone of the main Bushveld Complex, the Platreef contains a considerably greater modal percentage of sulphides (Sharman-Harris et al., 2005), and sulphide mineralisation is generally greater, PGE mineralogy is more complex and grades are generally lower and more variable (Armitage et al., 2002; Hutchinson and Kinnaird, 2005). The main base metal sulphides identified in the area, in order of abundance, are pyrrhotite, pentlandite, chalcopyrite with lesser amounts of pyrite, galena, sphalerite, millerite, chalcocite and other base metal sulphides (Armitage et al., 2002). The sulphide mineralisation is believed to be largely of magmatic origin, with contamination of country rocks considered to be an ore-modifying process, which could have also lead to an increase in sulphur content of the magma through assimilation of local S-containing country rocks such as the Transvaal shales and anhydrites (Holwell et al., 2007). The chemical character of the sulphides in the area, as well as the sources of sulphur are described in chapter 5.

Hutchinson and Kinnaird (2005) identified four principal sulphide associations. (1) Early magmatic sulphides, which are typified by angular grains of pyrrhotite with flames and rims of pentlandite and lesser chalcopyrite (Figure 4.6 E). (2) Late magmatic sulphides associated with interstitial felsic assemblages, which mainly consist of chalcopyrite and pentlandite, with lesser pyrrhotite, is usually associated with interstitial assemblages of plagioclase and quartz-feldspar symplectites. Sulphides may occur along the contact between rounded, corroded and embayed silicates. These sulphides associated with more felsic assemblages are generally more complex than those associated with primarily magmatic processes. (3) Late magmatic sulphides associated with granite dykes and their accompanying quartz-feldspathic veins. This subdivision will not be discussed, as granite veins were not sampled in the study area. (4) Sulphides within secondary silicate assemblages.

Study areas

Stratigraphically, base metal sulphides are distributed heterogeneously on the Turfspruit property, with higher contents typically associated with more pyroxenitic units, and lesser sulphides

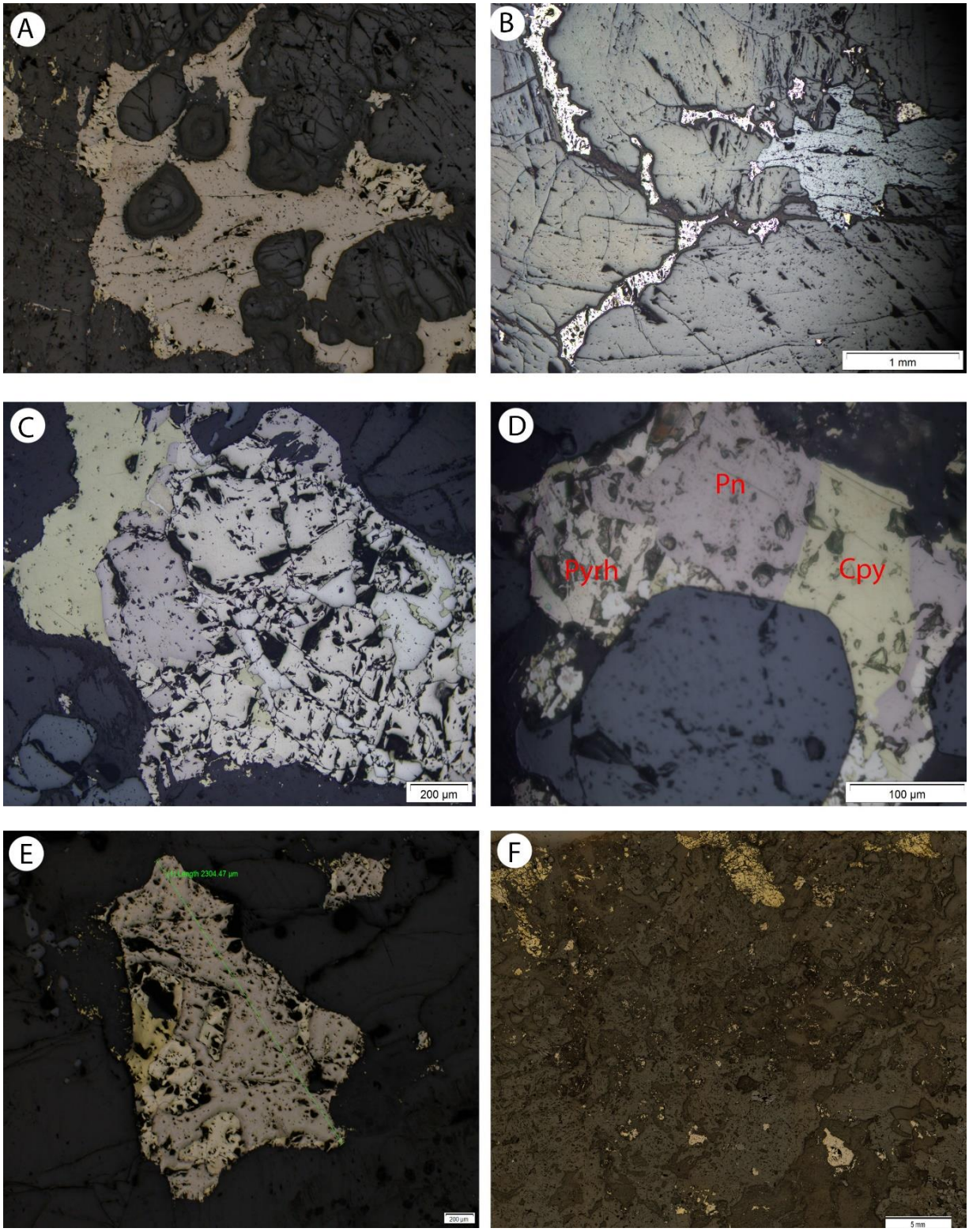


Figure 4. 8: Different morphologies and compositions of sulphide minerals in various rock types, taken under reflected light. (A) Intercumulus sulphide grains that mantle rounded pyroxenes in UMT366 at 1595.5 m. (B) Intercumulus sulphides occurring within the boundaries of pyroxenes. ZF116 at 1520 m. (C) Complex sulphide from UMT 366 at 1586 m, consisting out of a core of pyrrhotite, pentlandite exsolution, and rimmed by chalcopyrite. ZF 116 at 1537.15 m. (D) Multiphase sulphide grain that mantles a chromite grain. (Pyrh=Pyrrhotite; Pn=Pentlandite; Cpy=Chalcopyrite). ZF116 at 1537.15 m. (E) Angular grain of pyrrhotite with very little chalcopyrite and flames of pentlandite. Early magmatic sulphide as explained by Kinnaird (2005). ZF116 at 1538.3 m. (F) Isolated, large, disseminated sulphides (predominantly chalcopyrite) in a parapyroxenite in ZF116 at 1520 m.

occurring within more felsic units such as the norites. They are most commonly disseminated as polyphase, interstitial blebs, although there are at times zones of massive sulphide or net-textured ore.

Sulphides that display primary textures rarely consist of a single mineral phase, and in most instances, the grains contain a core of pyrrhotite, with chalcopyrite and pentlandite around the edges of the grain. In the Lower Chromite Zone on Zwartfontein sulphides commonly display this typical mineral assemblage (Figure 4.7 C). Pentlandite and pyrrhotite will typically be situated more towards the centre of a sulphide bleb, while chalcopyrite flanks the edges

In other instances, such as in UMT 366 at 1586 m, pentlandite occurs as exsolution flames within pyrrhotite (Figure 4.6 D & E). This can be explained in terms of the crystallisation sequence that takes place, as pyrrhotite and part of pentlandite crystallise from a monosulphide solid solution, which is the first in the crystallisation sequence from a sulphide liquid, with the residual liquid forming an intermediate solid solution, which on cooling forms chalcopyrite and some pentlandite (responsible for the exsolution flames) (Barnes et al., 2006).

There are several morphologies and textures in which sulphide minerals occur. In UMT 366, at 1595.5 m, a chromite stringer cross cuts a sulphide-rich pyroxenite, where interstitial sulphides occur mantling the chromite grains (Figure 4.7 A). Intercumulus blebs of sulphide are probably the most common morphology displayed on Turfspruit, and sometimes mantle other cumulus minerals such as pyroxene. On Zwartfontein, however, interstitial sulphides display a more vein-like morphology, occurring between the boundaries of cumulus mineral grains.

Many of the sulphides appear relatively fresh, even in rocks that have undergone extreme alteration. For example, some parapyroxenites (ZF116 at 1520 m) that are dominated by diopside and contain a considerable amount of metamorphic, and highly serpentinised olivine, contain unaltered interstitial base metal sulphide grains (Figure 4.6 F), with some PGE's locally as will be seen in Chapter 5. Sulphides in these rock types are considerably smaller, and monomineralic as opposed to the multiple sulphide phases encountered in unaltered host rocks, and consists out of a lot more pyrite. Other sulphides associated with alteration include secondary copper minerals such as bornite, covellite and chalcocite.

4.4 Discussion

Interpretations of detailed petrographic descriptions will be aided by comparing the results to previously published work on both the study areas, as well as work done elsewhere in the Bushveld Complex. Discussions are categorised in the same order as the rock types described and is followed by a section on the petrographic similarities and differences between the study areas and the Main Bushveld Complex.

4.4.1 Pyroxenite

The elongated, lath-shaped orthopyroxene grains present in the lower parts of the Platreef on Turfspruit are typical of Lower Critical- and Lower Zone pyroxenites (Kinnaird et al., 2005), but were especially prominent in more plagioclase-rich rocks such as feldspathic pyroxenites and norites in this study. Most of the pyroxenites that contained lath-shaped orthopyroxene grains had some moderately developed foliation, that was defined by the sub-parallel alignment of the elongated grains (Figure 4.2 B). Mondal and Mathez (2007) explains that elongated orthopyroxene grains with a defined orientation could have grown by coalescence of equant grains during a near-solidus shearing event. The area is known to have a number of large structures that run parallel to the Thabazimbi-Murchison lineament.

As is the case in most Bushveld rocks, evidence for recrystallisation of pyroxenes grains is rather common in the study areas. Orthopyroxene grains commonly engulf small plagioclase grains, which is shown in Figure 4.1 C, and orthopyroxene and chromite grains commonly meet at an angle of 120° (Figure 4.6.B). Recrystallisation textures such as these have been attributed to post-accumulation enlargement (For example: Cawthorn and Boerst, 2006).

Clinopyroxene grains occur as a number of different morphologies in the study area, which is usually determined by the rock type within which it occurs. Pyroxenites typically have large, poikilitic clinopyroxenes that may form rounded to semi-rounded oikocrysts of up to a centimetre in diameter, enclosing older phases (Figure 4.1 D). Eales et al. (1990) describe a similar occurrence and behaviour of clinopyroxene within the footwall of the UG1 chromitite in the western limb of the Bushveld Complex. Clinopyroxene grains may also mantle other orthopyroxenes, or plagioclase grains, appearing almost as a corona texture. In a lot of serpentinised rocks, the only recognisable minerals may be clinopyroxenes, as they formed considerably later, probably through late-stage fluid ingress.

An unusual occurrence in many pyroxenites on Turfspruit was the presence of cross-cutting serpentine veins that did not influence surrounding minerals in any way (Figure 4.1 A and Figure 4.2 A). This may provide some insight into the nature of how these fluids entered these rocks. One

would expect that the serpentinisation of a certain lithological horizon would be laterally extensive, and the contacts with the surrounding rocks would be more gradational unless there is an impermeable layer that is restricting the flow. Although looking at these two examples, the contacts are sharp, with no presence of impermeable layers such as chromitite. One way to explain this could be that these fluids flowed vertically as shoots or 'chimneys', and could possibly have been facilitated by structures, although this theory would obviously require some further study. Another possibility is that the hydration of surrounding rocks could be localised if the lenses of country rock (responsible for the hydration) were small.

4.4.2 Feldspathic Pyroxenite

Feldspathic pyroxenite is a term that is unique to the Bushveld complex due to its association with higher PGE grades, especially at the base of the Merensky Reef in the main Bushveld Complex. Most of the textures described for the Merensky Reef pegmatoidal pyroxenite (Cawthorn and Boerst, 2006; Viljoen, 1999), are present in similar rocks in the study area. The modal percentages and textures described for both pyroxenite and pegmatoidal pyroxenite in the Merensky, correlate with those on Turfspruit, containing large orthopyroxene oikocrysts, with accessory olivine and clinopyroxene.

Cawthorn and Boerst (2006) attribute the origin of the pegmatoidal feldspathic pyroxenite in the Merensky Reef to the addition of a superheated liquid. One distinctive petrographic aspect, which was crucial to their model, involved plagioclase inclusions within orthopyroxene that displayed a very characteristic texture. The plagioclase inclusion has a tricuspidate shape, with concave-inward boundaries (Figure 4.2 C) that resemble interstitial plagioclase grains occurring in pyroxenite. When looking at some of the orthopyroxene grains that host the plagioclase inclusions it appears that it may have consisted out of a number of orthopyroxene grains with interstitial plagioclase, but now occur as a single grain. Cawthorn and Boerst (2006) have attributed this, along with chain-textured chromitite, to have grown by reaction between primary orthopyroxene grains and a superheated liquid.

4.4.3 Parapyroxenite

Economic sulphide mineralisation in parapyroxenite was one of the lines of evidence that were used by Harris and Chaumba (2001) to show how the Platreef was affected by fluid-rock interaction to a much greater extent than is generally the case in the rest of the Bushveld, especially in the Merensky Reef. Parapyroxenite occur in all the holes studied on both Turfspruit and Zwartfontein, and has a spatial association with xenoliths. There are often disseminated, as well as small 1-2 cm seams of chromitite that occur within these rocks and according to Yudovskaya and Kinnaird (2010), these are

mostly Cr-spinels, instead of true chromitite, which will be investigated in Chapter 5. The presence of norite patches within a hornfels xenolith demonstrates how the Platreef magma had to intrude into what was an already existing Transvaal hornfels rocks.

Harzburgite

Harzburgitic rocks are common in the Lower Zone on Turfspruit, as well as within the Platreef on Zwartfontein. Apart from the extensive serpentinisation, the granular harzburgite on Zwartfontein closely resembles the primary layers of feldspathic harzburgite from the Pseudo Reef unit in the north-western Bushveld Complex, described by Scoon and de Klerk (1987). They describe an unusual abundance of olivine cumulates in the cyclic units between the UG1 chromitite and the Bastard Reef, which they attributed to new influxes of magma. The new influxes intruding the chamber at the level of the UG2 and Merensky Reefs did not intrude as a buoyant plume, but rather as a flow along the crystal-liquid interface. The abundance of ultramafic cumulates is believed to be a product of fractional crystallisation of a distinctly stratified layer of new magma.

The presence of olivine cumulates at Akanani as a dominant phase is in conflict with the generic model of the Bushveld stratigraphy. If one were to compare, as many previous authors have done, the mineralised zones of the Platreef with the Merensky Reef, then olivine should be present as a mere accessory mineral. The Upper Critical Zone is typified by large amounts of cumulus orthopyroxene and plagioclase, Cameron (1982) calculated a 47.1 modal % orthopyroxene and 45.1 modal % plagioclase for the Upper Critical Zone of the eastern limb. Although looking at the stratigraphy of ZF116 in Figure 3.9, it is shown that the Main Mineralised Zone (MMZ) is hosted by serpentinised harzburgite. This must surely indicate that the north-western area described by Scoon and de Klerk (1987) must have been replenished by new influxes of relatively primitive magma to explain the increased cumulus olivine content.

Scoon and de Klerk (1987) gave some detailed petrographic descriptions of the olivine-bearing rocks of the Amandelbult and Union Section mines of the Rustenburg platinum mines. As mentioned in Chapter 3, Jackson (1961) made an important distinction between poikilitic and granular harzburgites whilst working on the Stillwater Complex, which is based on textural relationships between olivine and orthopyroxene. Poikilitic harzburgites, described in Figure 3.2 A and Figures 4.4 A and B, is present in the upper Pseudoreefs in the western limb and is characterised by coarse to medium-grained feldspathic harzburgite, containing 60-70% cumulus olivine, intercumulus orthopyroxene (10-30 modal %) and intercumulus plagioclase (10-15 modal %), as well as accessory chromian-spinel. Harzburgite with more than 60 % olivine is absent from the study area, and it is

possible that the primary growth of olivine was halted through reaction replacement (by orthopyroxene) and by crystallisation of plagioclase in the interstitial sites.

Granular harzburgite is characterised by lesser olivine and more orthopyroxene and is texturally comparable to olivine orthopyroxenite. They are identified in the UG2 hanging wall, the Pseudo marker and the Merensky Reef on Amandelbult and the Union Section in the western limb. Scoon and de Klerk (1987) describe the UG2 hanging wall as a pegmatoidal, feldspathic, granular harzburgite that contains cumulus olivine (35-45 modal %), cumulus and intercumulus orthopyroxene (30-40 modal %), intercumulus plagioclase (10-20 modal %) and cumulus chromite. This is comparable to the harzburgite in this study as similar rock types occur on Turfspruit in hole UMT366, at 1585 m (Figure 3.3 A and Figure 4.3 A and B).

The rocks described in the hanging and footwall of the 'UG2' in UMT366 show many similarities to those in the north-western limb, except for significant serpentinisation in UMT366. It must be noted that the presence of olivine-dominant rocks in the Critical Zone of the Bushveld intrusion is limited, and those described in the north-western parts is anomalous. Although, that does not mean olivine is completely absent, as it is a fairly common accessory mineral in the Merensky Reef, and Cawthorn and Boerst (2006) describe Merensky Reef rocks at the Impala Platinum mine containing up to 10 modal % olivine. They describe how the pegmatitic pyroxenite units of the Merensky contain higher olivine content than that of the normal pyroxenites, and attributed this to higher degrees of melting which could have resulted in the formation of olivine through incongruent melting of the orthopyroxene. There is no obvious link between grain sizes of pyroxenite and the abundance of olivine on Turfspruit or Zwartfontein, rather with the presence of serpentinised rocks.

All the comparisons and contrasts mentioned above highlights the fact that petrographic similarities between the study area and parts of the main Bushveld Complex do not necessarily indicate the correlation. If one were to compare ultramafic rocks from other layered intrusions around the world, such as the Stillwater Complex or Skaergaard intrusion, there would be some petrographic similarities with that of the Bushveld Complex. Therefore, elaborate conclusions should not be drawn from something as widely distributed as petrographic features.

Chromite

Atoll- and mantle-type chromite growth, along with spherical grains mentioned in the sub-coalescent morphologies, suggest two generations of chromite growth (Hulbert and von Gruenewaldt, 1985). Perfect spheres of plagioclase that occur as inclusions in some chromite have also been observed by Hulbert and von Gruenewaldt (1985) in the UG2-like chromitite south of Mokopane in the Grasvally area.

Inclusions that occur within and are mantled by chromite are optically continuous (Figure 4.7), which indicates that these silicate spheres formed though postcumulus growth processes. However, Roeder et al. (2001), describes with the aid of experimental analysis that the rounded shape of chromite grains, as well as atoll-like morphologies, is a primary growth feature and not the result of recrystallisation or postcumulus growth. He explains that these inclusion-rich chromite grains are a product of fast skeletal growth and preferential development of edges and apices.

Inclusions within chromite grains have been described by other authors, and these atoll-like grains are not restricted to the northern limb. Kruparz and van Rensburg (1965) described inclusion-rich chromite deposits at Nietverdiend, in the Marico district (far western limb), that contain drop-like silicate intrusions of around 20 µm in size. McDonald (1965) described chromites on the Ruighoek farm, also in the western limb, that contained rounded silicate inclusions of 0.05 to 0.2 mm. Similar to the observations made in this study, the inclusions contained mostly intercumulus mineral grains. Minerals such as biotite and clinopyroxene are almost always interstitial in the lower part of the Critical Zone, and therefore it is thought that these inclusions had formed as part of a postcumulus enlargement of chromite. Jackson (1966) studied inclusion-rich chromite in the Stillwater Complex, as well as those from the Ruighoek farm, and believed them to represent overgrowth features. The theory implied that postcumulus enlargement occurred either at the surface of the crystal mush, or very close to the surface, while the chromite was still in contact with a magma saturated with respect to crystallising chromite.

Chain-textured

Chromian spinel most commonly forms 5-20 µm octahedra, along with the occasional chain of where the individual grains are attached to each other at the corners (Roeder et al., 2001). Wagner (1929) noted similar chain-like chromite stringers in a pegmatitic pyroxenite of the Merensky Reef in the eastern limb of the Bushveld Complex, shown in Figure 4.6 E. It depicts a very thin layer of chromite grains that cross-cut several atypically large orthopyroxene grains. He suggested that these stringers formed through chromite grains that remained suspended in the melt at a certain level and the orthopyroxene crystallised around them. However, this is rather unlikely as it would require all the orthopyroxene grains to subsequently sink as a single sheet, so as to preserve the continuity of the chromite stringer. The large size of the pyroxenes, as well as their density, makes this process very improbable. Instead, Cawthorn and Boerst (2006) suggested that there were probably two discrete layers of normal-sized pyroxene grains that formed with an intervening chromite layer. Orthopyroxene grains then went through a process of *in situ* enlargement and engulfed the chromite grains in their original stratigraphic position. They, therefore, suggest that this texture is a result of

postcumulus textural growth and are not primary igneous textures. Hulbert and von Gruenewaldt (1985) also attribute chain-like chromite to postcumulus growth processes This contrasts with Roeder et al. (2001) experimental data that showed these textures to be of a primary origin.

Postcumulus enlargement of chromite grains has been proposed as a solution to the problem of how a chromite cumulate with a high porosity (30 to 40%; Cameron and Desborough, 1969) can become densified to massive chromite layers such as the UG2, which contain less than 15% intercumulus silicates. A variety of solutions have been proposed, such as partial re-melting of cumulus chromite (Cameron and Emerson, 1959); chromite-rich liquids (McDonald, 1967); increase in the volume of chromite by postcumulus reaction of chromite with plagioclase and liquid to form Al-rich chromite, all of these have been refuted for various reasons. In situ growth of cumulus chromite, proposed by Hulbert and von Gruenewaldt (1985), is also unlikely due to the very low concentration of chromium in the interstitial liquid. A very simple approach by Spry (1969), involves enlargement of grains through annealing or sintering. This implies that fine-grained aggregates under strain anneal to become a coarse-grained aggregate with unstrained grains. Growth is driven by lattice strain energy and grain boundary energy, which leads to coarse polygonal boundaries that are fairly straight and form 120° triple junctions, as seen in Figure 4.6 B.

Sintering is a term used in the metallurgical and ceramics industry and is a process of compacting solid material through heat, without melting it. The presence of an interstitial fluid will improve the process, as it enhances the rearrangement of particles to get the most effective packing order. Cawthorn et al. (1983) refers to liquid sintering process for the enlargement of magnetite grains in the Upper Zone of the Bushveld Complex. The most common shape of sintered grains is angular grains that have triple junctions of 120°, with straight crystal faces (Figure 4.6 B). This is the reason why massive chromitite, such as in Figure 4.6 D, have considerably larger grains than disseminated chromites in silicate-rich areas. Atoll-like and mantle chromite are considered by Hulbert and von Gruenewaldt (1985) to be postcumulus textures associated with the sintering process.

It is important to note that just because the chromite from the study areas share a lot of similarities, in terms of its morphologies and textures, with that of the main Bushveld Complex, it does not necessarily mean that they are analogues to one another. For instance, in a study by Proenza et al. (2008), where they describe textures of chromite and platinum-group minerals in the chromitites from the western ophiolitic belt from the Pampean Ranges of Cordoba, Argentina, several similarities exist even though it is not even a layered mafic intrusion. They describe similar replacement textures and atoll-type chromites encountered in the study areas, as well as the exsolution of an Fe-rich Cr-spinel within a chromite grain. Therefore, based on the fact that certain

textures and morphologies are present in both the northern limb, as well as the main Bushveld Complex, does not at all mean that the two are analogues to each other.

Sulphides

The most common morphology of sulphides within both study areas were intercumulus blebs, that occurs in between cumulus silicate or chromite. Holwell and McDonald (2008) have interpreted these intercumulus sulphides as a product of the percolation of a sulphide liquid through a network of intergranular pore space. Their study involved sulphides that occurred within footwall gneisses further north on the Overysel property, and they attributed the liquid phases to be a result of partial melting of the gneiss. In the case of Turfspruit and Zwartfontein, it may be a result of partial melting of some of the numerous calc-silicate and hornfels xenoliths in the area.

Most sulphide grains encountered in the study are not monomineralic, and consist of at least two different mineral types. Most of these grains consist of pyrrhotite and are flanked by pentlandite and chalcopyrite. The reason for chalcopyrite occurring at the flanks of the sulphide grains is explained by Kinnaird and Nex (2015) as follows: As the monosulphide solution (mss) exsolved pyrrhotite and pentlandite as intergrown phases and flame exsolutions of pentlandite within pyrrhotite, the concentration in the mss increased and eventually chalcopyrite crystallised at the margins of the earlier formed sulphides. Holwell et al. (2007) explains that even though all these sulphides are in fact low-temperature phases, it is the most primary of the assemblages in that they are left unaltered and a direct cooling product of a fractionating sulphide liquid from the original Platreef magma

On Zwartfontein it is common for there to be a positive correlation with the amount of sulphides and the degree of serpentinisation. The ‘Main Mineralised Reef’ on Akanani consist of a highly serpentinised harzburgite, with sulphide content above 8%. According to Hutchinson and McDonald (2008), there is frequently an association overlooked between the degree of alteration, the density of secondary silicates such as tremolite or symplectitic quartz, and the size and distribution of the sulphide minerals

Comparison between the Main Bushveld Complex and the study areas

Petrographic similarities between the study areas and the Main Complex

In broad terms, the modal mineralogy of the study areas can be likened to that of the Critical Zone, with all the rock types, apart from the metamorphic rocks in the Platreef, containing ortho- and clinopyroxene, plagioclase and olivine, in differing proportions. A typical Platreef pyroxenite can be compared to that of a pyroxenite occurring within the Critical Zone of the Main Complex, consisting

predominantly of cumulus orthopyroxene, interstitial plagioclase, along with accessory clinopyroxene, spinels and biotite. Comparing the results of a study by Mondal and Mathez (2007) on the UG2 and Merensky reef in the eastern limb, there appears to be correlating features in hole UMT377 regarding the difference in the footwall and hanging wall pyroxenites of the so-called UG2 layer. If one were to assume that the chromite layer on Turfspruit is in fact analogous to the UG2, it may still be considered a very localised opinion and pigeonholing of the data.

An unusual abundance of olivine cumulates, comparable to those in the Akanani core, is found in the north-western Bushveld in the cyclic units between the UG1 chromitite and the Bastard Reef. Although this is a localised occurrence, there is a similarity nevertheless.

Even though the chromite in the study areas are not nearly as well developed as those in the Main complex, there existed several textural and morphological similarities between them. Chain-textured chromite stringers that cross cut silicates, as shown in Figure 4.6 C, occur in the Merensky, Grasvally and the Platreef. Wagner (1929) first noticed this in a pegmatitic pyroxenite of the Merensky Reef in the eastern limb, while Cawthorn and Boerst (2006) mention a number of localities where this can be seen in the western limb. They attributed it to form because of postcumulus textural growth and not a primary igneous texture. Another example is the presence of atoll-like chromite that occur in the Grasvally area (Hulbert and von Gruenewaldt, 1985), Marico district in the western limb (Kruparz and van Rensburg, 1965), and in the Merensky Reef and UG2 of the eastern limb. It is still uncertain whether inclusion-rich chromite grains formed as a primary growth feature or as a result of recrystallisation, but it is fairly common in most mafic layered intrusions around the globe. The similarities described appear to involve very localised processes, which can occur within any system that contains the same mineralogy. It is also important to note that most of these similarities, involved processes and mechanisms that took place postcumulus, such as recrystallisation and alteration by late-stage fluids.

Petrographic differences between the study areas and the Main Complex

The core studied on Zwartfontein and Turfspruit is lithologically much more heterogeneous, not as well-layered and much more contaminated than that of the main Bushveld Complex. Pyroxenite in the study areas show great variability in terms of grain sizes, textures and modal mineralogy, with no obvious cyclicity that one might expect in the main Bushveld Complex. Lath-shaped orthopyroxene crystals is very common throughout the stratigraphic succession, especially on Turfspruit, whereas in the rest of the Bushveld it is more commonly found in the Lower Zone. Clinopyroxene grains occur as an accessory phase within pyroxenite, but as the dominant mineral in parapyroxenite, which is

unique to the Platreef. Country rock xenoliths, along with the associated 'metamorphic' or parapyroxenite, is absent in the main Bushveld Complex for the most part.

The degree of serpentinisation in pyroxenite was quite variable, ranging from such intense alteration that recognition of individual mineral grains was almost impossible, to unaltered, primary magmatic pyroxenite. The Zwartfontein core is extremely serpentinised due to the high modal % of olivine in the rocks, which is not common in the Main Complex. The presence of olivine cumulates at Akanani as a dominant phase, conflicts with the generic model of the Bushveld stratigraphy. If one were to compare, as many previous authors have done, the mineralised zones of the Platreef with the Merensky Reef, then olivine should be present as a mere accessory mineral. The upper Critical Zone is typified by large amounts of cumulus orthopyroxene and plagioclase, Cameron (1982) calculated a 47.1 modal % orthopyroxene and 45.1 modal% plagioclase for the Upper Critical Zone of the eastern limb. Although looking at the stratigraphy of ZF116 in Figure 3.8, it is shown that the Main Mineralised Zone (MMZ) is hosted by serpentinised harzburgites.

Massive chromite is limited to small patches rarely exceeding 4-5cm, dissimilar to the UG2, and most chromite in the Platreef occurred as rounded to sub-rounded disseminated grains. The chromite present in the Merensky reef is consistently the earliest phase to crystallise, forming layers and inclusions in the pyroxenes (McDonald et al. 2005), while a considerable amount of chromite grains in the Platreef formed at a later stage, such as those found associated with metamorphism.

In comparison to the Critical Zone rocks of the main Bushveld Complex, the study areas contain a considerably greater modal percentage of sulphides, and base metal sulphide mineralisation is more abundant. The source is thought to be mainly magmatic, while a significant amount of sulphur may have been added through assimilation of pyrite-bearing shales and anhydrite (Holwell et al., 2007). Base metal sulphides are not restricted to magmatic lithologies, and a significant amount occur within xenoliths, as well as the associated parapyroxenite. Economic sulphide mineralisation in parapyroxenite was one of the lines of evidence that were used by Harris and Chaumba (2001) to show how the Platreef was affected by fluid-rock interaction to a much greater extent than is generally the case in the rest of the Bushveld, especially in the Merensky Reef.

Chapter 5

Chemistry

Introduction

Spinels have been used as 'petrogenetic indicators' since the term was introduced by Irvine (1965), and this application stems from the fact that these minerals crystallise from a wide range of conditions, and in the case of chromites, are usually the first to crystallise. In addition, they are refractory and relatively resistant to alteration in comparison to other high temperature phases (Barnes and Roeder, 2001).

Techniques

A FEI Quanta 200 Scanning electron microscope (SEM) coupled to an Oxford Instruments INCA energy dispersive X-ray analysis system was used, mainly as a qualitative technique to analyse both mineral chemistry, morphologies and textures. The advantages of using the SEM includes the high spatial resolution that cannot be obtained by a normal petrographic microscope, as well as a large depth of field. The electron dispersive spectrometer (EDS) provided mineral chemistry results through a 'point and shoot' option, and was used to distinguish between various spinel endmembers, sulphides, silicates and PGE minerals. Whole-rock geochemical data for hole UMT-336, and mineral chemistry for ZF-48 and ZF-116 was provided by Dr Marina Yudovskaya, while assay results for UMT -366, 377 and 335 was supplied by Ivanplats.

5.1 Mineral Chemistry

Electron microprobe analysis (EMPA) on chromite and olivine from hole ZF116 and ZF48 was provided by Dr Marina Yudovskaya. In some cases, where the EDS data from the SEM was accurate enough to be used as quantitative data, it was included in the table, which was important to include some mineral chemistry on Turfspruit rocks. Chemical data from a few different sources on the Main complex of the Bushveld was used to provide some comparative insights.

5.1.1 Chromite

A total of 64 chromite grains were analysed for all the major elements on holes ZF48 and ZF116. On hole ZF116, 27 samples were analysed, while on ZF48, 36 samples were analysed. The exact positions of the chromites analysed on Zwartfontein is shown in Table 1 in the appendix. Chromite compositions for the rest of the Bushveld Complex was sourced from several authors, which included UG2 grains from the Rustenburg section (Opoubou-Lando, 2010), UG1 and UG2 data from the Union section (Eales

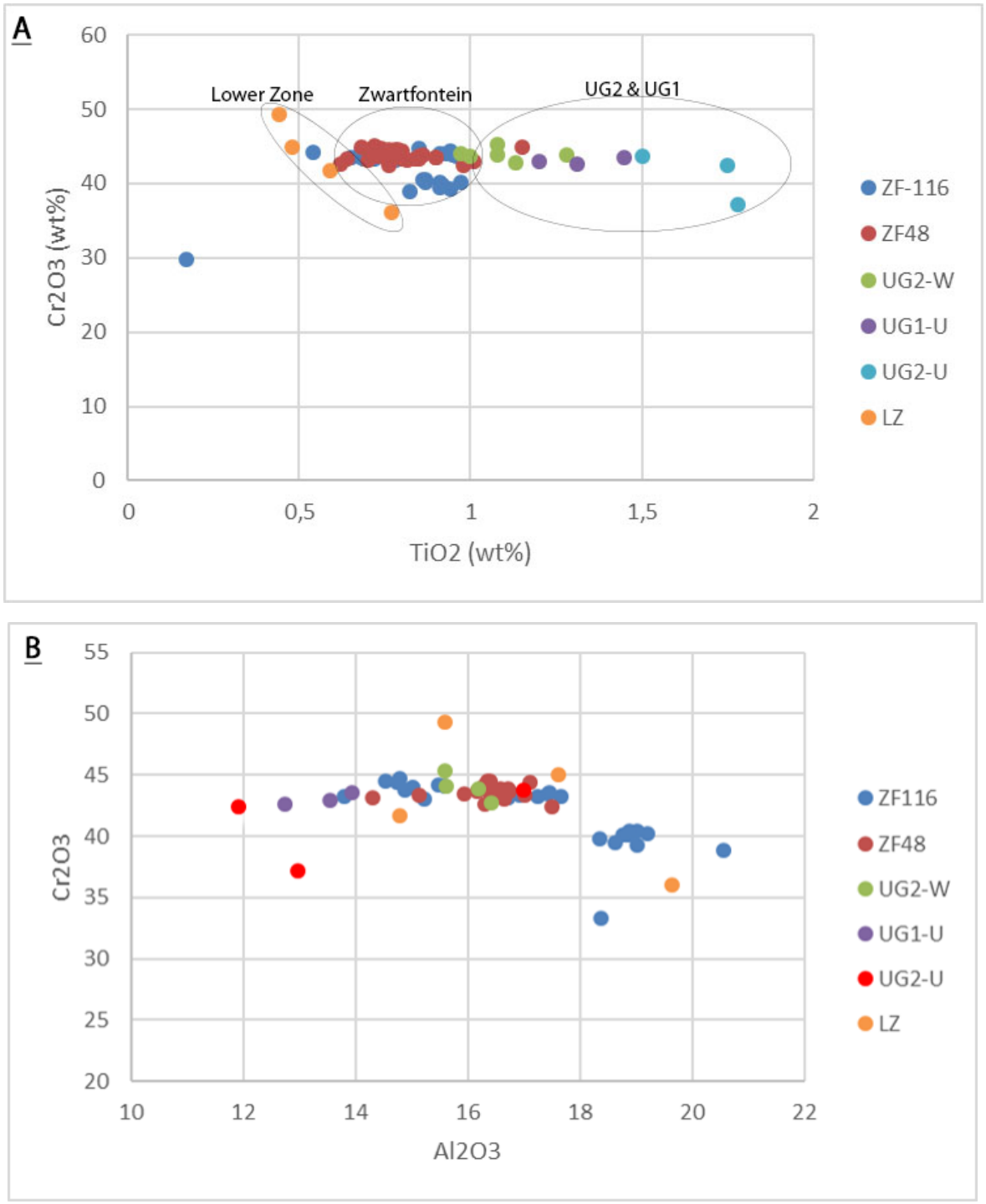


Figure 5. 1: Binary diagram of Cr vs Ti and Cr vs Al for different parts of the Bushveld Complex, including ZF (Zwartfontein), UG2-W (Waterval mine), UG1-U and UG2-U (Union section) and LZ (Lower Zone of the eastern limb). Chemical data and references are shown in Table 1 and 2 in the appendix.

and Reynolds, 1986), as well as disseminated chromite grains of the Lower Zone in the eastern limb, analysed by Cameron (1978). Chemical data for chromite from the western and eastern limbs can be found in Table 3, included in the appendix.

Figure 5.1 A shows the Cr vs Ti percentage of the grains analysed on Zwartfontein compared to data on chromite grains from elsewhere in the Bushveld Complex. The data from Zwartfontein is very well

grouped, with ZF48 having an average of 43.81 % Cr and 0.89 % for Ti, while ZF116 had a slightly lower Cr % of 41.82 % and a slightly higher Ti % of 0.9%. The position, as well as the composition of the Zwartfontein chromites that were analysed can be found in Table 1 in the appendix, and refer to Figure 3.9 to see the stratigraphic context of the samples.

To generate a valid comparison with the chromite from the main Bushveld Complex, the chromites chosen from Zwartfontein were all present in magmatic rock types, and as indicated by their chemistry, none formed as a product of contact metamorphism. Chromite that forms through metamorphic processes contains considerably more Fe, less Cr and higher Al values, and will be discussed separately. The Cr values of all the samples plotted are very similar, while Ti values varied between samples. Chromite grains from the UG1 and UG2 from the western Bushveld Complex show higher Ti values, while Lower Zone chromites have slightly lower Ti values than those on Zwartfontein.

The trace amounts of Ti within the chromite can be attributed to ilmenite, which is the main Ti-bearing mineral in the Bushveld Complex. Cameron (1979) describes that there is a stable association between that of ilmenite in the Critical Zone and the Platreef, although ilmenite is rare in Platreef chromites compared to Merensky chromitites (Legg, 1969). In the Bushveld Complex the chromitites progressively increase in V and Ti content upwards, which is attributed to increasing fractionation of the magma responsible for them (For example, Reynolds, 1985; Naldrett et al., 2012). Unfortunately, there were not a large enough interval of chromite minerals sampled in the stratigraphy to provide a large-scale trend of Ti values (Table 1 in appendix).

Interestingly, the chromitites of the Lower Zone, analysed by Cameron (1979), correlated more with those of Zwartfontein than that of either the UG1 or UG2. Therefore, it is probable the chromitites of the study areas crystallised from a magma(s) which has not undergone the amount of fractionation as that of the Main Complex magmas.

Small chromite stringers, as well as disseminated chromite grains are common in metamorphic parapyroxenites. Chemically, they are distinctive from those chromites found in magmatic rock types, and are more appropriately termed as Ti-Fe-Cr spinels. One such chromite from Zwartfontein was analysed by EMPA, and include sample ZF116-1225-19 (Table 1), which represents a high-Al Fe-Ti-Cr spinel. The single sample collected in hole TMT870 on Turfspruit also contains a high-Al Cr spinel, which is strange as there are no signs of metamorphism in the rock. The chemistry for the Cr spinel in TMT870 is shown in Table 3 in the appendix. Yudovskaya and Kinnaird (2010) highlighted two types of Fe-Ti-Cr spinels, namely a (1) low-Al type (4,9 - 7,5 wt% Al_2O_3), and a (2) high-Al type (8.8 – 19.3 wt% Al_2O_3).

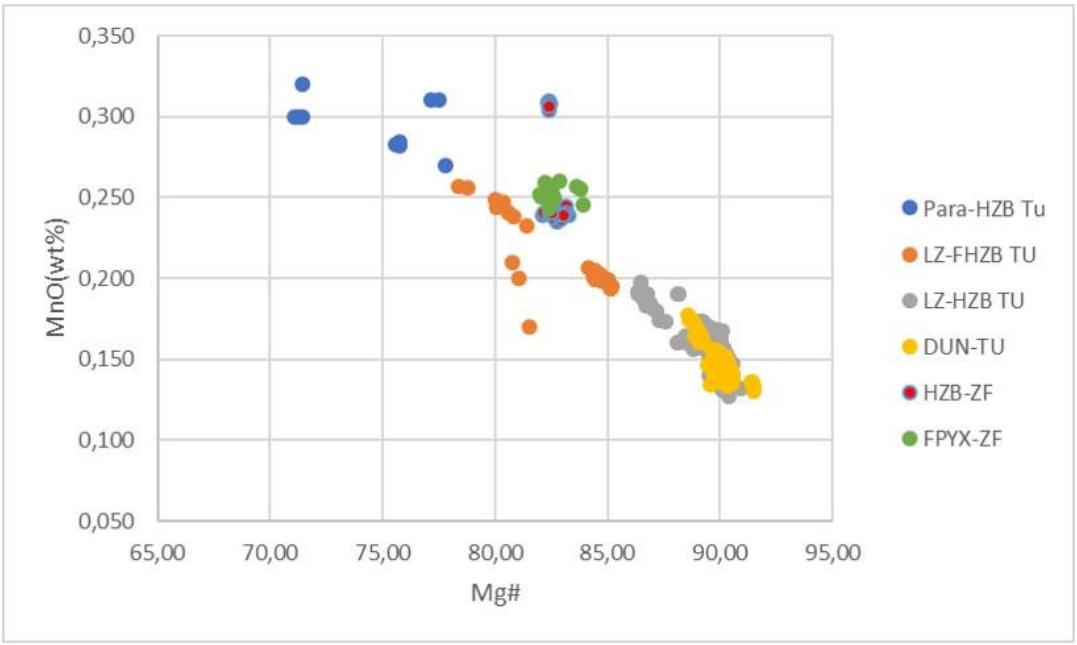
There is one low-Al type Cr spinel analysed in a parapyroxenites on Turfspruit, at 998 m in UMT377 (Table 3, Appendix). It is characterised by a very high Fe content (49.35 %), increased Ti (3.42 %), while it has considerably lower Cr (34.69 %) and Al (6.54 %) values. This decrease in Al values is probably an indication of postcumulus reequilibration of chromite grains. The increase in Fe content could possibly be explained by the presence of metamorphic magnetite rims found on chromite grains in many metamorphosed ultramafic rocks (for example: Onyeagocha, 1974; Barnes, 2000), although no magnetite was encountered during SEM studies. Both magnetite and chromite is likely to lose Al content, relative to Cr, during metamorphism and reaction with silicates and metamorphic fluids. The low-Al chromites that formed through metamorphism are often referred to as 'ferritchromite' (Barnes and Roeder, 2001).

The high-Al Fe-Ti-Cr spinels are more common on Zwartfontein, and these are characterised chemically by higher Cr content, and lower Ti. Most of the electron probe analyses on Zwartfontein show chromites with higher Al weight percentages when compared to those from elsewhere in the Bushveld Complex (Figure 5.1.B), with some grains showing Al values of up to 27 wt%. There is a marked difference in the extent of postcumulus equilibration on either massive or disseminated chromite grains. Disseminated grains experience considerably greater changes in their chemistry, and this is probably due to a greater surface area that is exposed to postcumulus fluids.

5.1.2 Olivine Chemistry

Limited analyses of olivine grains were available for this study, and therefore most of the data was provided by Dr Marina Yudovskaya who did EMPA work on both Turfspruit and Zwartfontein, while other data was sourced from research on the Union section (Scoon and de Klerk, 1987), Merensky Reef in the Rustenburg area (Naldret et al., 2009) and the Lower Zone in the eastern limb (Cameron, 1977). On Turfspruit, olivine grains were restricted to Lower Zone rocks or associated with serpentinised lithologies, such as paraharzburgites, while on Zwartfontein it was much more abundant due to the presence of harzburgitic rocks.

Looking at the data from Turfspruit (Table 2) and Zwartfontein (Table 4), the Mg# of chromite generally ranges between 71 for paraharzburgites and up to 91 for dunites. It has been shown that olivine composition does not have a defined trend over stratigraphic height, but is related to the host rock within which it occurs, which is illustrated in Figure 5.2. Yudovskaya and Kinnaird (2010) showed that olivine grains within metamorphic rocks in the Platreef, such as calc-silicates, have lower Mg# at Mg_{73}, while magmatic hosts may contain olivine grains with a Mg# of up to Mg_{83}.



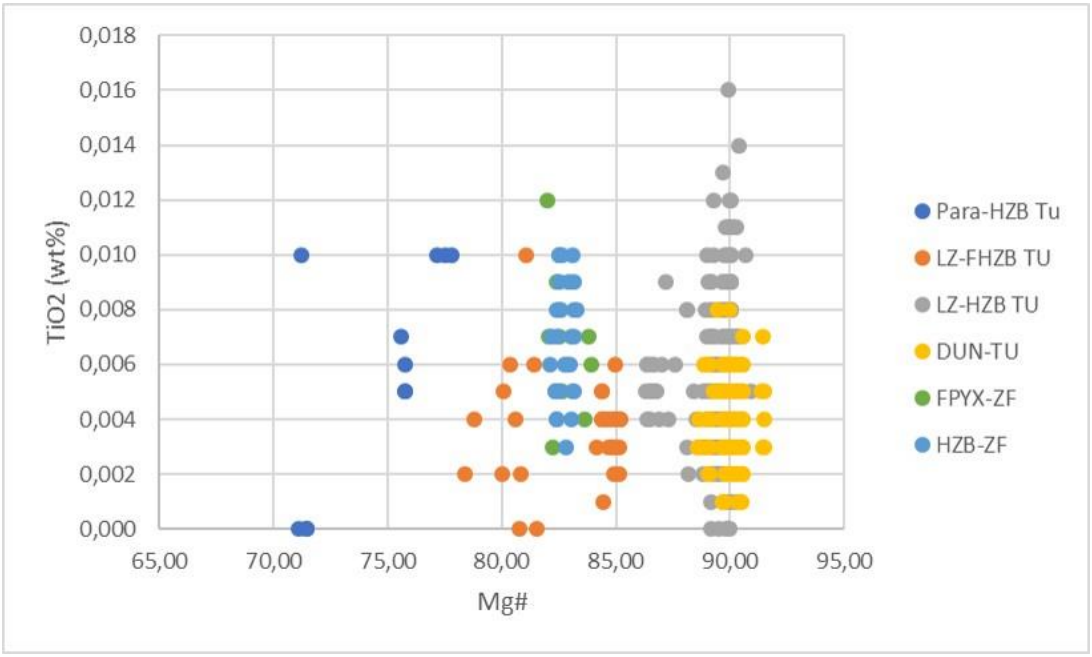


Figure 5. 2: Binary diagrams of both Ti and Mn vs Mg# for different lithologies in the study area. The abbreviations in the legend are as follows: TU (Turfspruit), ZF (Zwartfontein), Para-HZB (Paraharzburgite), LZ-FHZB (Lower Zone feldspathic harzburgite), DUN (Dunite), FPYX (Feldspathic pyroxenite), HZB (Harzburgite). Chemical data is shown in Table 2 and Table 4.

The Mn and Ti content of olivine is a measure of the degree of fractionation which the melt experienced, and it is clearly seen that Lower Zone harzburgite and dunite contain considerably less Mn, while paraharzburgite on Turfspruit consists of high Mn values (Figure 5.3). It is interesting to note that the olivine occurring in harzburgite within the Platreef on Zwartfontein, share the same composition as Lower Zone feldspathic harzburgites on Turfspruit, indicating a much lower degree of fractionation that took place on Zwartfontein.

Data on olivine from the Merensky Reef, Pseudo Reef, UG2 hanging- and footwall, as well as the Lower Zone of the eastern limb (Jagdlust), were all included in the comparative study. Figure 5.3 shows various elements plotted against the Mg#, and a number of trends can be observed. One of the most well-defined relationships is that an increase in Mg leads to a decrease in Mn. This is to be expected, as hotter and more primitive melts have not undergone significant fractional crystallisation. Olivine from both Turfspruit and Zwartfontein were predominantly Mg-rich, with Fe-rich varieties occurring within metamorphic lithologies, such as paraharzburgites, as well as feldspathic pyroxenites.

The Ni content of olivines are generally higher than that of orthopyroxene cumulates. Analyses of olivine from the Lower Zone rocks on Turfspruit shows poor Ni values in comparison to the Lower Zone of the eastern Bushveld at Jagdlust. The Ni content in olivine grains is controlled by both fractionated melt composition and partitioning into any coexisting sulphide melt.

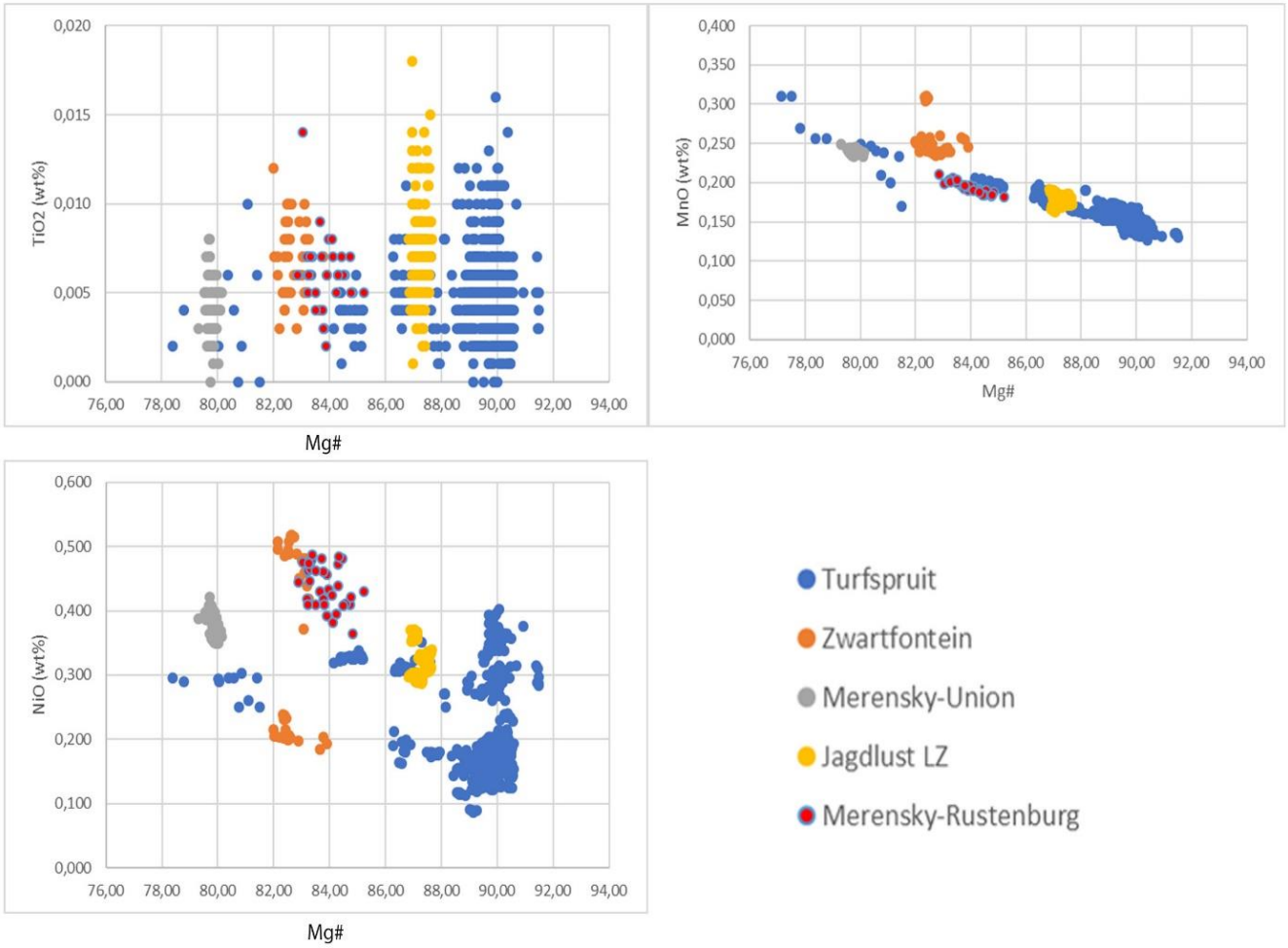


Figure 5. 3: Binary diagrams of Ni, Ti and Mn vs Mg# of different areas around the Bushveld Complex.

A similar Mg# vs Mn trend is seen in both Figure 5.3 and 5.2, even though a different classification scheme was used. Lower Zone olivine analysed on the Turfspruit property shows more primitive compositions as compared to that of eastern limb Lower Zone, while the Merensky in the Rustenburg section is less fractionated than that of the Union section. An exception to the trend were the Zwartfontein samples, which had more primitive Mg#, but lacked the expected Mn values.

5.2 Mineralisation

Introduction

The areas under investigation on Turfspruit do not form part of the economically PGE mineralised zones, although some PGM and Au grains were encountered, albeit sporadically, while the two holes on Zwartfontein were slightly more enriched in PGE's, as it occurred on the edge of the so-called Main Mineralised Zone (MMZ) of the Akanani site. Kinnaird and MacDonald (2005) define the Platreef as 'Mafic units enriched in Ni-Cu-PGE that occur between the Archaean granite basement or the Transvaal Supergroup and the gabbronorites of the Main Zone, north of the Planknek Fault'. Therefore, the mineralisation consists of a combination of platinum group elements and base metals, which are not always related. PGE mineralisation is typically associated with base metal sulphides and chromite grains when it occurs within fresh, unaltered rocks, specifically with pentlandite (Figure 5.3 A and D). In rocks that have undergone significant fluid-rock interaction, leading to serpentinisation, the PGE grains and base metal sulphides are commonly decoupled and PGE grains are present within secondary mineral assemblages. Mineralisation may also extend to some considerable depths into the footwall of the Platreef, such as at Sandsloot, where significant grades are still found within the dolomitic footwall (for example Armitage et al., 2002). Generally, the mineralised sections of the Platreef have lower grades than that of the Merensky Reef, or UG2, although the thickness of the economic portion of the Platreef is considerably thicker than both these ore horizons. According to Grobler (2017, personal communication) the upper part of the Turfspruit Cyclic unit has shown to contain high Merensky-like grades associated with Cr stringers.

One of the possible reasons that very few PGE grains were encountered during this study, may be a result of preferentially sampling chromite-rich rocks, as it is one of the focal points. Unlike the Merensky Reef and the UG2, mineralisation in the Platreef is not necessarily associated with chromitite seams or stringers. In some of the mineralised sections of the Platreef, chromite stringers may be associated with exceptional PGE grade, although high-grade zones occur without any associated chromite. In the case of hole UMT336 on Turfspruit, there is almost no correlation between chromite content and PGE grades whatsoever (Figure 5.5). This is, however, a very localised

opinion, as Ivanplats has found significant correlation across the property (Grobler 2017, personal communication.

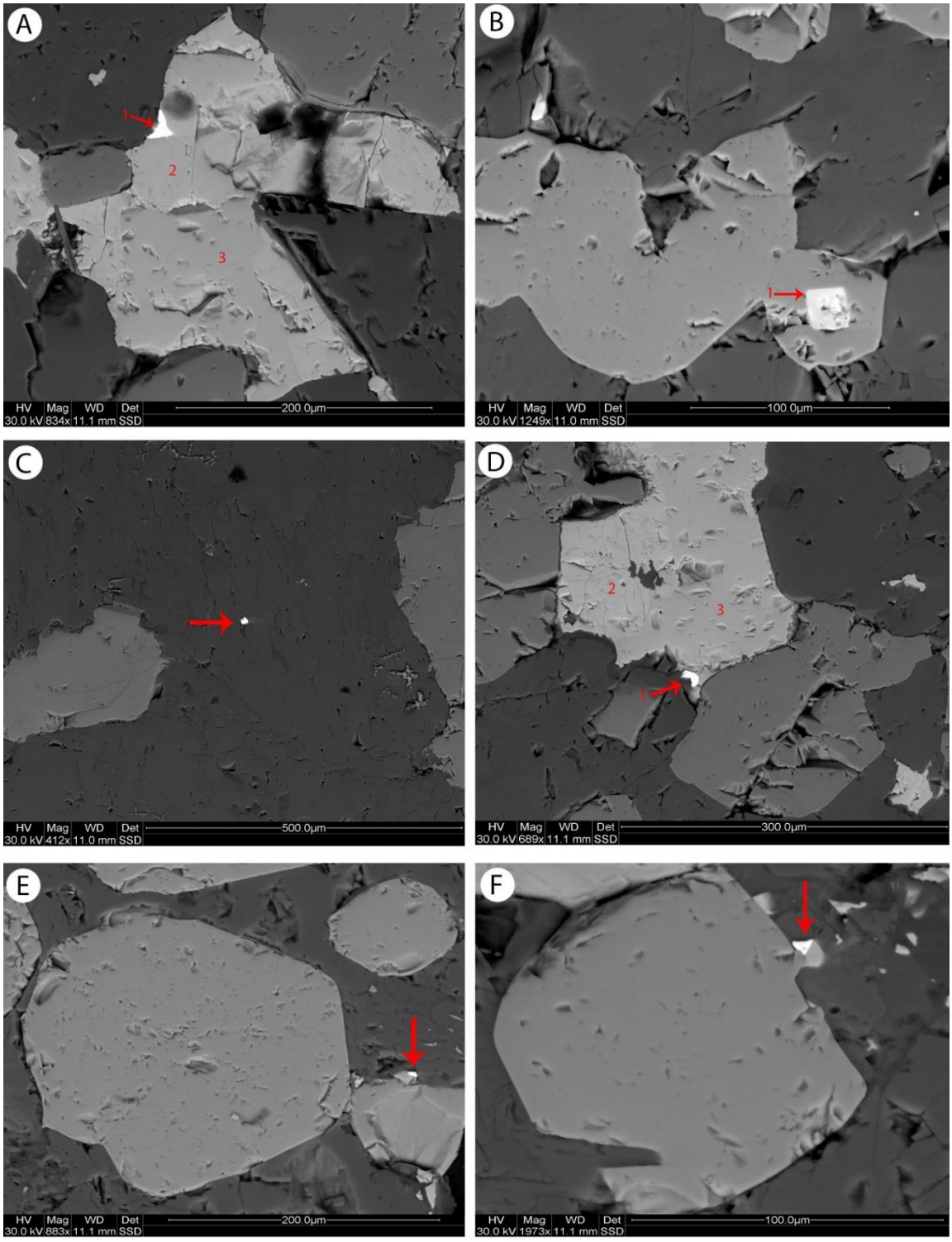


Figure 5. 4: Back-scattered electron images of the positions and morphologies of base metal sulphides and Platinum group minerals. Table 5.1 on the next page lists the chemical composition of the points shown on the figures above. (A) A multiphase sulphide consisting of pentlandite and pyrite, with a grain of Pd-sulphide on the edge. (TMT 870). (B) Cubic chalcopyrite grain. (C) Extremely small grain of a gold-mercury alloy. (D) Pd-dominated bismuthotelluride, occurring on the flanks of pentlandite and an arsenic-sulphide. (E) Small grain of Pd-Pt sulphide. (F) A strange Pt-sulphide mineral, with high amounts of Cu, Rh and Fe.

Table 5.1: Mineral chemistry of different grains shown in figure.

	Ore Mineralogy												
	S	Fe	Ni	Cu	As	Se	Rh	Pd	Te	Pt	Au	Hg	Bi	Total
A1	13,61	1,36	1,25			3,5	1,43	81,46						102,61
A2	35,4	29,8	32,87											98,07
A3	39,85	53,87						1,31						95,03
B	35,4	32,4	13,7	15,5										97
C											60,23	37,84		98,07
D1					2,37			23,66	25,58	2,18			46,1	99,89
D2	34,82	28,65	32,48											95,95
D3	40,23				54,73									94,96
E	18,98							16,54		62,45				97,97
F	28,73	3,55		10,2			8,58			34,82				85,88

Study areas

Although mineral chemical analyses done by the EDS is not very accurate, it was useful as a qualitative measure to identify the ore mineralogy. Figure 5.4 shows electron images of various PGE minerals, with the associated mineral chemistry listed in Table 5.1 According to Yudovskaya et al. (2011), the composition of the platinum group minerals encountered is largely dependent on the footwall composition, as well as the magmatic rock lithologies. The grains encountered in the study area were restricted to hole ZF116, ZF48 as well as TMT870, which is a metallurgical test hole consisting of significantly more platinum than any of the other holes investigated. Most of the grains in TMT870 occur on the edges of sulphides, especially pentlandite, and chromite, and have very small grains sizes, typically >5 µm (Figure 5.4 D). Compositionally, all the platinum minerals found on Turfspruit, which were restricted to one sample in hole TMT870, consist of palladium-dominated Pd-Pt-bismuthotellurides (Table 5.1). On Zwartfontein, hole ZF48 contains both Pt-Pd sulphides (Figure 5.4 E), as well as increased concentrations of Rh. The mineral identified in D1 may be michenerite $(Pd,Pt)(Te,Bi)_2$, situated on the edge of pyrite, which is rare, as these grains are more commonly found on the edge of either pentlandite or pyrrhotite. A grain of gold-mercury alloy was also found associated with PGE's, but not in the same manner, as it occurred within interstitial material (Figure 5.4 C1). The mineralised section in hole TMT870 is characterised by a greater variety of other sulphide minerals, particularly galena.

The increase in Rh content in PGE grains, as seen in Zwartfontein (Figure 5.4 F), is a good indicator of the type of mineralisation which has occurred. Early magmatic crystallisation is associated with higher Rh-Ir-Ru PGM and associated with harzburgite and chromite, while the typical pyroxenite-hosted PGE mineralisation exsolved from a PGE-rich sulphide liquid. According to Yudovskaya et al. (2011), the PGE characteristics of the mineralised harzburgite is more comparable to those of the Lower chromitite than that of the mineralised pyroxenite, and show an enrichment in Rh, with a Pt/Rh value of less than 10.

The widespread prevalence of platinum minerals is one of the distinguishing features of the Platreef, along with the lack of Pt-Pd sulphides and Pt alloys, which are both the dominant platinum phases in the Merensky Reef and UG2. Although there was a lack of PGM-sulphides in the holes studied, Ivanplats have shown significant Pt-sulphides near the upper contact of the "Merensky mineralised horizon" on Turfspruit. Bismuthotellurides crystallised under lower temperatures, and according to findings by Armitage et al. (2002), is associated with oxides, which is not the case in this study as most of these grains occur on the rims of sulphides. Although, the number of PGE's encountered during this study was far too little to be statistically representative of the study area, and therefore data from other authors were relied on to accommodate conclusions.

5.3 Geochemistry of hole UMT366

Introduction

Assay data on the economic elements of interest, which included Ni, Cu, Pt, Pd, Au, Cr, Rh, and S, were provided for hole UMT336, which is correlated with the stratigraphic succession (Figure 5.5). The major element chemistry of the Platreef lithologies can be modelled as a function of the proportions of the most common minerals that the rock contains, namely orthopyroxene, clinopyroxene, plagioclase and lesser olivine and chromite (Harris and Chaumba, 2001). The presence of hybrid lithologies (those that contain both magmatic and sedimentary features) tend to change the composition of geochemical plots to more Al and Ca-rich, and Mg-poor. The igneous Platreef is characterised by elevated values of Cr, Co and Fe (Harris and Chaumba, 2001), and this may serve as a useful geochemical indicator as to whether rocks are magmatic, hybrid or country rocks, in cases where it is not immediately clear from the modal mineralogy (McDonald and Holwell, 2011). For example, there is an abrupt drop in Cr values over calc-silicate rocks, slight increase over hybrid rocks such as parapyroxenites, and generally higher Cr values associated with magmatic lithologies (Figure 5.5).

The Platreef package has been interpreted to consist of a series of sills, based on geochemical studies of major element ratios, PGE ratios and changes in trace element abundances (Kinnaird, 2005; Manyeruke et al., 2005). Each package, or sill, is separated by differences in Mg#, SiO_2/Al_2O_2, CaO/Al_2O_3, K_20/TiO_2, and Sr/Al_2O_3, trace element abundances and Pt:Pd, and Ni:Cu ratios. Although this study has far too little data to support this theory, there are clear packages that can be identified in the assay data.

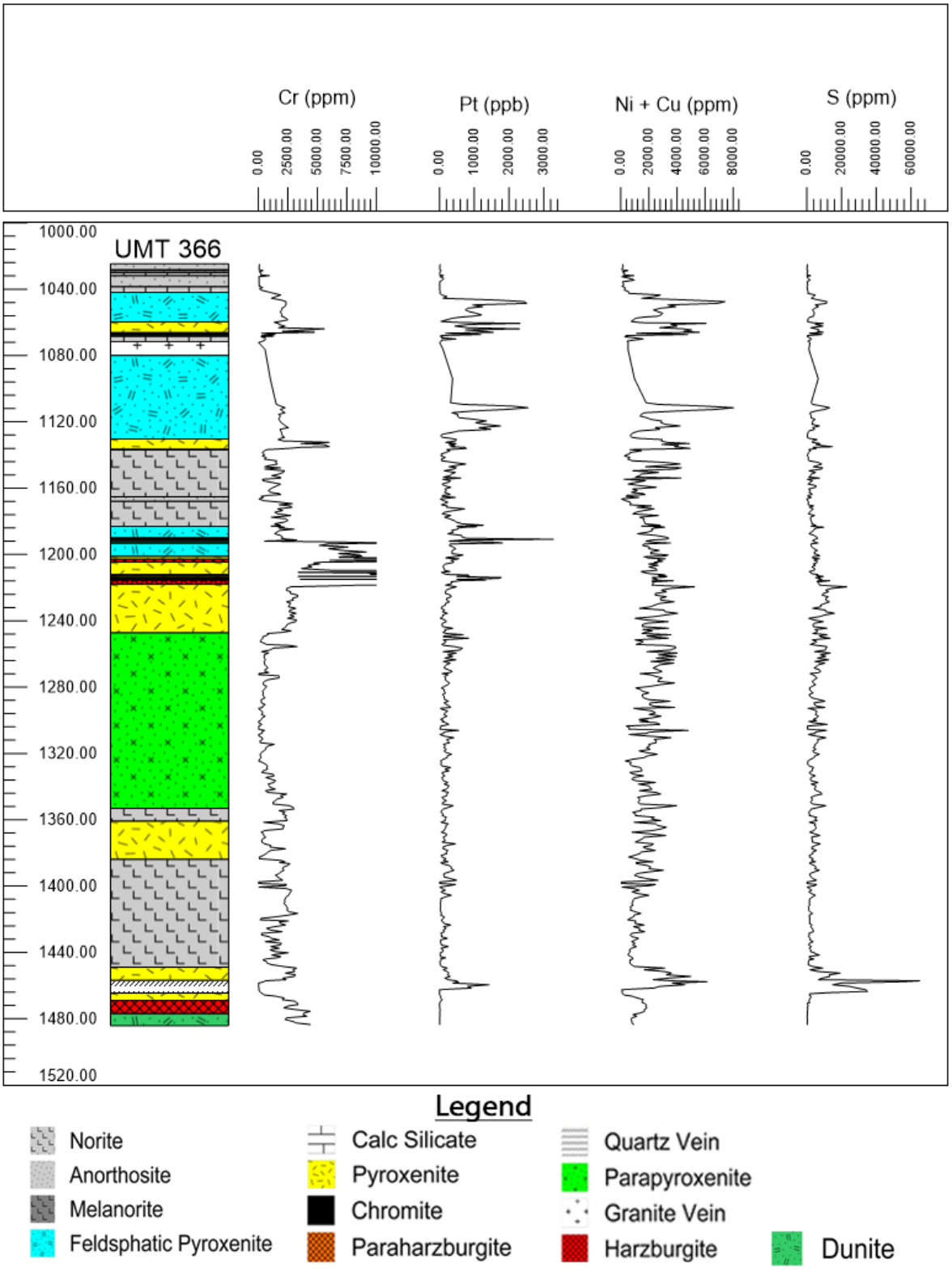


Figure 5. 5: A stratigraphic column of hole UMT336, with the associated chemistry of the economic elements.

Study areas

Whole-rock geochemical data on the economic minerals of interest are used in combination with the stratigraphy of hole UMT366, and their relationship is shown in Figure 5.5. Three poorly mineralised sections can be identified in the hole, the first of which occurs in pyroxenite and is interrupted by a calc-silicate xenolith, the second is associated with chromite horizons, and the third consists of only a small peak at the boundary between a quartz vein and pyroxenite. The mineralised section at the top of the hole shows the greatest economic potential, as the peaks occur over a wider area, as compared to the second and third which consist of only one or two small peaks. In the first mineralised section there is only a slight correlation between Pt and Cr, with a considerably stronger association between Pt and the base metals, which are in part associated with the sulphur content (Figure 5.6).

The second mineralised section corresponds with the 'so-called' UG2 layer, and only shows 3 or 4 small peaks. It is interesting to note that there is not such a strong relation between the Pt peaks and base metals, as these Pt grains are associated with chromites. The lower portion shows a very strange increase in sulphur around the quartz vein, with associated peaks in base metal sulphides and platinum, and sharp decrease in Cr. Lee (1996) explains that metasedimentary xenoliths frequently have a reaction halo of serpentine, as mentioned before, and these zones may have elevated concentrations of Cu, Ni and PGE.

Figure 5.6 show a few different plots which are categorised according to the different lithologies. It is shown that the Ni and Cu content has a positive correlation with PGE grade for the most part, except for harzburgites and dunites which fall out of this trend, as they contain higher amounts of Ni and Cu than the expected PGE grades. This is possibly due to the high amounts of olivine in these rocks, which are known to carry elevated amounts of Ni. Also, on Turfspruit, all the harzburgites and dunites encountered are of Lower Zone origin and are therefore not mineralised, and in fact, have a reduced metal content according to McDonald and Holwell (2007). The most consistently mineralised lithologies in UMT366 appears to be, in order of decreasing abundance, feldspathic pyroxenite (which has slightly lower base metal values, but the highest PGE grades), pyroxenites (which have slightly higher Ni+Cu values, with lower PGE's), chromites and parapyroxenites which show a wide range of grades. Norites, which are not typically a favourable host rock in the Bushveld Complex, have a number of samples which show good base metal and PGE mineralisation. Strangely, as mentioned earlier, some high-grade values came from a xenolith, which at the same time showed some of the lowest grades alongside anorthosites.

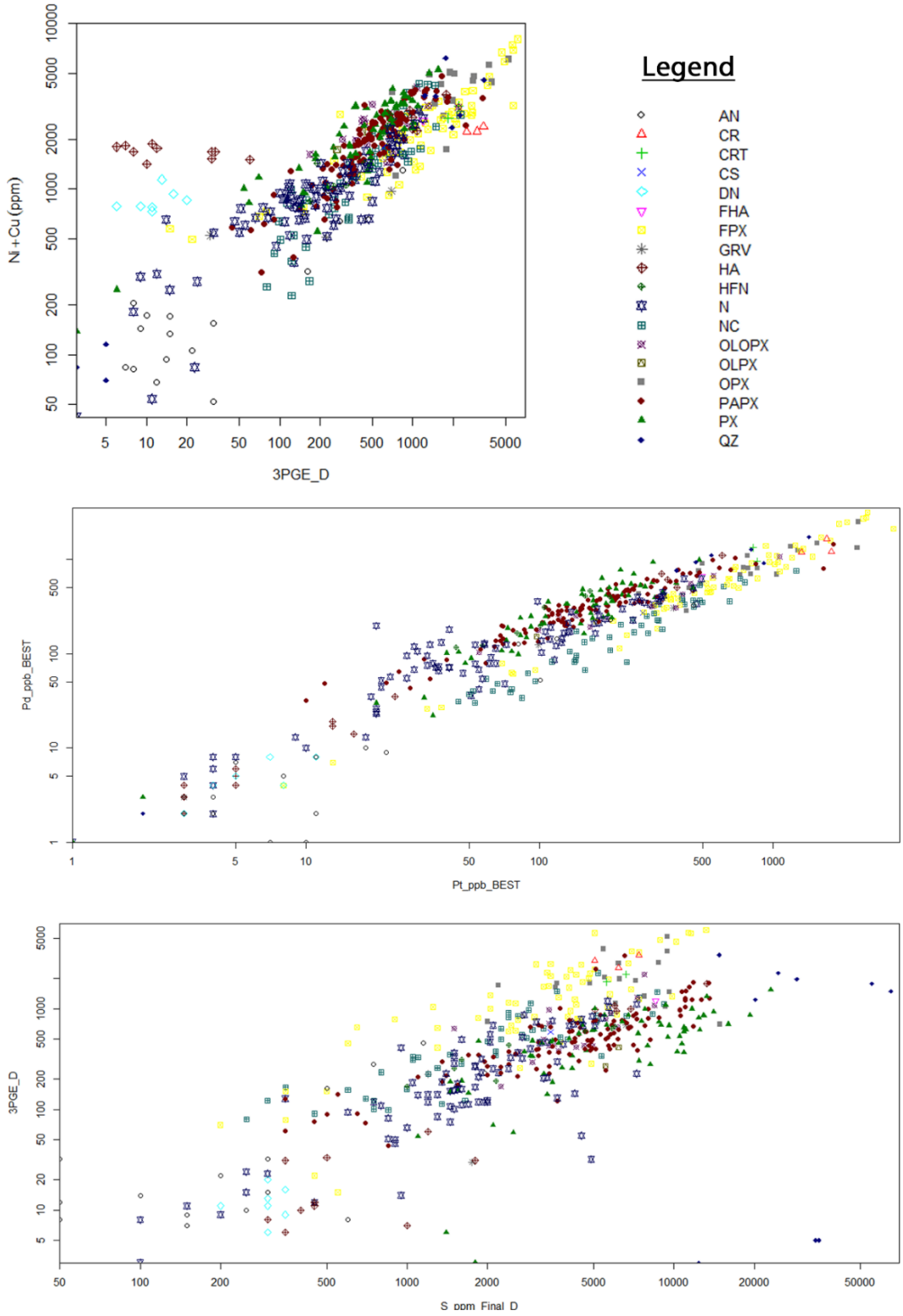


Figure 5. 6: Binary diagrams with different elemental plots, highlighting chemical differences between various lithologies in hole UMT366 on Turfspruit. The graphs show the relationship between PGE's and S and base metals, as well as the relationship between Pt and Pd. The abbreviations in the legend are as follows: AN (Anorthosite), CR (Chromite), CRT (Chromitite), CS (Calc-silicate), DN (Dunite), FHA (Feldspathic harzburgite), FPX (Feldspathic pyroxenite), GRV (Granite vein), HA (Harzburgite), HFN (Hornfels), N (Norite), NC (Norite cycle), OLOPX (Olivine orthopyroxenite), OLPX (Olivine pyroxenite), OPX (Orthopyroxenite), PAPX (Parapyroxenite), PX (Pyroxenite), QZ (Quartz vein).

The Pt:Pd ratio for UMT 366 averages 0.88 from the 485 samples analysed, with higher ratio values associated with norite cycles and anorthosites, while the lowest values were associated with parapyroxenites. This average ratio is similar to elsewhere in the northern limb, such as 0.93 for Drenthe in the far north (Maier et al. 2007). The Merensky Reef PGE data compiled by Kinnaird et al. (2002) and Cawthorn et al. (2002) show a variation in the Pt/Pd ratio between the different areas to be 1.9 to 2.9, which clearly show a notably higher Pt content. This shows that throughout both the eastern and western limbs the units are significantly richer in Pt than Pd, regardless of whether rocks contain sulphide or not. The reasons for this striking enrichment of Pt is not well understood, but it appears to be a fundamental compositional feature of the magmas that formed the upper Critical Zone. However, according to Grobler (2017, personal communication), the Pt:Pd ratio comparison between the Platreef and the Merensky is flawed. He claims that the mistake authors make is to calculate a ratio for the Platreef which includes several different mineralised units across the upper part of the proposed Upper Critical Zone, and compare these values with the Merensky elsewhere. According to him, if one were to only sample the Merensky equivalent in the Northern limb it shows a ratio comparable to that of the Merensky Reef elsewhere.

5.4 Discussion

5.4.1 Chromite

Evidence for post-cumulus fluid-rock interaction is abundant in the Platreef, including serpentinisation, textural and morphological evidence, as well as some chemical indications. Accessory chromite can undergo extensive postcumulus equilibration with surrounding ferromagnesian silicates (Irvine, 1969), and changes in the chemistry of chromite should indirectly reflect changes in the crystallisation conditions of a magma, particularly when these changes are viewed in combination with the chemistry of the associated silicates (Hulbert and von Gruenewaldt, 1985). Through studying chromites with different morphologies in both disseminated and massive chromite samples, Yudovskaya and Kinnaird (2010) showed how re-equilibration of chromite leads to a decrease in Mg and Al, with an increase in Ti and Fe. In the petrography chapter, it is shown that some disseminated and angular chromite grains appear to have been replaced by intercumulus plagioclase. Since both Al and Cr are 3^+ cations, they are fully interchangeable in the crystal lattice of the chromite grain. Looking at the data on chromites in table 1 and 3, this would make sense, as chromites with lower Al values have higher Cr values and vice versa, therefore supporting the substitution theory.

Yudovskaya and Kinnaird (2010) highlighted two types of Fe-Ti-Cr spinels, namely a (1) low-Al type (4.9 – 7.5 wt% Al_2O_3), and a (2) high-Al type (8.8 – 19.3 wt% Al_2O_3). This is comparable to the two spinel end-members described by Scoon and Eales (2002) in the sections where the iron-rich

ultramafic pegmatite cross-cuts the chromites on the Amandelbult mine. They describe a Ti-poor, Al-rich chromite, as well as a titanomagnetite low in Cr and Al, which was encountered on point in table.

5.4.2 Olivine

Olivine was restricted to the Lower Zone on Turfspruit, but it is common in the Platreef on Zwartfontein. The reason for the higher amount of olivine-bearing rocks at Akanani has been debated, some suggesting that it may have been in closer proximity to the feeder zone of the Platreef (McDonald and Holwell, 2007). Generally, the olivine in the Platreef show considerably higher Mg# in comparison to the eastern and western limbs and is comparable to olivine studied in the Lower Zone of the Grasvally area, studied by Hulbert and von Gruenewaldt (1985). In addition, the satellite Lower Zone rocks north of Mokopane studied by Mcdonald et al. (2005), also contain Mg# higher than the Lower Zone rocks elsewhere in the Bushveld. It is interesting to note that the olivine occurring in harzburgite within the Platreef on Zwartfontein, share the same composition as Lower Zone feldspathic harzburgites on Turfspruit, indicating a much lower degree of fractionation that took place on Zwartfontein. This supports the theory by McDonald and Holwell (2007) about a potential feeder zone in the area close to Zwartfontein.

According to McDonald et al. (2005), the best current estimate of primary Platreef olivine composition is grains analysed by Buchanan et al. (1981) with olivines of Fo_{75-76}. Other Fe-rich olivine encountered in the Platreef has been ascribed to non-magmatic processes such as the assimilation of banded ironstones into the reef, or as a replacement of orthopyroxene.

There are generally lower Ni values for the olivine of the Lower Zone on Turfspruit when compared to the Lower Zone olivine in the eastern limb of the Bushveld Complex (Figure 5.3). McDonald and Holwell (2007) show that Lower Zone cumulates in the northern limb, which pre-date the Platreef, are depleted in both Ni and Cu compared to Lower Zone rocks in other limbs. They propose that base metals, such as Ni and Cu, were concentrated in conduits that fed magma chambers of the Lower Zone and that these sulphides were transported by a later magma into the Platreef.

Lower Zone olivine analysed on the Turfspruit property show more primitive compositions as compared to that of the eastern limb Lower Zone, while the Merensky in the Rustenburg section is less fractionated than that of the Union section. A possible explanation for this could be late fluids that disturbed the chemistry of the olivine, seeing that there are very few fresh olivine grains in the Zwartfontein holes studied (refer to chapter 4). Also, according to McDonald et al (2005), replaced reef tends to be enriched in Ti and Mn, although one would expect a decrease in Mg and increase in Fe.

5.4.3 Mineralisation

All the PGE grains, except for point E in Figure 5.4 (ZF116 1538 m), are dominated by palladium. Most of the investigations on the Platreef have shown that the economic reefs are more Pd-rich, with Pt: Pd ratios less than 1, compared to those of the eastern and western limbs with Pt: Pd values greater than 1 (McDonald et al., 2005).

According to Yudovskaya et al. (2001) bismuthotellurides are distributed uniformly, but it occurs as the main Pd-bearing mineral on Turfspruit, in both the upper pyroxenitic reef (Hole TMT870), as well as the lower chromite zones. Armitage et al. (2002) explains that the general distribution of platinum group minerals in the Platreef is completely different to that of the PGE reefs in the main Complex, except for some pothole reef, as well as reef that has been affected by late-stage iron-rich ultramafic pegmatoid (IRUP). Evidence for late stage fluid ingress in the Platreef is plentiful, and it is possible that this may have altered the platinum group mineralogy, leading to the similarities with the more volatile-rich portions of the Merensky Reef.

There is a clear relationship between sulphur and PGE grade in UMT366 (Figure 5.5). This, however, is in contrast with some authors (for example Mitchell and Scoon, 2012) who claim that the relationship between PGE grades and base metals sulphides are poorly constrained and that grades correlate far more effectively with the occurrence of ultramafic lithologies. This does not seem to be the case in UMT336, which is by no means economically mineralised, but mineralisation does occur in feldspathic pyroxenite, pyroxenite, chromites and harzburgite. It also does not explain the presence of mineralisation extending into the dolomitic footwall on Sandsloot. It would make sense that PGE's are associated with sulphides, as most of the grains studied under the SEM occurred on the edges of both pentlandite and pyrrhotite. Kinnaird et al. (2005) explains the relation more clearly, saying that there is a close correlation between PGE's and base metals at low concentrations, but not necessarily between higher grades of PGE's and base metals. Therefore, S and base metals do not serve as a useful indicator for economic PGE mineralisation.

5.5 Comparison between the study areas and the Main Bushveld Complex

Although limited chemical data were available for this study, it is believed that a good representation of the chemistry of the rocks on both Turfspruit and Zwartfontein was obtained. Many authors have equated the Platreef with the Upper Critical Zone of the Bushveld Complex, but after scrutinizing the chemical character, especially the mineral chemistry of the Platreef, there appears to be a significant difference in the make-up of these rocks.

Chemical differences between the study areas and the Main Bushveld Complex

Bushveld chromites progressively increase in V and Ti content upwards in the succession due to increased fractionation of the magma responsible for them. When comparing the Ti and V content of upper Critical Zone chromites with Platreef chromites, it is clear that chromites in the Platreef crystallised from a magma which has not undergone the amount of fractionation as that of the Main Complex magmas. Not all the chromites in the study area formed solely through magmatic processes, and some Fe-Ti-Cr spinels formed through metamorphism, which is not common in the Main Complex due to the absence of xenoliths. The only instance where chromites in the Main Complex consists out of Fe-Ti-Cr-spinels is in potholed reef, or where chromite layers were intruded by iron-rich ultramafic pegmatoid (IRUP).

Although olivines are not common in the upper Critical Zone, there are certain areas, especially in the western limb, where they may be present between and within the UG2 and Merensky Reef. The Ni content of Lower Zone olivines on Turfspruit was depleted in comparison with stratigraphic equivalents in the eastern limbs, which could be explained by McDonald and Holwell (2007) theory about magmatic conduits that stored sulphides. Olivine grains from Zwartfontein appeared to have higher Mn values than those from the Upper Critical Zone in the western limb, which does not correlate with the idea that Platreef magmas underwent less fractionation. It could be explained by late-stage fluids altering the chemistry of the olivines.

Mineralisation in the study areas is dispersed over different lithologies, unlike the reefs of the eastern and western limbs which are well-defined within certain rock packages. Generally, the grades in the Platreef are much lower than that of the Merensky Reef and the UG2, but occur over thicker portions. The so-called ‘UG2’ in the study area is not nearly as well-endowed in PGE’s as its counterpart in the Main Complex, with extremely variable grades occurring within it. The type of platinum group minerals present in the study areas differs from those found in the Merensky and UG2. The main PGM on Turfspruit were bismuthotellurides, which were dominated by palladium, whereas Pt-Pd sulphides and alloys are far more common in the reefs of the main Bushveld Complex (Yudovskaya et al., 2011). The lower Pt : Pd ratio of less than 1 is also unique to the Platreef, as ratios are considerably higher in the eastern and western limbs. Another unique feature is the presence of moderate, and in some cases quite good PGE grades in norites, which are usually an unfavourable host rock. One of the major differences between the Platreef and the Upper Critical Zone is the high sulphide content in the Platreef, with some whole-rock assays reaching up to 7% sulphur. This has led to economic exploitation of both Ni and Cu on the Platreef, which is unheard of in the rest of the Bushveld and is more comparable to Norilsk-type Ni-Cu-PGE.

Chapter 6

Conclusion

Stratigraphically, the Platreef is situated in a similar position as the Critical Zone, between the Main- and Lower Zone, which lead early authors such as Wagner (1929) and Willemse (1969) to link the PGE-mineralised zones in the Platreef with that of the Merensky Reef. The eastern and western lobes of the Bushveld Igneous Complex are linked throughout the Critical, Main and Upper Zones (Cawthorn and Webb, 2001), but a connection with the northern limb is less certain and remains a contentious topic. Some industry geologists on Turfspruit claim to have recognised the Merensky equivalent within the Platreef, which they have termed the Turfspruit Cyclic Unit (TCU). Although, during this study a number of fundamental problems with this approach were recognised.

The Platreef lacks the spectacular layering of the Critical Zone present within the eastern and western limbs of the Bushveld Complex, with no obvious indication of cyclic sequences. Apart from the very broadly developed norite cycles present in the holes of Turfspruit, most of the lithologies in the study areas appear to occur very heterogeneously. The majority of the norite cycles on Turfspruit are incomplete, and Kinnaird et al. (2005) have attributed incomplete cycles to an interruption to normal steady-state fractionation processes.

Well-developed chromite horizons such as the UG2 and LG6 are absent in the Platreef, and instead there are two main 'chromite-rich zones', which are difficult to trace. The lower boundary of the upper Critical Zone is defined in the main Complex as the first appearance of cumulus plagioclase, although on Turfspruit there are norite packages that occur a few metres from the Lower Zone boundary with that of the Platreef, which is clearly in conflict with the stratigraphic constrains set for the Critical Zone. The presence of numerous xenoliths, and the fact that in some areas the immediate footwall of the Platreef is Transvaal sediments is a unique feature of the Platreef.

The 'Main Mineralised Zone' on Zwartfontein is very similar to the Merensky Cyclic Unit in the north-western Bushveld in the Union Section. Both contain granular harzburgite as one of the main lithologies, which is comparable in composition and texture to an olivine orthopyroxenite. However, the Zwartfontein reef is extensively serpentised, and the olivine contains a much lower Ti value as compared to the Union section Merensky Reef. Although the chemistry of the 'Main Mineralised Reef' may not be extremely indicative of the parental magma, as postcumulus fluids have probably altered it a great deal.

In terms of the petrographic character of the rocks on Turfspruit and Zwartfontein, a great deal of similarities exists with the Merensky and other Upper Critical Zone rocks. The general modal mineralogy is quite similar, with all rock types containing ortho- and clinopyroxene, plagioclase and olivine, in differing proportions. Even though chromite is not as well developed in the study areas, their textural and morphological character is comparable to those of the Upper Group chromites. Although, most of the similarities described, involved very localised processes that formed these textures, such as postcumulus growth, and could have occurred within any system that contain the same mineralogy. Therefore, the mere fact that rocks appear comparable does not indicate that similar processes formed them. Lithologically, the Platreef was significantly more heterogeneous, with a high degree of contamination, which in turn led to serpentinisation and other forms of alteration.

Mineralisation in the study areas appear to be different to those in the UG2 and Merensky Reefs. Whereas Pt-Pd sulphides and Pt-Pd alloys are far more prevalent in these reefs, the study areas have a different PGE facies. Turfspruit was dominated by Pd-dominant Pd-Pt-bismuthotellurides, while Zwartfontein had high Rh values in PGE grains. In both study areas, there is a considerably higher Pd-content compared to Pt, which is true for the entire northern limb. The average Pt:Pd ratio of hole UMT366 was 0.88, which is significantly lower than the 1.9 to 2.9 of the Merensky Reef (Cawthorn et al., 2002). It must be said that the conclusions are made from a statistically very unrepresentative sample size. The reasons for this striking enrichment of Pt in the main Bushveld Complex is not well understood, but it appears to be a fundamental compositional feature of the magmas that formed the upper Critical Zone.

The chemical character of the Platreef rocks was a lot more primitive when compared to Upper Critical Zone rocks elsewhere. V and Ti content of chromites on Turfspruit and Zwartfontein showed a magma which has not undergone the amount of fractionation as its ‘so-called’ stratigraphic equivalent in the western limb. Also, not all chromites formed through purely magmatic processes and were not true chromitites, but rather Fe-Ti-Cr spinels. In the Main Complex, these rocks are only present locally where the Iron-rich ultramafic pegmatite intruded. The Platreef has a considerably higher sulphide content, such that Ni and Cu is exploited at economic grades, and is far more Pd-rich than that of the Merensky or UG2 reefs.

This work has shown that the Platreef probably formed from a different magma which generated the upper Critical Zone in the eastern and western limbs of the Bushveld Igneous Complex, and there is substantial evidence to support the fact that the formation of the Platreef is not linked to that of the upper Critical Zone either genetically or temporally.

References

Armitage, P.E.B., McDonald, I., Edwards, S.J. and Manby, G.M. (2002) Platium-group element mineralisation in the Platreef and calc-silicate footwall at Sandsloot, Potgietersrus district, South Africa. Transactions of the institute of mining and metallurgy, v. 111, B36-B45.

Ashwal, L.D., Webb S.J. and Knoper, M.J. (2005). Magmatic stratigraphy in the Bushveld northern lobe: continuous geophysical and mineralogical data from the 2590 m Bellevue drillcore. South African Journal of Geology, v. 108, 199-232.

Barnes, S-. J., Cox, R.A. and Zientek, M.L. (2006). Platinum group element, gold, silver and base metal distribution in compositionally zoned sulphide droplets from the Medvezky Creek Mine, Noril'sk, Russia. Contributions to mineralogy and petrology, v. 152, 187-200.

Barnes, S.J. (2000). Chromite in komatiites, II. Modification during Greenschist to mid-amphibolite facies metamorphism. Journal of Petrology, v. 41, 387-409.

Barret, D.M., Jacobsen, J.B.L., McCarthy, T.S. and Cawthorn, R.G. (1978). The structure of the Bushveld Complex south of Potgietersrus, as revealed by a gravity survey. Transactions, Geological Society of South Africa, 81, 271-276.

Barton, J.M., Holzer, L., Karnber, B., Doig, R., Kramers, J.D. and Nyfeler, (1994). Discrete metamorphic events in the Limpopo belt, Southern Africa: Implications for the application of P-T paths in complex metamorphic terrains. Geological Society of America, v. 22, no. 11, 1035-1038.

Bates, R.L. and Jackson, J.A. (1987). *Glossary of Geology* American Geological Institute, Alexander, Virginia (3rd Edition).

Beard, J.S., Frost, B.R., Fryer, P. McCaig, A., Searle, R., Ildefonse, B., Zinin, P. and Sharma, S.K. (2009). Onset and Progression of Serpentinisation and Magnetite formation in Olivine-rich troctolite from IODP Hole U1309D. Journal of Petrology, v. 00, 1-17.

Buchanan, D.L., Nolan, J., Suddaby, P., Rousse, J.E., Viljoen, M.J. and Davenport, W.J. (1981). The genesis of sulphide mineralisation in a portion of the Potgietersrus limb of the Bushveld Complex. Economic Geology, v. 76, 568-579.

Cameron, E.N. (1975). Postcumulus and subsolidus equilibration of chromite and coexisting silicates in the eastern Bushveld Complex. Geochemica et Cosmochimica Acta, v. 39, 1021-1024.

Cameron, E.N. (1978). The Lower Zone of the eastern Bushveld Complex in the Olifants River trough. Journal of Petrology, v. 19, 437-462.

Cameron, E.N. (1979). Titanium-bearing oxide minerals of the Critical Zone of the Eastern Bushveld Complex, Am Mineral, v. 64, 140-150.

Cameron, E.N. (1980). Evolution of the Lower Critical Zone, central sector, eastern Bushveld Complex and its chromite deposits. Economic Geology, v. 75, 845-871.

Cameron, E.N. (1982). The upper critical zone of the eastern Bushveld Complex – precursor of the Merensky Reef. Economic Geology, v. 77, 1307-1327.

Cameron, E.N. and Desborough, G.A. (1969) Occurrence and characteristics of chromite deposits – eastern Bushveld Complex, Economic Geology, v. 4, 23-40.

Cameron, E.N. and Emerson, M.E. (1959) The origin of some of the chromite deposits of the eastern part of the Bushveld Complex, Economic Geology, v. 54, 1151-1213.

Cawthorn, R.G and Boerst, K. (2006). Origin of the pegmatitic pyroxenite in the Merensky unit, Bushveld Complex, South Africa. Journal of Petrology, v. 47, 1509-1530.

Cawthorn, R.G. (1996). Re-evaluation of magma compositions and processes in the Upper critical zone of the Bushveld complex. Mineralogical magazine, v. 60, 131-148.

Cawthorn, R.G. (1999). Platinum-group element mineralisation in the Bushveld Complex – a critical reassessment of geochemical models. South African Journal of Geology, v. 102, 268-281.

Cawthorn, R.G. (2007) a. Cr and Sr: Keys to parental magmas and processes in the Bushveld Complex, South Africa. Lithos, v. 95, 381-198.

Cawthorn, R.G. (2015), A review of the Bushveld complex and its mineralisation, *in* Platinum-group element mineralisation and resources of the Bushveld Complex, South Africa. Council for Geoscience, 2015.

Cawthorn, R.G. and Lee, C.A. (1998). 'Field excursion guide to the Bushveld Complex'. 8th international platinum symposium. Geol Soc of South Africa and South African institute of mining and metallurgy, v. 113.

Cawthorn, R.G. and Walvaren, F. (1998). Emplacement and Crystallisation time for the Bushveld Complex. Journal of petrology, v. 39, 1669-1687.

Cawthorn, R.G. and Webb, S.J. (2001). Connectivity between the western and eastern lobes of the Bushveld Complex. Tectonophysics, v. 330, 195-209.

Cawthorn, R.G., Barton, J.R. and Viljoen, M.J. (1985). Interaction of floor rocks with the Platreef on Overysel, Potgietersrus, Northern Transvaal. Economic Geology, v. 80, 988-1006.

Cawthorn, R.G., Eales, H.V., Walvaren, F., Uken, R., and Watkeys, M.R. (2006). The Bushveld Complex. Geological society of South Africa, Council for Geoscience, 261-282.

Cawthorn, R.G., McCarthy, T.S. and Davies, G. (1983) Vertical chemical gradients in a single grain of magnetite from the Bushveld Complex, South Africa. Mineralogical magazine, v. 47, 27-34.

Cousins, C.A. (1959). The structure of the mafic portion of the Bushveld Igneous Complex. Trans. Geol. Soc. South Africa, v. 62, 179-189.

Crockett, R.N. (1969). The geological significance of the margin of the Bushveld basin in Botswana with particular reference to the Lobatse Ramotswa areas. Trans. Geol. Soc. South Africa., v. 74, 211-235.

Crowson, P. (2001). Mineral handbook 2000-2001. Mining Journal books, Edenbridge, 486.

Darracott, B.W. (1975). A note on the 'Bushveld Line of intrusives'. Trans. Geol. Soc. South Africa, v. 78, 371-372.

De Klerk, W.J. (1992). Petrogenesis of the Upper critical zone of the Western Bushveld complex with emphasis on the UG1 footwall and Bastard units. Ph.D. thesis, Rhodes University, Grahamstown. 294.

De Wit, M.J. (1987). Gondwana break-up and the tectonic setting of the Dufek layered intrusion, with speculation on the tectonic setting of the Bushveld complex. Indaba on the tectonic setting of layered intrusives, University of Pretoria, South Africa.

Deer, W.A., Howie, R.A. and Zussman, J. (1992). An introduction to the Rock-Forming Minerals. Pearson Education Limited, England.

Du Plessis, C.P. and Walvaren, F. (1990). The tectonic setting of the Bushveld Complex in Southern Africa, Part 1. Structural deformation and distribution. Tectonophysics, v. 179, 305-319.

Eales, H.V (1987). Upper critical zone chromitite layers at R.P.M. Union Section Mine, wester Bushveld Complex. *In* Stowe, C.W., Evolution of chromium ore fields. Van Nostrand Reinhold, New York. 109-143.

Eales, H.V. and Cawthorn, R.G. (1996). The Bushveld Complex. In: Cawthorn, R.G. (ed) Layered Intrusions. Elsevier, Amsterdam, 191-229.

Eales, H.V. and Reynolds, I.M. (1986). Cryptic variations within chromitites of the Upper Critical Zone, North-western Bushveld Complex. Economic Geology, v. 81, 1056-1066.

Eales, H.V., de Klerk, W.J. and Teigler, B. (1990). Evidence for magma mixing processes within the Critical and Lower zones of the north-western Bushveld complex. South African Chemical Geology, v. 88, 261-278.

Eales, H.V., Marsh, J.S., Mitchell, A.A., de Klerk, W.J., Kruger, F.J. and Field, M. (1986). Some geochemical constraints upon models for crystallisation of the Upper critical zone - Main zone interval, birth-western Bushveld Complex. Mineralogical Mag, v 50, 567-582.

Finn, C.A., Bedrosian, P.A., Cole, J.C., Khoza, T.D. and Webb, S.J. (2015) Mapping the 3D extent of the Northern Lobe of the Bushveld layered mafic intrusion from geophysical data, Precambrian Research, v. 268, 279-294.

Friese, A. and Chunnet, G. (2004) Tectono-magmatic igneous development of the northern limb of the Bushveld Igneous Complex with special reference to the mining area of Potgietersrus Platinum Limited. Geoscience Africa, University of the Witwatersrand, Johannesburg, South Africa, 209-210.

Gain, S.B. and Mostert, A.B (1982). The geological setting of the platinoid and base metal sulphide mineralisation in the Platreef of the Bushveld Complex in Drenth, North of Potgietersrus. Econ Geol 77: 1395-1404.

Good, N. and De Wit, M.J. (1997). The Thabazimbi-Murchison lineament of the Kaapvaal Craton, South Africa: 2700 Ma of episodic deformation. Journal of the Geological Society, v. 154, 93-97.

Griffin, W.L., Graham, S., O'Reilly, S.Y. and Pearson, N.J. (2004). Lithosphere evolution beneath the Kaapvaal Craton: Re-Os systematics of sulphides in mantle-derived peridotites. Chemical Geology, v. 208, 89-118.

Grobler, D.F. and Nielsen, S.A. (2012). Upper Critical Zone (Merensky Reef – UG2) correlates within the Platreef, Turfspruit 241KR, Northern Limb, Bushveld Igneous Complex: Unpublished internal company report, Platreef Resources Pty Ltd., 27:31.

Grobler, D.F., Nielsen, S.A. and Broughton, D. (2012). Upper Critical Zone (Merensky Reef – UG2) correlates within the Platreef on the Turfspruit 241KR, Northern Limb, Bushveld Complex: 5th Platreef workshop, Mokopane, 9th – 11th November, 2012.

Groves, D.I., Ho, S.E., Rock, N.M.S., Barley, M.E. and Muggeridge, M.T. (1987). Archaean cratons, diamond and platinum: evidence for coupled long-lived crust-mantle systems. Geology, v. 15, 801-805.

Hall, A.L. (1932). The Bushveld igneous complex in the central Transvaal. Geological Society South Africa, Mem. 28, 544.

Hall, A.L. and Du Toit, A.L. (1923). 'On the section across the floor of the Bushveld Complex at the Hartebeestpoort Dam, West of Pretoria'. Trans. Geol. Soc. South Africa, v. 26, 69-96.

Harmer, R.E. and Armstrong, R.A. (2000). Duration of Bushveld (sensu lato) magmatism: constraints from new SHRIMP zircon chronology, Abstract, workshop on the Bushveld Complex, Gethlane Lodge, Burgersfort.

Harmer, R.E. and Sharpe, M.R. (1985). Field relations and strontium isotope systematics of the marginal rocks of the eastern Bushveld Complex. Economic Geology, v. 80, no. 4, 813-837.

Harris, C. and Chaumba, J.B. (2001). Crustal contamination and fluid-rock interaction during the formation of the Platreef, northern limb of the Bushveld Complex, South Africa. Journal of Petrology, v. 42, 1321-1347.

Hatton, C.J. and Schweitzer JK. (1995). Evidence for synchronous extrusive and intrusive bushveld magmatism. Journal of African Earth Sciences, v. 21, 579-594.

Hatton, C.J. and Von Gruenewaldt, G. (1987). The geological setting and petrogenesis of the Bushveld chromitite layers. *In* Stowe, C.W. (Ed), Evolution of chromium ore fields. Van Nostrand Reinhold, New York. 109-143.

Holwell, D.A. and McDonald, I. (2008). Chromite-hosted sulphide inclusions in the Platreef. Preservation of the parental sulphide liquid? 3rd Platreef Workshop, Mokopane, South Africa, 11-13th July, 2008.

Holwell, D.A., Armitage, P.E.B. and McDonald, I. (2005). Observations on the relationships between the Platreef and its hanging wall. Transactions, Institute of Mining and Metallurgy B, 114, 199-207.

Holwell, D.A., Boyce, A.J. and McDonald, I. (2007). Sulfur isotope variations within the Platreef Ni-Cu-PGE Deposit: Genetic implications for the origin of sulphide mineralisation, Economic Geology, v. 102, 1091-1110.

Hulbert, L.J. (1983). A petrological investigation of the Rustenburg layered suite and associated mineralisation south of Potgietersrus. Ph.D thesis, University of Pretoria, 501.

Hulbert, L.J. and Von Gruenewaldt, G. (1982). Nickel, copper and platinum mineralisation in the Lower Zone of the Bushveld Complex, south of Potgietersrus. Economic Geology, 77, 1296-1306.

Hulbert, L.J. and Von Gruenewaldt, G. (1985). Textural and compositional features of chromite in the lower and critical zones of the Bushveld complex south of Potgietersrus. Economic Geology, v. 80, 872-895.

Hunter, D.R. (1975). The regional geological setting of the Bushveld Complex. University of the Witwatersrand, Economic Geology Research Unit.

Hutchinson, D. and Kinnaird, J.A. (2005) Complex multistage genesis for the Ni-Cu-PGE mineralisation in the southern region of the Platreef, Bushveld Complex, South Africa. Applied Earth Science, v. 114, 208-224.

Hutchinson, D. and McDonald, I. (2008). Laser ablation ICP-MS study of platinum group elements in sulphides from the Platreef at Turfspruit, northern limb of the Bushveld Complex, South Africa. Mineralium deposita, v. 43, 695-711.

Irvine, T.N. (1965). Chromian spinel as a petrogenetic indicator. Part 1. Theory. Canadian Journal of Earth Sciences, v. 2, 648-672.

Ivanplats Limited, Platreef Project, Limpopo Province, Republic of South Africa. NI 43-101 Technical report on Updated Mineral Resource Estimate.

Jackson, E. (1966). Liquid immiscibility in chrome seam formation. Economic Geology, v. 61, 777-780.

Kinnaird, J.A. and Nex, P.A.M. (2015). An overview of the Platreef, *In* Platinum-group element (PGE) mineralisation and resources of the Bushveld Complex, South Africa. Council for Geosciences.

Kinnaird, J.A., Hutchinson, D., Schurmann, L., Nex, P.A.M. and de Lange, R. (2005). Petrology and mineralisation of the southern Platreef, northern limb of the Bushveld Complex, South Africa. Mineralium Deposita, v. 40, 576-597.

Kinnaird, J.A., Kruger, F.J., Nex, P.A.M. and Cawthorn, R.G. (2002). Chromitite formation – a key to understanding processes of platinum enrichment. Australian institute of mining and metallurgy, v. 307, B23-B34.

Kruger, F.J. (1990). The stratigraphy of the Bushveld Complex: a reappraisal and the relocation of the Main Zone boundaries. South African Journal of Geology, v. 93, 376-381.

Kruger, F.J. (1994). The Sr-isotopic stratigraphy of the western Bushveld Complex. South African Journal of Geology, v. 97, 393-398.

Kruger, F.J. (2005). Filling the Bushveld complex magma chamber: lateral expansion, roof and floor interaction, magmatic unconformities and formation of giant chromitite, PGE and Ti-V-magnetite deposits. Mineralium Deposita, v. 40, 451-472.

Kruger, F.J. and Marsh, J.S. (1982). Significance of $^{87}Sr/^{87}Sr$ ratios in the Merensky Cyclic Unit of the Bushveld Complex. Nature, v. 298, 53-55.

Kruparz, H. and Van Rensburg, W.L. (1965). The chromite deposits at Nietverdiend, Marico district, Transvaal, South Africa Geol. Survey Annal, v. 4, 137-150.

Le Bas, M.J. and Streckeisen, A.L. (1991) The IUGS systematics of igneous rocks. Journal of the Geological Society, London. V. 148, 825-833.

Le Maitre, R.W. (2002) Igneous Rocks, A classification and glossary of terms. Cambridge University Press, Cambridge, 236.

Lee, C.A (1996) A Review of mineralisation in the Bushveld Complex and some other layered intrusions. In: Cawthorn, R.G. (ed) Layered Intrusions. Elsevier Science, BV, Amsterdam, 103-145.

Legg, C.A. (1969) Some chromite-ilmenite associations in the Merensky Reef, Transvaal. Amer Mineral, v. 54, 1347-1354.

Longhi, J., Fram, M.S., Vander Auwera, J. and Montieth, J.N. (1993). Pressure effects, kinetics, and rheology of anorthositic and related magmas. American Mineralogist, v. 78, 1016-1030.

Lonmin (2014). Mineral Resource and Mineral Reserve Statement, 30 September

Maier, W.D. and Barnes, S.-J. (1998). Concentrations of rare earth elements in silicate rocks of the Lower, Critical, and Main Zones of the Bushveld Complex. Chem Geol, v. 150, 85-103.

Maier, W.D. and Barnes, S.-J. (2010). The petrogenesis of PGE reefs in the upper Main zone of the northern lobe of the Bushveld Complex on the farm Moorddrift, South Africa. Economic Geology, v. 105, 841-854.

Maier, W.D. and Eales, H.W. (1994). A facies model for the interval between the UG2 chromitite and Merensky Reef, western Bushveld Complex. Appl Earth Science (Trans Inst Min Metall B), v. 103, 22-30.

Maier, W.D. and Groves, D.I. (2011). Temporal and spatial controls on the formation of magmatic PGE and Ni-Cu deposits. Min Deposita, v. 46, 841-857.

Maier, W.D., Barnes, S.-J. and Groves, D.I. (2013). The Bushveld Complex, South Africa: formation of platinum-palladium, chrome- and vanadium-rich layers via hydrodynamic sorting of a mobilised cumulate slurry in a large, relatively slowly cooling, subsiding magma chamber. Mineral Deposita, v. 48, 1-56.

Maier, W.D., Barnes, S.-J. and van der Merwe, M.J. (2001). The concentrations of PGE in the pyroxenite marker, Bushveld Complex: implications for the formation of the Main zone. South African Journal of Geology, v. 104, 335-342.

Maier, W.D., de Klerk, L., Blaine, J., Manyeruke, T., Barnes, S.-J., Stevens, M.J.A. and Mavrogenes, J.A. (2007a). Petrogenesis of contact-style PGE-mineralisation in the northern lobe of the Bushveld; Comparison from the data from the farms, Rooipoort, Townlands, Drenthe and Nonnewerth. Mineral Deposita, v. 43, 255-280.

Marsh, B.D. (1998) On the interpretations of crystal size distributions in magmatic systems, Jounrla of Petrology, v. 39, 553-599.

McDonald, I., Holwell, D.A. and Armitage, P.E.B. (2005). Geochemistry and mineralogt of the Platreef and 'Critical Zone' of the northern lobe of the Bushveld Complex, South Africa: implications for Bushveld stratigraphy and the development of PGE mineralisation. Mineralium deposita, v. 40, 526-549.

McDonald, J.A. (1965) Liquid immiscibility as a factor in chromitite seam formation in the Bushveld Igneous Complex: Economic Geology, v. 60, 1674-1685.

McDonald, J.A. (1967) Liquid immiscibility in chromite seam formation- a reply. Economic Geology, v. 62, 288-292.

Merensky, H. (1925). The platinum areas of Lydenburg. South African Mining and Engineering Journal (Jan 10th), Johannesburg, South Africa, 474-475.

Mitchell, A.A. (1990). The stratigraphy, petrography and mineralogy of the Main Zone of the north-western Bushveld Complex. South African Journal of Geology, v. 93, 818-831.

Mitchell, A.A. and Scoon, R.N. (2012) The Platreef of the Bushveld Complex, South Africa: A new hypothesis of multiple, non-sequential magma replenishment based on observations at the Akanani project, north-west of Mokopane. South African Journal of Geology, v. 115, 535-550.

Mondal, S.K. and Mathez, E.A. (2007). Origin of the UG2 chromitite layer, Bushveld Complex. Journal of Petrology, v. 48, 495-510.

Nex, P.A.M. (2006) The Structural setting of mineralisation on Tweefontein hill, Northern Limb of the Bushveld Complex, South Africa: Transactions of the Institution of Mining and Metallurgy, v. 114, B243-B291.

Nex, P.A.M., Cawthorn, R.G. and Kinnaird, J.A. (2002) Geochemical effects of magma addition: compositional reversals and decoupling of trends in the Main Zone of the western Bushveld Complex. Mineralogical Magazine, v. 66, no.6, 833-856.

Nex, P.A.M., Kinnaird, J.A., Jones, B. and Colloty, A. (2006). Platreef rock type definitions and descriptions. Unpublished.

Onyeagocha, A.C. (1974) Alteration of chromite from the Twin Sisters dunite, Washington. American Mineralogist, v. 59, 609-612.

Opoubou-lando, S.D. (2010). Mineralogical characterisation of chromite in the UG2 Reef from Waterval Mine, Western Bushveld: Implications for mineral processing. Master of Science, Stellenbosch University.

Proenza, J.A., Zaccarini, F., Escayola, M., Cabana, C., Schalamuk, A. and Garuti, G. (2008) Composition and textures of chromite and platinum group minerals in chromitites of the western ophiolitic belt from Pampean Ranges of Cordoba, Argentina. Ore Geology Reviews, v. 33, 32-48.

Reczko, B.F.F., Oberholzer, J.D., Eriksson, P.G. and Schreiber, U.M. (1995). A re-evaluation of the Palaeoproterozoic Pretoria Group (Kaapvaal Craton) and a hypothesis on basin development. Journal of African Earth Sciences, v. 21, 505-519.

Reichhardt, F.J. (1994). The Molopo Farms Complex, Botswana: History, stratigraphy, petrography, petrochemistry, and Ni-Cu-PGE mineralisation. Exploration and mining Geology, v. 3, 263-284.

Reynolds, I.M. (1985). The nature and origin of titaniferous magnetite-rich layers in the upper zone of the Bushveld Complex; a review and synthesis. Economic Geology, v. 80, 1089-1108.

Roeder, P.L., Poustovetov, A. and Oskarsson, N. (2001). Growth form and composition of chromian spinel in MORB magma: diffusion-controlled crystallisation of chromian spinel. The Canadian Mineralogist, v. 39, 397-416.

SACS (South African Committee for Stratigraphy), 1980. Stratigraphy of South Africa. Part 1: Lithostratigraphy of the Republic of South Africa, South West Africa/Namibia, and the republics of Bophuthatswana, Transkei and Venda (L.E. Kent, Comp). Handbook, Geological survey of South Africa, Pretoria, v. 8, 690.

Schürmann, L.W., Grabe, P.J. and Steenkamp, C.J. (1998). Chromium, *In* Wilson, M.G.C. and Anheausser, C.R. (Eds), The Mineral Resources of South Africa. Handbook, Council for Geoscience, 16, Pretoria, 90-105.

Scoates, J.S. and Friedman, R.M. (2008), Precise age of the platiniferous Merensky reef, Bushveld Complex, South Africa, by the U-Pb zircon chemical abrasion ID-TIMS technique, Economic Geology, v. 103, 465-471.

Scoates, J.S. and Friedman, R.M. (2008). Precise age of the platineferous Merensky Reef, Bushveld Complex, South Africa, by the U-Pb zircon chemical abrasion ID-TIMS technique. Economic Geology, v. 103, 465-471.

Scoon, R.N. and de Klerk, W.J. (1987) The Relationship of olivine cumulates and mineralisation to cyclic units in part of the upper critical zone of the western Bushveld Complex. Canadian Mineralogist, v. 25, 51-77.

Scoon, R.N. and Eales, H.V. (2002). Unusual Fe-Ti-Cr spinels from discordant bodies of iron-rich ultramafic pegmatite at the Amandelbult Platinum mine, north-western Bushveld Complex. Mineralogical magazine, v. 66, 857-879.

Scoon, R.N. and Teigler, B. (1994). Platinum-group element mineralisation in the Critical Zone of the western Bushveld Complex: 1 Sulfide-poor chromitites below the UG2. Economic Geology, v. 89, 1094-1121.

Sekerka, R.F. (1993) Role of instabilities in determination of the shapes of growing crystals. Journal of crystal growth, v. 128, 1-12.

Sharman-Harris, E.R., Kinnaird, J.A., Harris, C. and Horstmann, U.E. (2005). A new look at sulphide mineralisation in the northern limb, Bushveld Complex: a stable isotope study. Applied Earth Science, v. 114, 252-261.

Sharpe, M.R. (1985). Strontium isotope evidence for preserved density stratification in the main zone of the Bushveld Complex. Nature, v. 316, 119-126.

Spry, A. (1969) Metamorphic textures: New York, Pergamon Press, 350.

Tankard, A.J., Jackson, M.P.A., Eriksson, K.A., Hobday, D.K., Hunter, D.R., and Minter, W.E.L. (1982). Crustal evolution of Southern Africa, 3.8 billion years of earth history: New York, Heidelberg, Berlin, Springer-Verlag, 523.

Teigler, B. and Eales, H.V. (1996). The Lower and Critical Zones of the western limb of the Bushveld Complex as intersected by the Nooitgedagt boreholes. Bulletin, Geological Survey of South Africa, v. 111, 126.

Teigler, B., Eales, H.V. and Scoon, R.N. (1992). The cumulate succession in the critical zone of the Rustenburg layered suite at Brits, western Bushveld Complex. South African Journal of Geology, v. 95, 17-28.

Van Biljon, W.J. (1976). Goud is nie waar dit gevind word nie! Trans. Geol. Soc. South Africa, v. 79, 155-167.

Van der Merwe, F., Viljoen, F. and Knoper, M. (2012). The mineralogy and mineral associations of platinum group elements and gold in the Platreef at Zwartfontein, Akanani project, Northern Bushveld Complex, South Africa. Miner Petrol, v. 106, 25-38.

Van der Merwe, M.J. (1976). The layered sequence of the Potgietersrus limb of the Bushveld Complex. Economic Geology, v. 71, 1337-1352.

Vermaak, C.F. (1995). The Platinum-group metals – a global perspective. Mintek, Randburg, South Africa, v. 247.

Vermaak, C.F. and van der Merwe, M.J. (2002). The platinum mines and deposits of the Bushveld complex. Mintek, Johannesburg, 118

Viljoen, M.J. (1999). The nature and origin of the Merensky Reef in the Western limb of the Bushveld Complex based on geological facies and geophysical data, South African Journal of Geology, v. 102, 192-208.

Von Gruenewaldt, G. (1973). The Main and Upper Zones of the Bushveld Complex in the Roossenekal area, eastern Transvaal. Transactions, Geological Society of South Africa, v. 76, 207-227.

Von Gruenewaldt, G., Hulbert, L.J. and Naldrett, A.J. (1989). Contrasting platinum group element concentration patterns in cumulates of the Bushveld Complex. Mineralium deposita, v. 24, 219-229.

Von Gruenewaldt, G., Sharpe, M.R. and Hatton, C.J. (1985), The Bushveld Complex: Introduction and Review*, Economic Geology*, v. 80, 803-812.

Von Gruenewaldt, G., Sharpe, M.R. and Hatton, C.J. (1985). The Bushveld Complex: Introduction and Review. Economic Geology, v. 80, 803-812.

Wagner, P.A. (1929) The platinum deposits and mines of South Africa, Struick, Lodon, 338.

Walvaren, F. (1987). Geochronological and isotope studies of Bushveld Complex rocks from the Fairfield borehole at Moloto, northeast of Pretoria. South African Journal of Geology, v. 90, 352-360.

Walvaren, F., Armstrong, R.A. and Kruger, F.J. (1990), A chronostratigraphic framework for the north-central Kaapvaal Craton, The Bushveld Complex and the Vredefort structure, *Tectonophysics*, v. 171, 23-48.

Walvaren, F., Armstrong, R.A. and Kruger, F.J. (1990). A chronostratigraphic framework for the north-central Kaapvaal craton, the Bushveld Complex and the Vredefort structure. Tectonophysics, v. 171, 23-48.

Wenk, H. and Bulakh, A. (2004). Minerals: Their Constitution and Origin. Cambridge University Press, Cambridge, United Kingdom.

White, J.A. (1994). The Potgietersrus prospect geology and exploration history XVth CMMI congress, Johannesburg SAIMM, v. 3, 172-181.

Willemse, J. (1969). The vanadiferous magnetic iron ore of the Bushveld Igneous Complex. Economic Geology Monograph, v. 4, 137-208.

Yudovskaya, M.A. and Kinnaird, J.A. (2010). Chromitite in the Platreef (Bushveld Complex, South Africa): Occurrence and evolution of its chemical composition. Mineral Deposita, v. 45, 369-391.

Yudovskaya, M.A., Kinnaird, J.A., Naldrett, A.J., Mokhov, A.V., McDonald, I. and Reinke, C. (2011). Facies variation in PGE mineralisation in the Central Platreef of the Bushveld Complex, South Africa. The Canadian Mineralogist, v. 49, 1349-1384.

Yudovskaya, M.A., Kinnaird, J.A., Sobolev, A.V., Kuzmin, D.V., McDonald, I. and Wilson, A.H. (2013). Petrogenesis of the Lower Zone Olivine-rich cumulates beneath the Platreef and their correlation with recognized occurrences in the Bushveld Complex. Economic Geology, v. 108, 1923-1952.

Zeh, A., Ovtcharova, M. and Schaltegger, U. (2015). The Bushveld Complex was emplaced and cooled in less than one million years – results of zirconology, and geotectonic implications. Earth and Planetary Science letters, v. 418, 103-114.

Appendix

Table 1: EMPA on chromite from holes ZF116 and ZF48 on the Zwartfontein property.

Analysis No.	SiO2	TiO2	V2O5	Al2O3	Cr2O3	FeO	MnO	MgO	CoO	NiO	ZnO
ZF116-1225-11	0.02	0.87	0.31	18.89	40.47	30.3	0.26	8.98	0.04	0.23	0.12
ZF116-1225-12	0.01	0.86	0.31	19.01	40.45	30.51	0.26	8.91	0.04	0.24	0.09
ZF116-1225-13	0.02	0.87	0.34	19.2	40.19	30.56	0.25	8.87	0.05	0.23	0.1
ZF116-1225-14	0.01	0.97	0.35	18.86	40.13	31.19	0.33	8.71	0.04	0.18	0.11
ZF116-1225-15	0.01	0.94	0.35	19.01	39.24	32.89	0.33	7.33	0.04	0.2	0.2
ZF116-1225-16	0.02	0.91	0.35	18.62	39.5	32.38	0.31	7.77	0.07	0.21	0.16
ZF116-1225-17	0	0.92	0.35	18.35	39.75	33.39	0.3	6.86	0.06	0.2	0.29
ZF116-1225-18	0.02	0.91	0.35	18.76	40.15	31.8	0.28	8.25	0.06	0.22	0.14
ZF116-1225-19	0.02	0.17	0.18	34.26	29.85	24.79	0.21	11.23	0.07	0.12	0.5
ZF116-1226.1-73	0	1.31	0.38	18.37	33.33	39.78	0.37	5.62	0.05	0.31	0.43
ZF116-1537.75-52	0.17	3.26	0.33	13.8	43.23	30.15	0.26	7.58	0.05	0.1	0.09
ZF116-1537.75-53	0.02	0.91	0.36	15.59	44.09	30.72	0.3	8.38	0.05	0.12	0.1
ZF116-1537.75-54	0	0.85	0.35	14.79	44.71	31.21	0.28	8.23	0.05	0.1	0.1
ZF116-1537.75-55	0.01	0.96	0.37	14.88	43.73	31.49	0.31	8.25	0.06	0.12	0.09
ZF116-1537.75-56	0.01	0.93	0.39	15.02	44.03	31.36	0.26	8.38	0.04	0.09	0.11
ZF116-1537.75-57	0.01	0.94	0.35	14.53	44.46	31.22	0.27	8.19	0.05	0.13	0.1
ZF116-1537.75-58	0.02	0.95	0.35	15.01	43.94	31.28	0.27	8.31	0.04	0.12	0.11
ZF116-1537.75-59	0.06	0.68	0.39	14.75	44.41	31.33	0.28	8.27	0.04	0.12	0.11
ZF116-1537.75-60	0.01	0.54	0.36	15.49	44.21	31.08	0.25	8.4	0.04	0.11	0.1
ZF116-1538-43	0	0.72	0.32	16.92	43.37	29.72	0.28	8.79	0.04	0.14	0.09
ZF116-1538-44	0	0.71	0.31	16.77	43.6	29.67	0.25	8.73	0.06	0.13	0.09
ZF116-1538-45	0.02	0.78	0.32	16.27	43.83	29.99	0.3	8.63	0.04	0.12	0.08
ZF116-1538-46	0.01	0.69	0.32	17.24	43.3	29.14	0.28	8.79	0.05	0.13	0.09
ZF116-1538-47	0.01	0.74	0.34	16.44	43.79	30.14	0.24	8.69	0.06	0.11	0.1
ZF116-1538-48	0.01	0.65	0.3	17.44	43.44	29.1	0.3	8.9	0.06	0.12	0.12
ZF116-1538-49	0.01	0.68	0.29	17.46	43.59	29.26	0.26	8.79	0.03	0.13	0.1
ZF116-1538-50	0	0.69	0.31	17.66	43.26	29.22	0.26	8.85	0.04	0.14	0.11
ZF116-1538-51	0	0.78	0.32	16.72	43.11	30.53	0.27	8.46	0.05	0.11	0.09
ZF48-1718-1	0.03	0.9	0.37	16.58	43.38	29.93	0.29	8.58	0.03	0.1	0.08
ZF48-1718-2	0.02	0.84	0.33	16.44	43.61	29.8	0.28	8.62	0.03	0.09	0.09
ZF48-1718-3	0.02	0.85	0.35	16.41	43.52	30.08	0.31	8.36	0.05	0.08	0.1
ZF48-1718-4	0.01	0.9	0.35	16.39	43.4	29.72	0.26	8.61	0.05	0.12	0.1
ZF48-1718-5	0.02	0.8	0.37	17.03	42.4	30.22	0.27	8.76	0.05	0.1	0.08
ZF48-1718-6	0.02	0.76	0.36	17.51	42.64	29.3	0.25	8.94	0.03	0.12	0.12
ZF48-1718-7	0.01	0.62	0.34	16.31	43.26	30.6	0.25	8.15	0.05	0.13	0.08
ZF48-1718-9	0.02	0.85	0.38	16.59	43.09	30.03	0.24	8.65	0.04	0.1	0.1
ZF48-1753.5-22	0.01	0.7	0.32	14.82	44.9	30.91	0.3	8.05	0.04	0.16	0.11
ZF48-1753.5-23	0	0.68	0.29	15.32	44.69	30.73	0.27	8.16	0.06	0.15	0.12
ZF48-1753.5-24	0.02	0.74	0.3	15.2	44.7	30.99	0.28	8.24	0.04	0.17	0.09

ZF48-1753.5-25	0	0.73	0.3	14.6	45.13	30.98	0.3	8.01	0.04	0.14	0.13
ZF48-1753.5-26	0.01	0.72	0.3	14.87	44.49	31.31	0.28	8.02	0.05	0.13	0.1
ZF48-1753.5-27	0.01	0.78	0.32	15.18	44.62	30.99	0.28	8.28	0.05	0.17	0.1
ZF48-1753.5-28	0.01	0.79	0.34	15.25	44.56	30.62	0.26	8.24	0.06	0.16	0.09
ZF48-1753.5-29	0	0.76	0.34	16.21	44.11	30.19	0.27	8.59	0.04	0.11	0.11
ZF48-1753.5-30	0.01	0.76	0.33	16.46	44	29.81	0.29	8.72	0.04	0.08	0.1
ZF48-1753.5-31	0	0.74	0.35	15.17	44.93	30.85	0.28	8.26	0.05	0.14	0.1
ZF48-1753.5-33	0	1.43	0.4	12.92	43.73	33.54	0.33	7.22	0.05	0.11	0.08
ZF48-1753.5-34	0.02	1.47	0.41	13.08	43.3	33.93	0.32	7.09	0.06	0.12	0.12
ZF48-1753.5-35	0.01	1.18	0.42	12.48	43.81	34.1	0.32	6.88	0.05	0.13	0.1
ZF48-1753.5-36	0.02	1.25	0.41	12.45	44.02	34.36	0.3	6.92	0.03	0.12	0.09
ZF48-1753.5-37	0	1.15	0.36	14.27	42.91	33.21	0.31	7.31	0.05	0.12	0.1
ZF48-1753.5-38	0.01	1.01	0.41	14.64	42.49	33.09	0.28	7.33	0.04	0.13	0.1
ZF48-1753.5-39	0.01	1.19	0.38	14.45	42.42	33.22	0.28	7.22	0.05	0.14	0.13
ZF48-1753.5-40	0.01	1.39	0.43	12.15	44.21	33.99	0.34	6.8	0.05	0.12	0.08
ZF48-1753.5-41	0	1.4	0.42	11.49	43.57	35.44	0.33	6.36	0.04	0.12	0.09
ZF48-1768-62	0.02	0.71	0.33	16.28	43.7	30.27	0.3	8.34	0.02	0.09	0.1
ZF48-1768-63	0.02	0.72	0.34	16.75	43.88	29.73	0.27	8.61	0.05	0.11	0.1
ZF48-1768-64	0	0.74	0.35	16.72	43.47	30.29	0.29	8.51	0.05	0.12	0.08
ZF48-1768-65	0.01	0.75	0.33	15.95	44.54	29.71	0.31	8.47	0.05	0.12	0.1
ZF48-1768-66	0	0.72	0.39	16.4	43.9	30.21	0.29	8.47	0.05	0.1	0.08
ZF48-1768-67	0.01	0.86	0.37	16.59	43.31	30.77	0.27	8.27	0.04	0.1	0.1
ZF48-1768-68	0	0.64	0.38	15.13	44.36	32.07	0.33	7.36	0.03	0.08	0.09
ZF48-1768-69	0.01	0.8	0.31	17.11	43.62	29.42	0.28	8.79	0.05	0.12	0.09
ZF48-1768-70	0.02	0.73	0.36	16.17	44.48	29.88	0.21	8.65	0.05	0.11	0.08

Table 2: EMPA on olivine grains from hole UMT6 on Turfspruit

rock	depth, m	Mg#	SiO2	TiO2	FeO	CaO	MnO	MgO	NiO	Cr2O3	CoO	Al2O3
PR HZB	859	77.80	38.91	0.010	20.41	0.050	0.270	40.15	0.280	0.010	0.020	0.010
PR HZB	859	77.15	38.77	0.010	21.02	0.010	0.310	39.83	0.180	0.000	0.020	0.000
PR HZB	859	77.50	38.67	0.010	20.65	0.020	0.310	39.91	0.220	0.000	0.010	0.000
PARA HZB	967	71.24	37.96	0.010	26.00	0.040	0.300	36.14	0.120	0.010	0.020	0.000
PARA HZB	967	71.43	37.89	0.000	25.87	0.030	0.300	36.30	0.120	0.000	0.020	0.000
PARA HZB	967	71.08	37.66	0.000	25.99	0.030	0.300	35.85	0.120	0.010	0.030	0.000
PARA HZB	967	71.42	37.95	0.000	25.71	0.060	0.320	36.05	0.120	0.010	0.010	0.000
PARA HZB	989	75.74	38.89	0.005	22.84	0.050	0.283	40.00	0.144	0.005	0.025	0.002
PARA HZB	989	75.74	39.04	0.006	22.94	0.046	0.284	40.18	0.145	0.006	0.025	0.000
PARA HZB	989	75.74	39.01	0.005	22.87	0.038	0.282	40.07	0.143	0.007	0.025	0.000
PARA HZB	989	75.60	39.07	0.007	23.00	0.028	0.283	40.00	0.126	0.007	0.024	0.002
FPYX	1028	70.69	37.41	0.000	26.41	0.050	0.350	35.74	0.150	0.010	0.050	0.000
FPYX	1028	70.71	37.56	0.000	26.35	0.050	0.350	35.70	0.150	0.000	0.060	0.010
FPYX	1028	70.91	37.45	0.000	26.10	0.040	0.340	35.71	0.150	0.000	0.030	0.000
LZ FHZB	1195.8	81.51	39.85	0.000	17.53	0.030	0.170	43.36	0.250	0.020	0.030	0.010
LZ FHZB	1195.8	80.74	39.75	0.000	18.12	0.020	0.210	42.64	0.250	0.010	0.020	0.000
LZ FHZB	1195.8	81.09	39.62	0.010	17.75	0.040	0.200	42.70	0.260	0.050	0.010	0.020
LZ FHZB	1202.35	81.41	39.07	0.006	17.54	0.031	0.233	43.11	0.296	0.004	0.026	0.020
LZ FHZB	1202.35	80.02	38.53	0.002	18.80	0.025	0.249	42.27	0.294	0.005	0.017	0.000
LZ FHZB	1202.35	80.85	38.24	0.002	17.93	0.015	0.238	42.48	0.302	0.004	0.028	0.001
LZ FHZB	1202.35	78.79	37.83	0.004	19.82	0.025	0.256	41.32	0.289	0.003	0.028	0.001
LZ FHZB	1202.35	80.38	38.58	0.006	18.36	0.034	0.247	42.20	0.296	0.004	0.026	0.000
LZ FHZB	1202.35	78.39	37.97	0.002	20.03	0.025	0.257	40.75	0.295	0.006	0.030	0.000
LZ FHZB	1202.35	80.57	38.69	0.004	18.28	0.028	0.241	42.55	0.296	0.004	0.027	0.001
LZ FHZB	1202.35	80.06	38.37	0.005	18.64	0.016	0.244	42.00	0.289	0.004	0.028	0.001
LZ FHZB	1209.7	85.17	39.55	0.004	14.27	0.021	0.194	45.98	0.328	0.003	0.023	0.000
LZ FHZB	1209.7	84.37	38.73	0.005	14.82	0.026	0.203	44.92	0.321	0.005	0.024	0.000
LZ FHZB	1209.7	84.97	39.19	0.006	14.37	0.023	0.198	45.58	0.329	0.034	0.025	0.011

LZ FHZB	1209.7	84.90	39.31	0.002	14.47	0.024	0.199	45.65	0.327	0.003	0.025	0.002
LZ FHZB	1209.7	84.40	39.23	0.005	14.88	0.026	0.204	45.19	0.325	0.004	0.024	0.005
LZ FHZB	1209.7	84.69	39.50	0.003	14.77	0.025	0.202	45.84	0.329	0.001	0.024	0.000
LZ FHZB	1209.7	84.73	38.98	0.004	14.49	0.018	0.198	45.14	0.329	0.003	0.025	0.001
LZ FHZB	1209.7	85.04	39.50	0.004	14.33	0.021	0.199	45.69	0.338	0.003	0.025	0.000
LZ FHZB	1209.7	84.41	39.53	0.004	14.93	0.020	0.205	45.38	0.327	0.002	0.023	0.000
LZ FHZB	1209.7	84.93	39.55	0.004	14.43	0.025	0.198	45.63	0.328	0.005	0.025	0.000
LZ FHZB	1209.7	84.43	38.97	0.001	14.64	0.026	0.199	44.57	0.326	0.004	0.024	0.003
LZ FHZB	1209.7	84.50	39.04	0.004	14.77	0.030	0.201	45.17	0.323	0.004	0.023	0.000
LZ FHZB	1209.7	85.13	39.49	0.003	14.33	0.025	0.193	46.02	0.330	0.004	0.025	0.000
LZ FHZB	1209.7	84.15	39.10	0.003	14.96	0.026	0.206	44.56	0.318	0.003	0.025	0.000
LZ FHZB	1209.7	84.89	38.59	0.004	14.37	0.021	0.197	45.30	0.324	0.004	0.027	0.002
LZ FHZB	1209.7	84.57	38.92	0.004	14.77	0.025	0.200	45.43	0.327	0.004	0.026	0.000
LZ FHZB	1209.7	85.14	39.23	0.002	14.23	0.021	0.194	45.75	0.325	0.001	0.025	0.003
LZ FHZB	1209.7	84.79	39.23	0.003	14.55	0.018	0.198	45.50	0.324	0.004	0.026	0.004
LZ FHZB	1209.7	85.19	39.64	0.004	14.26	0.025	0.195	46.00	0.325	0.005	0.022	0.005
LZ FHZB	1209.7	84.38	38.77	0.004	14.75	0.024	0.201	44.73	0.328	0.034	0.023	0.000
LZ FHZB	1209.7	84.91	39.74	0.003	14.56	0.023	0.199	45.95	0.330	0.002	0.025	0.000
LZ HZB	1237.2	86.37	38.71	0.004	12.92	0.021	0.192	45.95	0.310	0.005	0.021	0.004
LZ HZB	1237.2	86.50	39.85	0.004	13.05	0.022	0.193	46.96	0.308	0.001	0.022	0.001
LZ HZB	1237.2	86.52	38.92	0.005	12.89	0.025	0.190	46.41	0.319	0.012	0.022	0.001
LZ HZB	1237.2	86.62	39.71	0.005	12.78	0.022	0.187	46.44	0.307	0.009	0.020	0.007
LZ HZB	1237.2	86.34	38.39	0.005	13.03	0.024	0.191	46.22	0.306	0.003	0.020	0.000
LZ HZB	1237.2	87.31	39.39	0.004	12.26	0.018	0.174	47.33	0.350	0.005	0.020	0.001
LZ HZB	1237.2	86.63	39.02	0.006	12.80	0.020	0.190	46.53	0.313	0.005	0.023	0.000
LZ HZB	1237.2	86.49	40.21	0.005	13.05	0.023	0.197	46.86	0.305	0.004	0.021	0.002
LZ HZB	1237.2	86.80	40.61	0.005	12.84	0.018	0.190	47.38	0.312	0.003	0.023	0.000
LZ HZB	1237.2	87.60	40.16	0.006	11.98	0.018	0.173	47.48	0.320	0.004	0.021	0.000
LZ HZB	1237.2	87.03	40.00	0.006	12.45	0.026	0.181	46.88	0.323	0.004	0.020	0.000
LZ HZB	1237.2	86.38	39.42	0.006	12.98	0.023	0.190	46.18	0.309	0.007	0.021	0.000
LZ HZB	1237.2	86.66	39.71	0.006	12.75	0.026	0.188	46.47	0.311	0.085	0.023	0.031
LZ HZB	1237.2	87.19	40.45	0.009	12.42	0.018	0.179	47.44	0.325	0.003	0.022	0.005
LZ HZB	1237.2	86.70	39.41	0.005	12.60	0.018	0.183	46.07	0.313	0.004	0.021	0.006
LZ HZB	1237.2	86.36	39.67	0.006	12.95	0.024	0.192	46.01	0.308	0.005	0.022	0.008
LZ HZB	1237.2	86.91	39.84	0.004	12.61	0.021	0.184	46.97	0.308	0.003	0.021	0.001
LZ HZB	1360.3	89.19	40.66	0.009	10.49	0.025	0.170	48.60	0.128	0.003	0.012	0.004
LZ HZB	1360.3	89.17	40.38	0.007	10.53	0.024	0.171	48.63	0.141	0.006	0.015	0.002
LZ HZB	1360.3	89.18	40.52	0.007	10.59	0.020	0.174	48.93	0.128	0.004	0.014	0.000
LZ HZB	1360.3	89.22	40.40	0.007	10.45	0.027	0.170	48.50	0.161	0.022	0.014	0.013
LZ HZB	1360.3	89.20	40.43	0.005	10.49	0.021	0.170	48.58	0.141	0.007	0.014	0.001
LZ HZB	1360.3	89.28	40.54	0.004	10.53	0.020	0.173	49.21	0.119	0.004	0.013	0.000
LZ HZB	1360.3	89.15	40.44	0.006	10.59	0.027	0.170	48.84	0.151	0.020	0.015	0.000
LZ HZB	1360.3	89.17	40.43	0.007	10.53	0.019	0.170	48.67	0.125	0.005	0.014	0.000
LZ HZB	1360.3	89.11	40.64	0.006	10.56	0.019	0.174	48.48	0.136	0.014	0.014	0.007
LZ HZB	1360.3	89.08	40.49	0.004	10.65	0.021	0.174	48.76	0.162	0.008	0.015	0.008
LZ HZB	1360.3	89.28	40.69	0.007	10.44	0.020	0.167	48.79	0.155	0.011	0.015	0.005
LZ HZB	1360.3	89.07	40.44	0.006	10.61	0.023	0.173	48.56	0.153	0.035	0.015	0.009
LZ HZB	1360.3	89.28	40.40	0.012	10.46	0.024	0.169	48.90	0.150	0.020	0.014	0.005
LZ HZB	1360.3	89.27	41.06	0.010	10.63	0.020	0.173	49.62	0.128	0.006	0.014	0.000
LZ HZB	1360.3	89.10	40.43	0.006	10.50	0.022	0.171	48.19	0.133	0.005	0.012	0.003
LZ HZB	1360.3	89.26	40.74	0.004	10.52	0.022	0.168	49.06	0.139	0.005	0.015	0.000
LZ HZB	1360.3	89.21	40.78	0.006	10.59	0.023	0.171	49.12	0.159	0.007	0.015	0.009
LZ HZB	1360.3	89.16	40.12	0.009	10.53	0.021	0.167	48.63	0.158	0.011	0.013	0.008
LZ HZB	1360.3	89.13	40.08	0.006	10.55	0.022	0.171	48.56	0.129	0.006	0.013	0.007
LZ HZB	1360.3	89.08	40.72	0.005	10.65	0.022	0.172	48.74	0.122	0.015	0.015	0.008
LZ HZB	1360.3	89.40	40.61	0.006	10.44	0.022	0.171	49.39	0.123	0.004	0.012	0.000
LZ HZB	1360.3	89.22	40.35	0.002	10.51	0.016	0.174	48.78	0.123	0.004	0.011	0.000
LZ HZB	1390	89.01	40.39	0.007	10.69	0.025	0.165	48.60	0.158	0.005	0.015	0.004
LZ HZB	1390	89.14	40.55	0.001	10.63	0.024	0.162	48.96	0.160	0.005	0.015	0.002
LZ HZB	1390	89.29	40.57	0.006	10.45	0.023	0.161	48.91	0.162	0.006	0.014	0.002
LZ HZB	1390	89.05	40.24	0.009	10.63	0.021	0.166	48.50	0.154	0.009	0.015	0.006
LZ HZB	1390	89.25	40.42	0.004	10.46	0.018	0.160	48.76	0.159	0.008	0.014	0.002

LZ HZB	1390	89.22	40.53	0.004	10.54	0.016	0.163	48.92	0.157	0.006	0.013	0.002
LZ HZB	1390	89.04	40.40	0.003	10.68	0.019	0.166	48.69	0.158	0.005	0.015	0.002
LZ HZB	1390	89.26	40.31	0.005	10.47	0.020	0.162	48.82	0.153	0.008	0.013	0.006
LZ HZB	1390	89.20	40.48	0.003	10.54	0.020	0.160	48.86	0.163	0.006	0.013	0.003
LZ HZB	1428	90.10	40.52	0.006	9.70	0.021	0.152	49.50	0.180	0.008	0.017	0.004
LZ HZB	1428	90.17	40.72	0.004	9.66	0.019	0.151	49.71	0.179	0.015	0.015	0.009
LZ HZB	1428	90.01	40.53	0.003	9.77	0.026	0.154	49.41	0.179	0.118	0.016	0.056
LZ HZB	1428	90.36	40.86	0.004	9.48	0.012	0.151	49.86	0.166	0.003	0.013	0.005
LZ HZB	1428	90.25	40.86	0.004	9.58	0.009	0.153	49.74	0.152	0.013	0.012	0.005
LZ HZB	1428	90.14	40.87	0.002	9.68	0.017	0.153	49.67	0.175	0.005	0.015	0.005
LZ HZB	1428	90.13	40.92	0.004	9.70	0.009	0.157	49.71	0.157	0.003	0.013	0.007
LZ HZB	1449	89.88	40.86	0.009	9.97	0.019	0.164	49.67	0.147	0.009	0.016	0.006
LZ HZB	1449	89.88	40.67	0.006	9.93	0.015	0.167	49.48	0.148	0.006	0.014	0.003
LZ HZB	1449	90.00	40.87	0.006	9.88	0.016	0.165	49.91	0.149	0.008	0.014	0.008
LZ HZB	1449	90.02	40.85	0.008	9.82	0.018	0.160	49.70	0.150	0.012	0.015	0.013
LZ HZB	1449	89.83	40.71	0.003	9.97	0.025	0.165	49.43	0.152	0.004	0.014	0.003
LZ HZB	1449.45	89.91	40.91	0.006	9.98	0.021	0.165	49.88	0.151	0.005	0.014	0.002
LZ HZB	1449.45	89.95	40.93	0.005	9.79	0.020	0.166	49.18	0.148	0.009	0.014	0.003
LZ HZB	1449.45	89.98	40.87	0.002	9.78	0.014	0.166	49.28	0.135	0.002	0.014	0.001
LZ HZB	1449.45	89.90	40.61	0.008	9.85	0.019	0.165	49.22	0.149	0.012	0.014	0.014
LZ HZB	1449.45	89.91	40.91	0.005	9.87	0.024	0.167	49.33	0.143	0.006	0.016	0.000
LZ HZB	1449.45	89.89	40.76	0.000	9.90	0.017	0.168	49.41	0.142	0.002	0.014	0.001
LZ HZB	1449.45	90.07	40.80	0.001	9.74	0.011	0.168	49.59	0.128	0.005	0.012	0.000
LZ HZB	1449.45	90.00	40.84	0.000	9.80	0.007	0.163	49.47	0.152	0.002	0.014	0.000
LZ HZB	1449.45	89.82	40.55	0.008	9.90	0.022	0.161	49.03	0.155	0.038	0.013	0.017
LZ HZB	1449.45	89.92	41.01	0.003	9.87	0.023	0.167	49.42	0.144	0.005	0.016	0.000
LZ HZB	1449.45	90.04	40.84	0.004	9.78	0.012	0.163	49.64	0.147	0.001	0.015	0.002
LZ HZB	1449.45	90.01	40.43	0.011	9.73	0.021	0.164	49.17	0.136	0.011	0.014	0.006
LZ HZB	1449.45	89.94	40.50	0.003	9.81	0.021	0.162	49.23	0.151	0.006	0.014	0.000
LZ HZB	1449.45	89.88	40.39	0.002	9.90	0.019	0.167	49.33	0.148	0.003	0.014	0.000
LZ HZB	1449.45	89.90	40.68	0.011	9.86	0.022	0.163	49.27	0.157	0.014	0.016	0.010
LZ HZB	1449.45	89.90	40.52	0.004	9.85	0.019	0.160	49.23	0.161	0.008	0.014	0.001
LZ HZB	1449.45	89.98	40.66	0.005	9.75	0.021	0.158	49.15	0.156	0.006	0.014	0.009
LZ HZB	1449.45	89.80	40.75	0.005	9.96	0.021	0.169	49.18	0.144	0.005	0.016	0.000
LZ HZB	1449.45	90.01	40.85	0.003	9.81	0.016	0.165	49.61	0.149	0.003	0.015	0.000
LZ HZB	1449.45	89.99	40.60	0.008	9.76	0.020	0.167	49.20	0.153	0.008	0.013	0.006
LZ HZB	1480	90.54	40.96	0.006	9.32	0.012	0.148	50.06	0.124	0.005	0.013	0.001
LZ HZB	1480	90.40	40.76	0.007	9.43	0.021	0.150	49.83	0.125	0.009	0.014	0.011
LZ HZB	1480	90.46	40.78	0.001	9.35	0.022	0.148	49.76	0.125	0.003	0.013	0.004
LZ HZB	1480	90.33	40.78	0.005	9.47	0.018	0.149	49.66	0.127	0.005	0.013	0.006
LZ HZB	1480	90.41	40.96	0.003	9.42	0.017	0.148	49.84	0.129	0.008	0.014	0.005
LZ HZB	1496	89.76	40.83	0.006	10.04	0.019	0.162	49.42	0.337	0.007	0.017	0.000
LZ HZB	1496	89.68	40.86	0.003	10.14	0.018	0.164	49.45	0.341	0.006	0.018	0.003
LZ HZB	1496	89.68	40.78	0.004	10.12	0.019	0.164	49.38	0.341	0.014	0.017	0.006
LZ HZB	1496	89.70	40.80	0.005	10.09	0.019	0.164	49.32	0.333	0.007	0.016	0.005
LZ HZB	1496	89.61	40.86	0.006	10.20	0.019	0.166	49.37	0.328	0.004	0.018	0.003
LZ HZB	1517	89.48	40.54	0.002	10.28	0.016	0.161	49.09	0.138	0.020	0.016	0.005
LZ HZB	1517	89.57	40.68	0.003	10.26	0.020	0.161	49.46	0.139	0.003	0.013	0.003
LZ HZB	1517	89.40	40.71	0.003	10.41	0.020	0.164	49.29	0.136	0.001	0.013	0.002
LZ HZB	1517	89.50	40.66	0.000	10.29	0.023	0.163	49.25	0.136	0.003	0.014	0.002
LZ HZB	1517	89.50	40.77	0.005	10.33	0.017	0.166	49.42	0.131	0.013	0.014	0.005
LZ HZB	1517.77	89.34	40.85	0.002	10.41	0.017	0.166	48.95	0.134	0.004	0.015	0.000
LZ HZB	1517.77	89.47	40.93	0.002	10.29	0.023	0.160	49.06	0.143	0.004	0.016	0.000
LZ HZB	1517.77	89.40	40.40	0.006	10.28	0.018	0.164	48.67	0.141	0.006	0.014	0.002
LZ HZB	1517.77	89.63	40.41	0.005	10.08	0.013	0.160	48.88	0.129	0.000	0.014	0.000
LZ HZB	1517.77	89.41	40.37	0.002	10.34	0.020	0.162	48.99	0.140	0.005	0.014	0.000
LZ HZB	1517.77	89.45	40.37	0.003	10.26	0.021	0.162	48.80	0.140	0.003	0.015	0.002
LZ HZB	1517.77	89.46	40.58	0.003	10.28	0.020	0.165	48.98	0.133	0.003	0.016	0.000
LZ HZB	1517.77	89.56	40.59	0.002	10.17	0.017	0.157	48.97	0.144	0.002	0.014	0.000
LZ HZB	1517.77	89.43	40.43	0.004	10.33	0.021	0.164	49.07	0.130	0.004	0.015	0.000
LZ HZB	1517.77	89.40	40.53	0.006	10.32	0.021	0.164	48.84	0.138	0.003	0.012	0.000
LZ HZB	1517.77	89.71	40.81	0.004	10.11	0.015	0.161	49.43	0.135	0.004	0.012	0.000

LZ HZB	1517.77	89.37	40.25	0.002	10.34	0.019	0.166	48.82	0.141	0.004	0.014	0.000
LZ HZB	1517.77	89.40	40.31	0.005	10.30	0.018	0.162	48.77	0.152	0.004	0.016	0.000
LZ HZB	1517.77	89.58	40.76	0.005	10.20	0.015	0.162	49.20	0.139	0.005	0.014	0.001
LZ HZB	1517.77	89.37	40.37	0.004	10.36	0.021	0.162	48.88	0.136	0.003	0.012	0.000
LZ HZB	1517.77	89.35	40.37	0.005	10.36	0.016	0.165	48.79	0.149	0.006	0.015	0.001
LZ HZB	1517.77	89.41	40.59	0.004	10.36	0.016	0.164	49.05	0.138	0.002	0.014	0.000
LZ HZB	1517.77	89.48	40.32	0.003	10.25	0.012	0.167	48.91	0.124	0.001	0.014	0.002
LZ HZB	1517.77	89.61	40.34	0.008	10.15	0.015	0.161	49.16	0.134	0.007	0.014	0.010
LZ HZB	1528	89.22	41.09	0.002	10.70	0.019	0.159	49.67	0.173	0.008	0.018	0.008
LZ HZB	1528	89.26	41.00	0.006	10.65	0.019	0.159	49.67	0.176	0.006	0.016	0.012
LZ HZB	1528	89.19	40.64	0.005	10.66	0.018	0.160	49.36	0.167	0.008	0.017	0.007
LZ HZB	1528	89.16	40.72	0.008	10.70	0.021	0.163	49.41	0.171	0.008	0.019	0.007
LZ HZB	1528	89.10	40.87	0.005	10.77	0.021	0.161	49.41	0.173	0.007	0.018	0.004
LZ HZB	1528	89.18	40.64	0.002	10.67	0.018	0.157	49.35	0.175	0.003	0.018	0.007
LZ HZB	1528	89.14	40.66	0.004	10.69	0.020	0.159	49.23	0.169	0.004	0.018	0.004
LZ HZB	1528	89.17	40.76	0.006	10.69	0.017	0.160	49.38	0.167	0.006	0.018	0.008
LZ HZB	1550	89.58	40.60	0.004	10.24	0.016	0.158	49.37	0.161	0.006	0.019	0.009
LZ HZB	1550	89.87	40.72	0.003	9.97	0.017	0.151	49.64	0.165	0.014	0.016	0.005
LZ HZB	1550	89.83	40.78	0.003	10.03	0.016	0.154	49.73	0.166	0.005	0.018	0.004
LZ HZB	1550	89.56	40.83	0.002	10.30	0.017	0.159	49.56	0.162	0.003	0.018	0.003
LZ HZB	1550	89.59	40.62	0.004	10.25	0.037	0.158	49.51	0.161	0.008	0.015	0.003
LZ HZB	1550	89.59	40.83	0.004	10.28	0.017	0.161	49.65	0.163	0.004	0.018	0.003
LZ HZB	1569	88.80	40.50	0.003	10.97	0.015	0.157	48.79	0.152	0.007	0.018	0.003
LZ HZB	1569	88.54	40.34	0.004	11.19	0.014	0.160	48.55	0.154	0.004	0.018	0.007
LZ HZB	1569	88.66	40.47	0.003	11.12	0.009	0.160	48.79	0.152	0.001	0.018	0.002
LZ HZB	1569	88.80	40.55	0.005	10.99	0.016	0.156	48.92	0.153	0.006	0.018	0.004
LZ HZB	1569	88.81	40.49	0.002	11.00	0.022	0.158	48.97	0.144	0.062	0.017	0.032
LZ HZB	1569	88.81	40.54	0.003	11.00	0.018	0.158	48.99	0.145	0.001	0.018	0.005
LZ HZB	1569	88.75	40.42	0.003	11.03	0.017	0.159	48.86	0.152	0.003	0.017	0.003
LZ HZB	1569	88.44	40.17	0.005	11.35	0.011	0.164	48.72	0.144	0.309	0.017	0.072
LZ HZB	1604.35	90.05	40.24	0.003	9.63	0.014	0.143	48.92	0.200	0.008	0.019	0.001
LZ HZB	1604.35	90.37	40.79	0.002	9.51	0.024	0.139	50.06	0.191	0.007	0.017	0.001
LZ HZB	1604.35	90.26	41.18	0.004	9.48	0.016	0.141	49.30	0.194	0.009	0.017	0.000
LZ HZB	1604.35	90.11	40.35	0.004	9.65	0.019	0.146	49.34	0.194	0.005	0.018	0.002
LZ HZB	1604.35	90.02	40.75	0.003	9.63	0.014	0.144	48.72	0.198	0.005	0.019	0.000
LZ HZB	1604.35	90.13	40.31	0.002	9.43	0.015	0.139	48.36	0.190	0.006	0.018	0.000
LZ HZB	1604.35	90.51	40.85	0.004	9.32	0.014	0.135	49.89	0.181	0.017	0.018	0.001
LZ HZB	1604.35	90.29	40.67	0.004	9.50	0.015	0.138	49.61	0.190	0.007	0.017	0.002
LZ HZB	1604.35	90.37	40.45	0.004	9.37	0.010	0.135	49.33	0.187	0.010	0.017	0.001
LZ HZB	1604.35	90.20	40.42	0.004	9.69	0.017	0.146	50.08	0.194	0.005	0.018	0.000
LZ HZB	1620	89.21	40.72	0.005	10.62	0.015	0.162	49.24	0.129	0.003	0.015	0.002
LZ HZB	1620	89.33	40.75	0.002	10.52	0.013	0.161	49.44	0.128	0.007	0.015	0.002
LZ HZB	1620	89.28	40.52	0.002	10.57	0.023	0.161	49.43	0.123	0.004	0.014	0.002
LZ HZB	1620	89.14	40.58	0.000	10.67	0.018	0.165	49.13	0.128	0.017	0.017	0.006
LZ HZB	1620	89.19	40.53	0.004	10.62	0.017	0.162	49.16	0.125	0.026	0.014	0.016
LZ HZB	1620	89.30	40.63	0.007	10.53	0.019	0.159	49.31	0.122	0.009	0.014	0.009
DUN	1630	88.75	40.76	0.003	11.08	0.022	0.174	49.08	0.114	0.005	0.018	0.007
DUN	1630	88.64	40.60	0.004	11.19	0.020	0.175	48.99	0.115	0.006	0.015	0.003
DUN	1630	88.64	40.70	0.003	11.15	0.021	0.174	48.82	0.117	0.007	0.016	0.002
DUN	1630	88.57	40.66	0.003	11.24	0.016	0.177	48.90	0.117	0.006	0.015	0.005
DUN	1630	88.88	41.03	0.006	11.01	0.018	0.171	49.38	0.113	0.005	0.015	0.002
DUN	1637	89.15	40.53	0.004	10.64	0.016	0.164	49.06	0.087	0.009	0.015	0.003
DUN	1637	89.10	40.52	0.002	10.70	0.013	0.164	49.09	0.089	0.013	0.016	0.007
DUN	1637	89.03	40.67	0.004	10.77	0.018	0.167	49.08	0.091	0.003	0.018	0.002
DUN	1637	89.26	40.61	0.005	10.56	0.020	0.160	49.23	0.090	0.007	0.017	0.005
DUN	1637	89.09	40.67	0.004	10.71	0.013	0.162	49.07	0.089	0.003	0.016	0.002
LZ HZB	1663	89.84	40.95	0.003	10.12	0.021	0.153	50.19	0.133	0.033	0.015	0.009
LZ HZB	1663	90.04	40.95	0.002	9.87	0.010	0.148	50.06	0.138	0.003	0.013	0.005
LZ HZB	1663	89.85	40.83	0.001	10.04	0.017	0.152	49.90	0.135	0.007	0.014	0.003
LZ HZB	1663	89.93	40.91	0.006	9.98	0.018	0.148	50.06	0.135	0.005	0.013	0.007
LZ HZB	1663	89.79	41.05	0.004	10.13	0.020	0.155	50.00	0.137	0.008	0.016	0.009
LZ HZB	1663.7	89.72	39.85	0.005	10.09	0.020	0.150	49.37	0.133	0.006	0.015	0.002

LZ HZB	1663.7	89.87	39.91	0.005	9.96	0.019	0.150	49.55	0.121	0.004	0.011	0.004
LZ HZB	1663.7	89.76	39.90	0.006	10.04	0.023	0.149	49.34	0.133	0.005	0.014	0.004
LZ HZB	1663.7	89.76	39.88	0.003	9.89	0.014	0.149	48.65	0.128	0.005	0.013	0.001
LZ HZB	1663.7	89.80	40.01	0.007	10.00	0.016	0.151	49.41	0.122	0.005	0.012	0.001
LZ HZB	1663.7	90.10	40.15	0.003	9.80	0.015	0.145	50.04	0.129	0.006	0.012	0.000
LZ HZB	1663.7	89.81	40.93	0.006	9.88	0.021	0.148	48.90	0.123	0.006	0.014	0.005
LZ HZB	1663.7	89.64	40.45	0.005	10.01	0.022	0.152	48.62	0.137	0.006	0.014	0.000
LZ HZB	1663.7	89.69	40.15	0.003	9.94	0.019	0.148	48.52	0.130	0.051	0.014	0.019
LZ HZB	1663.7	89.65	40.02	0.007	10.04	0.020	0.150	48.82	0.131	0.007	0.013	0.011
LZ HZB	1664.9	89.94	39.84	0.002	9.89	0.015	0.149	49.61	0.130	0.007	0.014	0.001
LZ HZB	1664.9	89.88	39.80	0.002	9.98	0.016	0.154	49.72	0.134	0.007	0.014	0.000
LZ HZB	1664.9	90.08	40.31	0.003	9.69	0.019	0.145	49.42	0.132	0.009	0.014	0.000
LZ HZB	1664.9	89.97	40.06	0.003	9.96	0.013	0.152	50.11	0.126	0.004	0.014	0.001
LZ HZB	1664.9	89.98	39.92	0.004	9.91	0.016	0.151	49.92	0.133	0.006	0.014	0.002
LZ HZB	1664.9	89.93	40.14	0.004	9.89	0.015	0.150	49.59	0.131	0.006	0.014	0.000
LZ HZB	1664.9	90.05	40.37	0.003	9.80	0.013	0.149	49.78	0.128	0.045	0.016	0.000
LZ HZB	1664.9	89.93	39.53	0.002	9.89	0.015	0.150	49.57	0.130	0.004	0.014	0.001
LZ HZB	1664.9	90.14	39.54	0.003	9.79	0.019	0.148	50.17	0.126	0.005	0.015	0.000
LZ HZB	1664.9	89.88	39.73	0.003	9.86	0.028	0.149	49.16	0.131	0.007	0.014	0.000
DUN	1665.5	90.00	40.04	0.003	9.95	0.013	0.151	50.29	0.132	0.006	0.014	0.000
DUN	1665.5	89.78	40.16	0.003	9.91	0.019	0.149	48.84	0.128	0.014	0.015	0.003
DUN	1665.5	89.85	40.00	0.005	9.86	0.007	0.150	49.00	0.127	0.006	0.014	0.000
DUN	1665.5	89.89	39.98	0.003	9.95	0.011	0.148	49.63	0.125	0.018	0.014	0.000
DUN	1665.5	89.88	40.21	0.004	9.90	0.014	0.150	49.35	0.132	0.006	0.017	0.003
DUN	1665.5	89.71	40.14	0.003	9.91	0.016	0.149	48.51	0.125	0.006	0.014	0.001
DUN	1665.5	89.78	40.51	0.005	9.87	0.012	0.147	48.65	0.130	0.004	0.016	0.002
DUN	1665.5	89.99	39.81	0.003	9.96	0.012	0.151	50.23	0.130	0.007	0.014	0.000
DUN	1665.5	89.75	40.51	0.004	9.99	0.013	0.152	49.09	0.133	0.009	0.016	0.002
DUN	1666.8	90.22	40.41	0.003	9.47	0.010	0.136	49.02	0.150	0.008	0.015	0.000
DUN	1666.8	90.30	40.22	0.003	9.50	0.027	0.138	49.64	0.152	0.004	0.015	0.000
DUN	1666.8	90.14	40.08	0.002	9.46	0.012	0.135	48.50	0.154	0.004	0.014	0.001
DUN	1666.8	90.40	40.28	0.002	9.47	0.026	0.135	50.05	0.154	0.003	0.015	0.002
DUN	1666.8	90.04	40.24	0.005	9.57	0.021	0.137	48.58	0.156	0.171	0.017	0.066
DUN	1666.8	90.21	40.49	0.004	9.42	0.020	0.135	48.75	0.152	0.007	0.015	0.002
DUN	1666.8	90.28	39.99	0.003	9.52	0.022	0.138	49.64	0.150	0.008	0.015	0.001
DUN	1666.8	90.27	40.37	0.003	9.42	0.022	0.135	49.02	0.149	0.004	0.014	0.001
DUN	1666.8	90.37	39.94	0.003	9.34	0.023	0.137	49.17	0.146	0.006	0.014	0.000
DUN	1666.8	90.43	40.31	0.003	9.35	0.020	0.135	49.60	0.146	0.008	0.015	0.002
DUN	1667	90.44	40.76	0.002	9.42	0.019	0.143	50.04	0.142	0.006	0.015	0.008
DUN	1667	90.44	40.83	0.002	9.47	0.016	0.140	50.24	0.140	0.007	0.014	0.005
DUN	1667	90.53	40.76	0.003	9.38	0.013	0.140	50.30	0.140	0.008	0.014	0.002
DUN	1667	90.55	40.62	0.005	9.35	0.017	0.140	50.29	0.143	0.006	0.014	0.000
DUN	1670.65	90.07	40.63	0.003	9.74	0.016	0.137	49.59	0.181	0.006	0.015	0.000
DUN	1670.65	90.19	40.69	0.004	9.69	0.016	0.136	49.96	0.174	0.006	0.016	0.000
DUN	1670.65	90.17	40.80	0.003	9.69	0.014	0.138	49.90	0.179	0.007	0.014	0.001
DUN	1670.65	90.00	40.37	0.003	9.70	0.014	0.139	49.03	0.178	0.009	0.015	0.002
DUN	1670.65	90.33	40.42	0.003	9.51	0.008	0.133	49.86	0.182	0.008	0.016	0.002
DUN	1670.65	89.85	41.15	0.002	9.65	0.011	0.139	47.93	0.181	0.007	0.018	0.000
DUN	1670.65	90.15	40.54	0.002	9.59	0.012	0.137	49.22	0.179	0.009	0.018	0.000
DUN	1670.65	90.24	40.69	0.004	9.65	0.017	0.139	50.08	0.184	0.015	0.017	0.000
DUN	1670.65	90.07	41.09	0.003	9.62	0.017	0.138	48.95	0.187	0.015	0.016	0.002
DUN	1670.65	89.99	40.45	0.003	9.80	0.015	0.144	49.44	0.187	0.006	0.017	0.000
DUN	1671.7	90.37	40.47	0.004	9.47	0.019	0.140	49.83	0.211	0.003	0.021	0.001
DUN	1671.7	90.24	40.25	0.003	9.52	0.023	0.143	49.40	0.206	0.007	0.020	0.000
DUN	1671.7	90.03	40.16	0.003	9.62	0.017	0.146	48.75	0.214	0.005	0.020	0.000
DUN	1671.7	90.41	40.71	0.003	9.31	0.015	0.136	49.23	0.200	0.006	0.018	0.000
DUN	1671.7	90.06	40.73	0.003	9.49	0.014	0.139	48.24	0.202	0.024	0.019	0.003
DUN	1671.7	89.94	40.61	0.003	9.55	0.015	0.144	47.90	0.206	0.008	0.019	0.000
DUN	1671.7	90.16	40.42	0.003	9.57	0.023	0.143	49.21	0.212	0.005	0.020	0.001
DUN	1671.7	90.22	40.51	0.004	9.45	0.012	0.142	48.95	0.193	0.004	0.019	0.000
DUN	1671.7	90.34	40.93	0.001	9.53	0.019	0.142	50.00	0.215	0.003	0.020	0.000
DUN	1671.7	90.33	40.48	0.004	9.47	0.016	0.142	49.62	0.212	0.005	0.019	0.000

DUN	1673.63	89.81	40.66	0.002	9.95	0.023	0.145	49.24	0.176	0.007	0.018	0.001
DUN	1673.63	89.61	40.94	0.004	9.96	0.017	0.146	48.19	0.177	0.004	0.022	0.000
DUN	1673.63	89.75	41.51	0.001	9.83	0.014	0.138	48.28	0.175	0.004	0.020	0.000
DUN	1673.63	89.78	41.35	0.003	9.92	0.019	0.145	48.92	0.188	0.008	0.021	0.002
DUN	1673.63	90.03	41.24	0.003	9.89	0.014	0.139	50.14	0.183	0.006	0.022	0.000
DUN	1673.63	89.70	40.64	0.003	9.92	0.014	0.143	48.51	0.184	0.006	0.019	0.001
DUN	1673.63	89.84	40.57	0.004	9.78	0.019	0.139	48.54	0.185	0.005	0.021	0.000
DUN	1673.63	89.97	40.63	0.005	9.91	0.019	0.144	49.91	0.185	0.025	0.020	0.003
DUN	1673.63	89.95	40.80	0.005	9.80	0.019	0.138	49.23	0.186	0.007	0.022	0.001
DUN	1673.63	89.87	40.70	0.004	9.83	0.016	0.141	48.94	0.177	0.007	0.019	0.000
DUN	1674.65	89.98	40.11	0.005	9.83	0.015	0.145	49.54	0.195	0.008	0.025	0.004
DUN	1674.65	90.23	40.11	0.003	9.60	0.010	0.140	49.75	0.180	0.009	0.022	0.004
DUN	1674.65	90.10	40.17	0.004	9.74	0.014	0.141	49.75	0.196	0.007	0.023	0.000
DUN	1674.65	89.95	40.33	0.004	9.87	0.021	0.144	49.55	0.192	0.007	0.024	0.000
DUN	1674.65	90.11	40.58	0.003	9.80	0.017	0.140	50.14	0.187	0.005	0.022	0.000
DUN	1674.65	90.09	40.39	0.002	9.79	0.016	0.143	49.93	0.191	0.007	0.024	0.000
DUN	1674.65	89.92	40.30	0.004	9.83	0.016	0.143	49.16	0.180	0.005	0.021	0.001
DUN	1674.65	90.20	40.20	0.002	9.78	0.015	0.143	50.49	0.190	0.005	0.022	0.000
DUN	1674.65	89.96	39.87	0.003	9.87	0.014	0.144	49.65	0.188	0.008	0.021	0.001
DUN	1674.65	89.83	39.93	0.006	9.91	0.022	0.147	49.09	0.184	0.007	0.023	0.000
DUN	1675.4	90.20	40.89	0.002	9.61	0.016	0.138	49.64	0.163	0.005	0.021	0.000
DUN	1675.4	89.96	40.47	0.006	9.73	0.022	0.140	48.96	0.167	0.413	0.023	0.119
DUN	1675.4	90.50	40.62	0.005	9.37	0.017	0.139	50.09	0.174	0.006	0.022	0.002
DUN	1675.4	90.27	40.97	0.003	9.46	0.016	0.136	49.28	0.171	0.008	0.021	0.004
DUN	1675.4	90.40	40.63	0.003	9.48	0.015	0.141	50.11	0.172	0.025	0.022	0.005
DUN	1675.4	90.29	40.66	0.005	9.55	0.010	0.139	49.83	0.170	0.005	0.022	0.000
DUN	1675.4	90.32	40.67	0.002	9.45	0.012	0.135	49.48	0.161	0.007	0.021	0.001
DUN	1675.4	90.13	40.81	0.002	9.81	0.014	0.142	50.27	0.193	0.007	0.022	0.000
DUN	1675.4	90.13	40.31	0.003	9.52	0.019	0.141	48.79	0.167	0.009	0.021	0.002
DUN	1675.4	90.46	40.72	0.005	9.37	0.015	0.137	49.85	0.179	0.006	0.022	0.004
DUN	1676.4	90.28	41.23	0.005	9.39	0.017	0.140	48.91	0.158	0.006	0.022	0.000
DUN	1676.4	90.55	40.56	0.002	9.33	0.013	0.135	50.19	0.152	0.009	0.021	0.000
DUN	1676.4	90.46	40.48	0.004	9.41	0.019	0.141	50.05	0.157	0.006	0.021	0.000
DUN	1676.4	90.46	40.06	0.006	9.36	0.015	0.138	49.80	0.156	0.010	0.021	0.002
DUN	1676.4	90.52	40.59	0.003	9.31	0.019	0.138	49.90	0.161	0.006	0.023	0.000
DUN	1676.4	90.19	40.55	0.003	9.36	0.022	0.139	48.27	0.154	0.005	0.022	0.001
DUN	1676.4	90.58	40.39	0.003	9.39	0.023	0.139	50.69	0.154	0.005	0.021	0.000
DUN	1676.4	90.56	40.49	0.007	9.37	0.022	0.138	50.48	0.154	0.010	0.020	0.003
DUN	1676.4	90.24	40.77	0.003	9.44	0.020	0.139	48.93	0.155	0.037	0.021	0.008
DUN	1676.4	90.13	41.15	0.004	9.51	0.019	0.141	48.75	0.158	0.006	0.021	0.000
DUN	1677.85	90.13	40.93	0.004	9.44	0.015	0.142	48.39	0.196	0.016	0.022	0.004
DUN	1677.85	90.18	41.10	0.004	9.43	0.014	0.142	48.56	0.191	0.007	0.021	0.000
DUN	1677.85	90.54	40.84	0.002	9.35	0.008	0.141	50.21	0.185	0.005	0.019	0.000
DUN	1677.85	90.49	40.81	0.002	9.37	0.016	0.143	50.01	0.179	0.003	0.020	0.000
DUN	1677.85	90.34	41.21	0.002	9.37	0.017	0.140	49.15	0.188	0.004	0.021	0.001
DUN	1677.85	90.59	41.08	0.004	9.34	0.016	0.141	50.45	0.192	0.005	0.022	0.002
DUN	1677.85	90.48	41.67	0.001	9.31	0.016	0.140	49.67	0.187	0.007	0.018	0.000
DUN	1677.85	90.41	41.10	0.003	9.37	0.017	0.142	49.60	0.190	0.006	0.020	0.000
DUN	1677.85	90.15	41.53	0.004	9.44	0.020	0.143	48.50	0.192	0.006	0.020	0.000
DUN	1677.85	90.19	41.32	0.003	9.45	0.021	0.142	48.72	0.187	0.006	0.019	0.001
DUN	1679.9	90.07	40.56	0.004	9.83	0.015	0.151	50.02	0.192	0.004	0.019	0.001
DUN	1679.9	90.02	40.87	0.004	9.81	0.019	0.151	49.64	0.195	0.006	0.019	0.000
DUN	1679.9	90.00	40.80	0.003	9.86	0.029	0.152	49.85	0.194	0.006	0.017	0.000
DUN	1679.9	90.17	40.95	0.006	9.77	0.014	0.151	50.27	0.194	0.007	0.019	0.001
DUN	1679.9	89.86	40.69	0.003	9.94	0.016	0.155	49.42	0.190	0.008	0.017	0.003
DUN	1679.9	90.04	40.89	0.003	9.82	0.020	0.151	49.82	0.198	0.010	0.019	0.000
DUN	1679.9	90.07	40.76	0.002	9.83	0.017	0.153	49.99	0.202	0.006	0.018	0.001
DUN	1679.9	90.11	41.16	0.005	9.75	0.012	0.149	49.83	0.192	0.005	0.018	0.000
DUN	1679.9	90.20	40.46	0.006	9.67	0.019	0.147	49.92	0.206	0.008	0.019	0.003
DUN	1679.9	90.14	40.70	0.006	9.70	0.013	0.147	49.76	0.208	0.009	0.017	0.004
DUN	1680.25	89.83	40.84	0.002	9.93	0.022	0.155	49.23	0.195	0.008	0.017	0.003
DUN	1680.25	89.93	41.04	0.006	9.82	0.024	0.153	49.25	0.202	0.005	0.017	0.001

DUN	1680.25	89.75	40.80	0.006	9.87	0.017	0.153	48.50	0.203	0.008	0.018	0.000
DUN	1680.25	90.02	40.72	0.003	9.86	0.017	0.153	49.92	0.201	0.014	0.018	0.004
DUN	1680.25	89.95	40.46	0.004	9.84	0.017	0.153	49.42	0.202	0.009	0.016	0.003
DUN	1680.25	89.77	40.35	0.003	9.96	0.019	0.155	49.03	0.191	0.005	0.018	0.000
DUN	1680.25	90.05	40.24	0.004	9.73	0.017	0.150	49.43	0.206	0.010	0.019	0.000
DUN	1680.25	90.20	40.86	0.006	9.64	0.015	0.144	49.78	0.212	0.006	0.018	0.002
DUN	1680.25	89.89	41.12	0.004	9.87	0.025	0.153	49.29	0.203	0.007	0.018	0.001
DUN	1680.42	90.31	40.08	0.006	9.72	0.019	0.149	50.87	0.201	0.008	0.019	0.002
DUN	1680.42	90.22	40.15	0.002	9.58	0.015	0.146	49.54	0.202	0.004	0.019	0.000
DUN	1680.42	89.77	40.08	0.003	9.92	0.021	0.155	48.85	0.197	0.078	0.018	0.042
DUN	1680.42	90.25	40.18	0.003	9.60	0.012	0.145	49.90	0.201	0.006	0.018	0.000
DUN	1680.42	90.03	40.56	0.002	9.78	0.020	0.153	49.58	0.189	0.005	0.017	0.000
DUN	1680.42	89.89	40.71	0.004	9.67	0.017	0.147	48.24	0.197	0.007	0.020	0.000
DUN	1680.42	90.02	40.52	0.004	9.77	0.021	0.151	49.50	0.202	0.008	0.020	0.001
DUN	1680.42	90.00	40.69	0.008	9.75	0.020	0.150	49.21	0.195	0.008	0.018	0.004
DUN	1680.42	90.04	40.49	0.003	9.80	0.020	0.150	49.71	0.191	0.008	0.018	0.002
DUN	1680.42	89.88	40.29	0.005	9.86	0.021	0.154	49.15	0.193	0.007	0.020	0.000
DUN	1683.81	89.73	41.46	0.005	9.96	0.024	0.145	48.80	0.184	0.004	0.014	0.003
DUN	1683.81	89.63	41.17	0.005	10.04	0.020	0.148	48.68	0.194	0.006	0.016	0.004
DUN	1683.81	89.44	40.64	0.008	10.18	0.024	0.146	48.43	0.194	0.004	0.016	0.007
DUN	1683.81	89.69	40.66	0.004	10.11	0.023	0.148	49.37	0.186	0.004	0.017	0.001
DUN	1683.81	89.57	41.08	0.005	10.10	0.012	0.134	48.68	0.149	0.007	0.014	0.005
DUN	1683.81	89.68	40.73	0.006	10.15	0.019	0.144	49.51	0.198	0.009	0.018	0.004
DUN	1712	91.50	40.99	0.005	8.42	0.018	0.131	50.85	0.287	0.011	0.015	0.009
DUN	1712	91.49	41.01	0.004	8.47	0.015	0.133	51.06	0.284	0.006	0.013	0.007
DUN	1712	91.44	40.94	0.007	8.49	0.020	0.136	50.88	0.288	0.006	0.018	0.005
DUN	1712	91.39	41.08	0.005	8.58	0.014	0.136	51.10	0.314	0.005	0.016	0.004
DUN	1712	91.45	40.88	0.003	8.51	0.013	0.135	51.07	0.310	0.007	0.018	0.002
DUN	1712	91.48	41.04	0.003	8.48	0.012	0.134	51.08	0.297	0.008	0.018	0.003
DUN	1722	90.35	40.28	0.005	9.40	0.017	0.148	49.37	0.235	0.013	0.015	0.007
DUN	1722	90.46	40.40	0.003	9.32	0.006	0.145	49.56	0.235	0.006	0.016	0.001
DUN	1722	90.26	40.50	0.004	9.54	0.013	0.151	49.58	0.239	0.005	0.014	0.003
DUN	1722	90.37	40.49	0.003	9.43	0.018	0.145	49.67	0.241	0.008	0.016	0.007
DUN	1722	90.57	40.47	0.006	9.23	0.013	0.141	49.74	0.229	0.007	0.014	0.004
DUN	1731	89.70	40.43	0.001	10.05	0.009	0.154	49.13	0.197	0.005	0.015	0.002
DUN	1731	89.62	40.54	0.003	10.13	0.011	0.156	49.07	0.198	0.005	0.014	0.006
DUN	1731	89.70	40.47	0.001	10.05	0.012	0.153	49.13	0.201	0.006	0.013	0.005
DUN	1731	89.71	40.53	0.004	10.05	0.015	0.154	49.15	0.203	0.006	0.014	0.008
DUN	1743	89.12	40.15	0.006	10.59	0.013	0.160	48.65	0.160	0.006	0.016	0.003
DUN	1743	89.08	39.92	0.003	10.63	0.016	0.160	48.66	0.161	0.003	0.019	0.004
DUN	1743	89.05	39.79	0.002	10.64	0.015	0.162	48.56	0.161	0.004	0.019	0.001
DUN	1743	89.10	39.75	0.004	10.59	0.016	0.162	48.55	0.159	0.010	0.017	0.007
DUN	1743	89.06	40.01	0.006	10.62	0.014	0.163	48.51	0.162	0.003	0.016	0.006
DUN	1743	88.96	39.85	0.004	10.71	0.020	0.163	48.46	0.164	0.004	0.018	0.006
DUN	1743	88.89	39.75	0.006	10.82	0.021	0.164	48.56	0.164	0.235	0.020	0.044
DUN	1743	89.13	40.07	0.003	10.59	0.016	0.161	48.70	0.154	0.003	0.017	0.001
LZ HZB	1908.44	88.17	40.88	0.002	11.44	0.030	0.190	47.85	0.250	0.006	0.030	0.003
LZ HZB	1908.44	88.13	40.92	0.008	11.51	0.030	0.160	47.96	0.270	0.013	0.010	0.007
LZ HZB	1908.44	88.10	40.84	0.008	11.53	0.020	0.160	47.90	0.270	0.003	0.020	0.011
LZ HZB	1908.44	88.14	40.77	0.003	11.43	0.010	0.190	47.67	0.270	0.002	0.020	0.008
LZ HZB	1916	88.94	40.91	0.008	10.91	0.020	0.161	49.25	0.289	0.006	0.016	0.003
LZ HZB	1916	88.93	40.93	0.005	10.92	0.017	0.160	49.23	0.278	0.006	0.018	0.007
LZ HZB	1916	88.94	40.94	0.003	10.93	0.022	0.159	49.32	0.276	0.013	0.018	0.011
LZ HZB	1916	88.99	40.96	0.010	10.86	0.021	0.160	49.24	0.285	0.003	0.018	0.008
LZ HZB	1916	89.09	40.95	0.005	10.75	0.018	0.157	49.29	0.298	0.002	0.016	0.007
LZ HZB	1932.2	89.56	40.86	0.002	10.10	0.010	0.150	48.62	0.320	0.006	0.020	0.003
LZ HZB	1932.2	89.66	41.02	0.008	10.03	0.020	0.150	48.80	0.330	0.013	0.020	0.007
LZ HZB	1932.2	89.51	40.88	0.008	10.17	0.010	0.170	48.71	0.320	0.003	0.020	0.011
LZ HZB	1932.2	89.50	40.79	0.003	10.18	0.010	0.140	48.68	0.330	0.002	0.040	0.008
LZ HZB	1948.6	90.33	40.70	0.002	9.68	0.017	0.140	50.77	0.297	0.005	0.016	0.001
LZ HZB	1948.6	89.52	40.47	0.008	10.29	0.016	0.162	49.31	0.271	0.004	0.018	0.000
LZ HZB	1948.6	89.20	40.18	0.008	10.52	0.018	0.158	48.78	0.270	0.008	0.016	0.006

LZ HZB	1948.6	89.51	40.45	0.003	10.22	0.018	0.151	48.91	0.277	0.003	0.016	0.003
LZ HZB	1948.6	89.45	41.22	0.005	10.34	0.014	0.156	49.19	0.277	0.005	0.017	0.000
LZ HZB	1948.6	89.88	41.07	0.004	9.81	0.019	0.144	48.91	0.298	0.004	0.015	0.003
LZ HZB	1948.6	90.00	40.70	0.007	9.85	0.022	0.143	49.74	0.290	0.004	0.015	0.006
LZ HZB	1948.6	89.42	40.58	0.005	10.59	0.019	0.160	50.20	0.268	0.103	0.016	0.027
LZ HZB	1948.6	89.82	40.68	0.004	10.15	0.016	0.155	50.28	0.288	0.008	0.016	0.000
LZ HZB	1949	90.20	40.06	0.001	9.75	0.017	0.144	50.35	0.289	0.004	0.016	0.002
LZ HZB	1949	89.63	39.63	0.004	9.94	0.011	0.144	48.18	0.300	0.166	0.015	0.101
LZ HZB	1949	90.09	40.15	0.005	9.79	0.019	0.141	49.93	0.291	0.004	0.017	0.002
LZ HZB	1949	89.92	40.18	0.010	9.84	0.080	0.141	49.28	0.297	0.076	0.016	0.044
LZ HZB	1949	89.88	40.11	0.006	9.77	0.014	0.142	48.72	0.294	0.014	0.017	0.009
LZ HZB	1949	90.13	40.44	0.005	9.70	0.020	0.139	49.66	0.302	0.004	0.018	0.001
LZ HZB	1949	90.16	40.53	0.002	9.65	0.017	0.139	49.61	0.301	0.004	0.016	0.000
LZ HZB	1949	89.99	40.78	0.010	9.70	0.017	0.138	48.91	0.306	0.010	0.018	0.017
LZ HZB	1949	89.94	40.34	0.006	9.72	0.017	0.142	48.74	0.297	0.004	0.016	0.006
LZ HZB	1949	90.29	40.48	0.007	9.67	0.019	0.141	50.47	0.298	0.007	0.016	0.009
LZ HZB	1949.5	89.93	40.15	0.006	9.79	0.014	0.143	49.09	0.294	0.006	0.016	0.004
LZ HZB	1949.5	89.98	40.49	0.009	9.77	0.023	0.143	49.19	0.302	0.006	0.018	0.005
LZ HZB	1949.5	90.06	40.58	0.005	9.77	0.016	0.142	49.68	0.284	0.004	0.017	0.001
LZ HZB	1949.5	90.08	40.21	0.003	9.85	0.019	0.145	50.22	0.293	0.005	0.017	0.005
LZ HZB	1949.5	90.11	40.57	0.004	9.74	0.019	0.140	49.82	0.295	0.004	0.018	0.001
LZ HZB	1949.5	90.10	40.16	0.005	9.84	0.021	0.144	50.29	0.302	0.005	0.020	0.001
LZ HZB	1949.5	90.06	40.55	0.003	9.76	0.020	0.142	49.64	0.290	0.004	0.017	0.001
LZ HZB	1949.5	90.07	40.42	0.004	9.81	0.021	0.144	49.96	0.286	0.003	0.016	0.007
LZ HZB	1949.5	90.18	40.72	0.005	9.80	0.018	0.144	50.52	0.301	0.003	0.016	0.003
LZ HZB	1949.5	89.93	40.14	0.008	9.82	0.022	0.144	49.25	0.291	0.007	0.016	0.007
LZ HZB	1950.16	90.06	40.15	0.008	9.68	0.019	0.140	49.25	0.288	0.008	0.015	0.006
LZ HZB	1950.16	90.16	40.55	0.006	9.59	0.016	0.137	49.31	0.308	0.004	0.017	0.000
LZ HZB	1950.16	90.08	40.45	0.003	9.68	0.017	0.139	49.34	0.309	0.003	0.016	0.000
LZ HZB	1950.16	90.09	40.56	0.003	9.66	0.017	0.138	49.28	0.313	0.003	0.018	0.001
LZ HZB	1950.16	90.05	40.62	0.006	9.72	0.022	0.140	49.33	0.311	0.003	0.017	0.000
LZ HZB	1950.16	90.07	40.59	0.004	9.70	0.015	0.141	49.40	0.302	0.005	0.018	0.000
LZ HZB	1950.16	90.05	40.43	0.003	9.67	0.013	0.142	49.16	0.313	0.002	0.016	0.000
LZ HZB	1950.16	90.06	40.02	0.004	9.71	0.017	0.142	49.37	0.315	0.002	0.017	0.000
LZ HZB	1950.16	89.95	40.45	0.010	9.82	0.016	0.141	49.34	0.288	0.007	0.016	0.007
LZ HZB	1950.16	89.98	40.45	0.006	9.76	0.019	0.140	49.19	0.308	0.002	0.016	0.003
LZ HZB	1950.16	90.06	39.94	0.009	9.66	0.012	0.141	49.09	0.306	0.006	0.015	0.002
LZ HZB	1950.16	90.46	40.52	0.002	9.34	0.018	0.135	49.71	0.313	0.029	0.016	0.013
LZ HZB	1950.16	90.45	40.36	0.006	9.31	0.014	0.133	49.47	0.296	0.004	0.017	0.011
LZ HZB	1950.16	89.96	40.55	0.003	9.81	0.015	0.144	49.31	0.298	0.074	0.017	0.025
LZ HZB	1950.16	90.25	40.42	0.002	9.50	0.015	0.131	49.34	0.307	0.004	0.016	0.000
LZ HZB	1950.16	90.02	40.28	0.010	9.67	0.017	0.140	48.93	0.310	0.003	0.017	0.003
LZ HZB	1950.16	89.96	40.51	0.011	9.77	0.018	0.140	49.12	0.306	0.007	0.016	0.001
LZ HZB	1950.16	90.19	40.55	0.004	9.59	0.014	0.137	49.44	0.308	0.006	0.016	0.000
LZ HZB	1950.16	89.99	40.67	0.005	9.76	0.020	0.141	49.25	0.298	0.023	0.017	0.004
LZ HZB	1950.16	90.04	40.38	0.010	9.71	0.018	0.140	49.25	0.297	0.007	0.015	0.013
LZ HZB	1950.3	90.69	40.76	0.010	9.17	0.020	0.134	50.11	0.315	0.007	0.014	0.011
LZ HZB	1950.3	90.26	41.03	0.005	9.34	0.012	0.137	48.57	0.337	0.110	0.016	0.041
LZ HZB	1950.3	90.25	41.03	0.005	9.47	0.020	0.140	49.17	0.364	0.005	0.017	0.006
LZ HZB	1950.3	90.94	40.46	0.005	8.83	0.017	0.132	49.75	0.376	0.012	0.014	0.007
LZ HZB	1950.3	90.51	40.73	0.003	9.23	0.012	0.137	49.36	0.356	0.045	0.017	0.015
LZ HZB	1950.3	90.30	39.95	0.005	9.47	0.021	0.138	49.48	0.358	0.016	0.015	0.017
LZ HZB	1950.3	90.29	39.97	0.005	9.41	0.017	0.135	49.06	0.358	0.004	0.017	0.004
LZ HZB	1950.3	90.13	39.92	0.007	9.54	0.014	0.141	48.90	0.356	0.034	0.018	0.013
LZ HZB	1950.3	90.35	40.32	0.007	9.37	0.017	0.138	49.25	0.365	0.026	0.016	0.012
LZ HZB	1950.55	89.75	40.32	0.010	9.94	0.020	0.146	48.86	0.351	0.011	0.016	0.007
LZ HZB	1950.55	89.96	40.78	0.005	9.90	0.021	0.147	49.79	0.363	0.028	0.016	0.011
LZ HZB	1950.55	89.93	40.95	0.008	9.93	0.022	0.147	49.74	0.370	0.057	0.016	0.045
LZ HZB	1950.55	89.99	40.62	0.009	9.75	0.022	0.144	49.18	0.356	0.011	0.018	0.009
LZ HZB	1950.55	90.05	40.48	0.005	9.79	0.014	0.147	49.75	0.337	0.006	0.016	0.005
LZ HZB	1950.55	89.83	40.98	0.011	9.89	0.023	0.147	49.00	0.347	0.005	0.015	0.008
LZ HZB	1950.55	89.96	40.96	0.003	9.82	0.020	0.146	49.40	0.345	0.004	0.015	0.002

LZ HZB	1950.55	89.70	41.01	0.008	9.71	0.016	0.144	47.41	0.364	0.005	0.017	0.008
LZ HZB	1950.55	89.71	40.27	0.009	10.10	0.021	0.148	49.41	0.380	0.079	0.017	0.037
LZ HZB	1950.55	90.26	40.45	0.011	9.64	0.013	0.151	50.14	0.304	0.011	0.014	0.021
LZ HZB	1951	90.11	40.52	0.005	9.65	0.012	0.143	49.32	0.357	0.003	0.015	0.002
LZ HZB	1951	90.10	40.54	0.004	9.65	0.017	0.144	49.31	0.361	0.003	0.016	0.001
LZ HZB	1951	90.19	40.37	0.011	9.71	0.017	0.144	50.09	0.356	0.009	0.016	0.006
LZ HZB	1951	89.69	41.23	0.009	9.88	0.019	0.148	48.21	0.349	0.005	0.016	0.006
LZ HZB	1951	90.03	40.44	0.009	9.87	0.016	0.148	50.00	0.357	0.011	0.016	0.007
LZ HZB	1951	90.04	40.16	0.012	9.84	0.014	0.146	49.88	0.375	0.012	0.017	0.002
LZ HZB	1951	89.81	39.99	0.007	9.85	0.012	0.145	48.73	0.368	0.016	0.018	0.007
LZ HZB	1951	90.05	39.99	0.008	9.78	0.014	0.147	49.67	0.355	0.006	0.015	0.006
LZ HZB	1951	89.81	40.21	0.002	9.89	0.018	0.147	48.87	0.357	0.012	0.017	0.005
LZ HZB	1951	90.12	39.95	0.007	9.84	0.013	0.149	50.39	0.347	0.114	0.016	0.028
LZ HZB	1951.5	90.07	40.12	0.008	9.74	0.131	0.136	49.57	0.370	0.087	0.018	0.073
LZ HZB	1951.5	89.97	40.10	0.003	9.90	0.009	0.145	49.85	0.396	0.005	0.016	0.000
LZ HZB	1951.5	89.93	40.38	0.004	9.88	0.011	0.145	49.53	0.393	0.007	0.017	0.003
LZ HZB	1951.5	89.92	40.17	0.005	9.98	0.021	0.145	49.93	0.366	0.011	0.016	0.005
LZ HZB	1951.5	89.87	40.17	0.006	9.96	0.007	0.149	49.55	0.385	0.007	0.016	0.002
LZ HZB	1951.5	89.83	40.65	0.005	9.86	0.013	0.143	48.88	0.351	0.004	0.013	0.003
LZ HZB	1951.5	89.89	40.55	0.004	10.04	0.022	0.151	50.10	0.337	0.003	0.014	0.003
LZ HZB	1951.5	89.86	40.67	0.005	9.89	0.016	0.147	49.18	0.357	0.005	0.014	0.002
LZ HZB	1951.5	89.69	40.40	0.005	9.77	0.018	0.143	47.74	0.393	0.004	0.018	0.002
LZ HZB	1951.5	90.06	40.17	0.005	9.83	0.010	0.143	50.02	0.402	0.008	0.017	0.001
LZ HZB	1952	90.10	40.61	0.007	9.60	0.013	0.138	49.03	0.230	0.010	0.016	0.015
LZ HZB	1952	89.96	40.63	0.005	9.81	0.016	0.141	49.34	0.305	0.005	0.016	0.005
LZ HZB	1952	89.87	40.15	0.008	9.85	0.013	0.146	49.01	0.306	0.010	0.017	0.003
LZ HZB	1952	89.96	40.17	0.008	9.88	0.012	0.142	49.68	0.268	0.022	0.019	0.012
LZ HZB	1952	90.01	40.79	0.012	9.79	0.013	0.142	49.50	0.305	0.006	0.015	0.005
LZ HZB	1952	90.03	40.43	0.009	9.80	0.018	0.141	49.67	0.296	0.008	0.014	0.006
LZ HZB	1952	89.95	40.36	0.003	9.97	0.012	0.146	50.03	0.297	0.158	0.015	0.049
LZ HZB	1952	90.30	40.80	0.005	9.55	0.017	0.136	49.90	0.261	0.004	0.015	0.005
LZ HZB	1952	89.94	40.66	0.016	9.76	0.021	0.138	48.98	0.301	0.009	0.016	0.016
LZ HZB	1952	90.10	40.56	0.011	9.69	0.019	0.140	49.51	0.294	0.008	0.017	0.014
LZ HZB	1952.5	89.70	40.38	0.013	9.79	0.018	0.142	47.85	0.282	0.007	0.015	0.009
LZ HZB	1952.5	89.82	39.55	0.006	9.92	0.019	0.143	49.12	0.260	0.005	0.014	0.004
LZ HZB	1952.5	90.06	39.72	0.002	9.78	0.014	0.141	49.73	0.279	0.004	0.016	0.001
LZ HZB	1952.5	90.00	40.24	0.007	9.75	0.013	0.141	49.22	0.287	0.012	0.017	0.005
LZ HZB	1952.5	90.09	40.94	0.003	9.61	0.017	0.140	49.03	0.268	0.005	0.015	0.001
LZ HZB	1952.5	89.95	40.75	0.004	9.71	0.014	0.141	48.79	0.279	0.004	0.017	0.005
LZ HZB	1952.5	90.09	40.02	0.003	9.65	0.013	0.136	49.20	0.283	0.003	0.015	0.002
LZ HZB	1952.5	89.93	40.06	0.006	9.91	0.019	0.144	49.65	0.284	0.004	0.017	0.003
LZ HZB	1952.5	89.87	40.01	0.007	9.87	0.016	0.144	49.11	0.272	0.015	0.016	0.008
LZ HZB	1952.5	89.89	39.92	0.010	9.92	0.018	0.142	49.50	0.298	0.005	0.017	0.006
LZ HZB	1953.15	89.87	40.18	0.006	9.81	0.016	0.138	48.87	0.152	0.002	0.020	0.000
LZ HZB	1953.15	89.99	40.28	0.002	9.76	0.014	0.137	49.26	0.147	0.004	0.017	0.000
LZ HZB	1953.15	89.85	40.26	0.007	9.87	0.022	0.140	49.00	0.144	0.004	0.017	0.002
LZ HZB	1953.15	89.98	40.56	0.005	9.80	0.018	0.139	49.41	0.141	0.002	0.015	0.000
LZ HZB	1953.15	90.06	40.42	0.007	9.71	0.025	0.138	49.36	0.154	0.006	0.016	0.004
LZ HZB	1953.15	89.95	40.54	0.002	9.87	0.019	0.139	49.55	0.149	0.003	0.016	0.007
LZ HZB	1953.15	90.01	40.10	0.004	9.75	0.020	0.138	49.29	0.152	0.005	0.017	0.005
LZ HZB	1953.15	90.12	40.21	0.003	9.64	0.014	0.131	49.36	0.151	0.002	0.020	0.000
LZ HZB	1953.15	89.81	40.24	0.004	9.94	0.015	0.141	49.16	0.144	0.003	0.020	0.000
LZ HZB	1953.15	89.81	39.83	0.002	9.87	0.016	0.140	48.79	0.146	0.004	0.017	0.000
LZ HZB	1953.15	89.80	39.91	0.004	9.91	0.013	0.138	48.98	0.146	0.002	0.016	0.003
LZ HZB	1953.15	89.82	39.70	0.007	9.88	0.018	0.137	48.88	0.134	0.005	0.018	0.003
LZ HZB	1953.15	90.40	40.02	0.006	9.29	0.017	0.127	49.09	0.141	0.015	0.023	0.018
LZ HZB	1953.15	89.87	40.08	0.005	9.84	0.017	0.137	49.00	0.155	0.002	0.017	0.000
LZ HZB	1953.15	89.87	40.07	0.000	9.86	0.014	0.139	49.10	0.131	0.004	0.020	0.000
LZ HZB	1953.15	89.86	40.08	0.005	9.87	0.019	0.138	49.04	0.152	0.002	0.015	0.000
LZ HZB	1953.15	90.01	39.80	0.005	9.70	0.016	0.133	49.03	0.147	0.038	0.016	0.010
LZ HZB	1953.15	90.09	39.74	0.003	9.68	0.016	0.136	49.34	0.145	0.002	0.017	0.000
LZ HZB	1953.15	90.02	39.83	0.007	9.72	0.017	0.133	49.21	0.155	0.023	0.016	0.013

LZ HZB	1953.15	90.02	39.89	0.006	9.73	0.017	0.135	49.29	0.149	0.016	0.016	0.001
LZ HZB	1953.3	89.93	40.20	0.005	9.97	0.018	0.142	49.98	0.159	0.006	0.016	0.004
LZ HZB	1953.3	89.74	40.53	0.004	10.03	0.014	0.143	49.20	0.176	0.004	0.018	0.002
LZ HZB	1953.3	89.67	40.04	0.006	10.03	0.021	0.143	48.85	0.175	0.003	0.019	0.004
LZ HZB	1953.3	89.73	40.49	0.005	10.13	0.019	0.145	49.69	0.179	0.004	0.018	0.003
LZ HZB	1953.3	89.79	39.95	0.005	9.96	0.014	0.143	49.13	0.180	0.005	0.016	0.005
LZ HZB	1953.3	89.88	40.74	0.009	9.90	0.020	0.140	49.31	0.166	0.009	0.016	0.013
LZ HZB	1953.3	89.83	40.39	0.002	9.86	0.016	0.137	48.85	0.179	0.003	0.016	0.004
LZ HZB	1953.3	89.98	40.29	0.005	9.96	0.019	0.142	50.20	0.173	0.003	0.016	0.004
LZ HZB	1953.3	89.97	39.97	0.005	9.93	0.014	0.140	49.99	0.176	0.004	0.018	0.002
LZ HZB	1953.3	90.12	39.97	0.003	9.77	0.011	0.139	50.02	0.173	0.003	0.016	0.002
LZ HZB	1954.12	90.49	40.27	0.004	9.28	0.013	0.136	49.56	0.179	0.003	0.017	0.000
LZ HZB	1954.12	90.47	40.39	0.003	9.46	0.020	0.141	50.39	0.154	0.004	0.017	0.002
LZ HZB	1954.12	90.37	39.40	0.004	9.37	0.016	0.135	49.34	0.168	0.006	0.018	0.006
LZ HZB	1954.12	90.27	40.48	0.005	9.48	0.017	0.139	49.36	0.176	0.010	0.019	0.007
LZ HZB	1954.12	90.39	39.76	0.014	9.52	0.019	0.139	50.27	0.180	0.015	0.020	0.008
LZ HZB	1954.12	90.48	40.03	0.005	9.53	0.016	0.138	50.82	0.175	0.007	0.017	0.004
LZ HZB	1954.12	90.18	39.76	0.006	9.72	0.019	0.142	50.12	0.175	0.005	0.018	0.004
LZ HZB	1954.12	90.31	39.82	0.004	9.59	0.018	0.140	50.14	0.174	0.005	0.018	0.000
LZ HZB	1954.12	89.98	39.89	0.005	9.81	0.013	0.143	49.42	0.183	0.005	0.017	0.000
FPYX Ol-bearing	1955	89.88	39.24	0.005	9.84	0.054	0.140	49.05	0.147	0.020	0.017	0.013
FPYX Ol-bearing	1955	89.88	40.02	0.003	9.68	0.014	0.137	48.24	0.155	0.003	0.017	0.000
FPYX Ol-bearing	1955	89.84	40.20	0.006	9.69	0.016	0.137	48.06	0.153	0.005	0.016	0.005
FPYX Ol-bearing	1955	90.05	39.68	0.006	9.91	0.014	0.143	50.29	0.149	0.009	0.019	0.010
FPYX Ol-bearing	1955	89.92	39.55	0.003	9.78	0.017	0.140	48.94	0.158	0.004	0.019	0.004
FPYX Ol-bearing	1955	89.99	39.77	0.006	9.88	0.020	0.139	49.88	0.153	0.004	0.017	0.005
FPYX Ol-bearing	1955	89.87	40.10	0.002	9.94	0.013	0.144	49.52	0.149	0.003	0.017	0.001
FPYX Ol-bearing	1955	89.99	40.00	0.003	9.87	0.014	0.143	49.80	0.147	0.002	0.019	0.002
FPYX Ol-bearing	1955	89.88	40.38	0.009	9.86	0.018	0.139	49.17	0.152	0.006	0.016	0.008
FPYX Ol-bearing	1955	89.93	40.87	0.002	9.91	0.018	0.141	49.64	0.156	0.005	0.017	0.000
FPYX Ol-bearing	1955.5	89.57	40.28	0.006	10.20	0.019	0.149	49.17	0.160	0.004	0.018	0.004
FPYX Ol-bearing	1955.5	89.43	40.89	0.004	10.13	0.020	0.150	48.14	0.168	0.003	0.017	0.002
FPYX Ol-bearing	1955.5	89.70	40.45	0.004	9.95	0.013	0.147	48.63	0.161	0.002	0.017	0.002
FPYX Ol-bearing	1955.5	89.57	40.27	0.003	10.15	0.018	0.150	48.93	0.166	0.034	0.019	0.009
FPYX Ol-bearing	1955.5	89.61	39.92	0.003	10.10	0.016	0.150	48.91	0.159	0.003	0.017	0.000
FPYX Ol-bearing	1955.5	89.47	39.77	0.010	10.08	0.020	0.150	48.04	0.161	0.007	0.018	0.015
FPYX Ol-bearing	1955.5	89.70	40.01	0.011	10.09	0.014	0.148	49.35	0.161	0.025	0.018	0.012
FPYX Ol-bearing	1955.5	89.73	40.04	0.010	10.03	0.018	0.147	49.17	0.171	0.014	0.017	0.012
FPYX Ol-bearing	1955.5	89.71	40.23	0.005	10.14	0.016	0.149	49.63	0.166	0.005	0.018	0.003
FPYX Ol-bearing	1955.5	89.50	39.83	0.007	10.12	0.018	0.148	48.41	0.169	0.028	0.017	0.011
FPYX Ol-bearing	1956	89.64	39.71	0.004	10.07	0.016	0.147	48.91	0.186	0.002	0.017	0.000
FPYX Ol-bearing	1956	89.46	40.28	0.011	10.29	0.014	0.154	49.01	0.184	0.010	0.019	0.004
FPYX Ol-bearing	1956	89.67	40.35	0.005	10.18	0.019	0.150	49.58	0.188	0.005	0.018	0.002
FPYX Ol-bearing	1956	89.35	40.08	0.007	10.32	0.013	0.154	48.58	0.179	0.003	0.017	0.003
FPYX Ol-bearing	1956	89.65	39.81	0.011	10.12	0.018	0.151	49.16	0.198	0.013	0.017	0.024
FPYX Ol-	1956	89.39	39.98	0.007	10.19	0.017	0.150	48.15	0.180	0.008	0.017	0.003

bearing												
FPYX Ol-bearing	1956	89.34	40.19	0.004	10.25	0.019	0.152	48.21	0.177	0.008	0.016	0.006
FPYX Ol-bearing	1956	89.44	40.29	0.006	10.21	0.012	0.151	48.50	0.191	0.004	0.018	0.001
FPYX Ol-bearing	1956	89.50	39.77	0.007	10.20	0.019	0.153	48.80	0.182	0.006	0.016	0.010
FPYX Ol-bearing	1956	89.27	40.27	0.004	10.45	0.016	0.156	48.80	0.189	0.003	0.018	0.003
FPYX Ol-bearing	1956.5	89.65	40.08	0.006	10.26	0.017	0.154	49.84	0.177	0.005	0.016	0.000
FPYX Ol-bearing	1956.5	89.76	39.98	0.004	10.12	0.012	0.150	49.78	0.175	0.004	0.016	0.000
FPYX Ol-bearing	1956.5	89.54	40.13	0.002	10.12	0.014	0.152	48.61	0.173	0.003	0.017	0.001
FPYX Ol-bearing	1956.5	89.58	40.24	0.004	10.20	0.012	0.152	49.18	0.184	0.005	0.018	0.000
FPYX Ol-bearing	1956.5	89.53	39.89	0.009	10.24	0.021	0.150	49.12	0.175	0.013	0.015	0.008
FPYX Ol-bearing	1956.5	89.60	40.22	0.002	10.25	0.019	0.151	49.52	0.177	0.002	0.016	0.002
FPYX Ol-bearing	1956.5	89.72	40.43	0.003	10.01	0.013	0.146	49.05	0.181	0.003	0.017	0.002
FPYX Ol-bearing	1956.5	89.57	39.66	0.008	10.08	0.013	0.150	48.60	0.189	0.006	0.018	0.010
FPYX Ol-bearing	1956.5	89.67	40.52	0.002	10.24	0.017	0.152	49.86	0.178	0.003	0.016	0.000
FPYX Ol-bearing	1956.5	89.49	40.33	0.006	10.30	0.019	0.149	49.23	0.177	0.026	0.017	0.008
FPYX Ol-bearing	1957	89.29	40.23	0.002	10.58	0.013	0.152	49.47	0.171	0.003	0.018	0.000
FPYX Ol-bearing	1957	88.83	40.18	0.004	10.68	0.013	0.152	47.64	0.167	0.004	0.020	0.000
FPYX Ol-bearing	1957	89.12	40.49	0.004	10.49	0.016	0.152	48.26	0.170	0.004	0.016	0.002
FPYX Ol-bearing	1957	88.98	40.27	0.003	10.53	0.019	0.152	47.74	0.165	0.003	0.016	0.002
FPYX Ol-bearing	1957	88.83	40.39	0.004	10.61	0.016	0.154	47.37	0.166	0.007	0.016	0.000
FPYX Ol-bearing	1957	89.35	40.10	0.002	10.46	0.019	0.151	49.24	0.151	0.003	0.016	0.000
FPYX Ol-bearing	1957	88.62	39.96	0.012	10.94	0.013	0.162	47.81	0.155	0.162	0.020	0.036
FPYX Ol-bearing	1957	88.91	40.20	0.003	10.65	0.024	0.156	47.89	0.182	0.038	0.018	0.019
FPYX Ol-bearing	1957	89.16	39.93	0.005	10.64	0.014	0.155	49.10	0.166	0.003	0.019	0.000
FPYX Ol-bearing	1957.5	88.93	39.36	0.004	10.74	0.021	0.158	48.41	0.157	0.003	0.015	0.004
FPYX Ol-bearing	1957.5	88.98	39.26	0.006	10.68	0.018	0.160	48.37	0.159	0.004	0.018	0.005
FPYX Ol-bearing	1957.5	89.06	39.18	0.006	10.64	0.017	0.158	48.57	0.158	0.009	0.015	0.006
FPYX Ol-bearing	1957.5	89.30	39.89	0.007	10.57	0.020	0.157	49.54	0.149	0.006	0.017	0.003
FPYX Ol-bearing	1957.5	89.12	39.70	0.008	10.66	0.016	0.158	49.00	0.160	0.009	0.018	0.006
FPYX Ol-bearing	1957.5	89.03	39.74	0.007	10.55	0.019	0.158	48.04	0.160	0.003	0.018	0.004
FPYX Ol-bearing	1957.5	89.26	39.58	0.007	10.58	0.017	0.160	49.33	0.157	0.006	0.016	0.003
FPYX Ol-bearing	1957.5	88.98	39.77	0.006	10.62	0.018	0.155	48.12	0.169	0.006	0.018	0.005
FPYX Ol-bearing	1957.5	89.03	39.80	0.011	10.67	0.018	0.157	48.62	0.166	0.008	0.018	0.011
FPYX Ol-bearing	1957.5	89.05	40.10	0.005	10.69	0.016	0.157	48.80	0.160	0.003	0.018	0.000
FPYX Ol-bearing	1959	88.84	40.05	0.012	10.90	0.023	0.159	48.71	0.177	0.010	0.016	0.006
FPYX Ol-bearing	1959	88.65	40.66	0.004	11.05	0.017	0.160	48.46	0.176	0.005	0.018	0.002
FPYX Ol-bearing	1959	88.69	40.74	0.005	10.82	0.014	0.155	47.64	0.179	0.006	0.017	0.004
FPYX Ol-bearing	1959	88.54	40.27	0.010	10.96	0.018	0.158	47.53	0.184	0.006	0.017	0.007

FPYX Ol-bearing	1959	88.84	40.88	0.005	10.66	0.012	0.151	47.62	0.176	0.006	0.017	0.003
FPYX Ol-bearing	1959	88.60	40.60	0.004	10.78	0.017	0.155	47.05	0.180	0.004	0.018	0.000
FPYX Ol-bearing	1959	88.74	40.73	0.010	10.90	0.020	0.156	48.19	0.174	0.007	0.018	0.012
FPYX Ol-bearing	1959	88.36	40.56	0.006	11.13	0.019	0.160	47.44	0.174	0.006	0.018	0.002
FPYX Ol-bearing	1959	88.84	40.14	0.003	10.88	0.019	0.159	48.61	0.178	0.004	0.018	0.004
FPYX Ol-bearing	1959	89.00	40.12	0.005	10.84	0.014	0.157	49.21	0.167	0.005	0.016	0.002
FPYX Ol-bearing	1961	87.62	40.11	0.004	11.84	0.013	0.165	47.01	0.172	0.003	0.020	0.001
FPYX Ol-bearing	1961	87.71	39.49	0.002	11.79	0.013	0.164	47.25	0.178	0.006	0.020	0.000
FPYX Ol-bearing	1961	87.94	40.60	0.001	11.58	0.009	0.162	47.38	0.179	0.003	0.019	0.003
FPYX Ol-bearing	1961	87.92	39.94	0.002	11.76	0.019	0.167	48.02	0.179	0.003	0.018	0.000
FPYX Ol-bearing	1961	87.63	39.80	0.007	11.98	0.017	0.166	47.63	0.179	0.003	0.020	0.001
FPYX Ol-bearing	1961	87.70	40.85	0.003	11.78	0.020	0.163	47.14	0.178	0.003	0.019	0.000
FPYX Ol-bearing	1961	87.85	39.96	0.003	11.78	0.018	0.166	47.80	0.175	0.003	0.019	0.001
FPYX Ol-bearing	1961	87.48	40.46	0.005	12.06	0.019	0.171	47.31	0.180	0.007	0.021	0.002
FPYX Ol-bearing	1961	87.87	39.89	0.005	11.84	0.012	0.164	48.11	0.176	0.003	0.021	0.001
FPYX Ol-bearing	1961	87.87	40.00	0.001	11.92	0.018	0.169	48.46	0.175	0.003	0.021	0.002
FPYX Ol-bearing	1962.5	86.60	39.25	0.003	12.89	0.018	0.176	46.72	0.197	0.005	0.021	0.003
FPYX Ol-bearing	1962.5	86.79	39.91	0.004	12.59	0.017	0.174	46.41	0.191	0.003	0.020	0.001
FPYX Ol-bearing	1962.5	86.59	39.53	0.005	12.99	0.020	0.179	47.06	0.162	0.007	0.027	0.006
FPYX Ol-bearing	1962.5	86.91	40.47	0.006	12.57	0.014	0.175	46.83	0.192	0.003	0.023	0.004
FPYX Ol-bearing	1962.5	86.48	40.05	0.008	13.06	0.021	0.182	46.90	0.164	0.006	0.026	0.007
FPYX Ol-bearing	1962.5	86.31	39.60	0.008	13.21	0.014	0.184	46.75	0.213	0.005	0.029	0.008
FPYX Ol-bearing	1962.5	86.71	39.93	0.008	12.84	0.021	0.177	47.01	0.179	0.008	0.025	0.014
FPYX Ol-bearing	1962.5	86.28	38.95	0.007	13.23	0.017	0.180	46.67	0.191	0.009	0.027	0.014
FPYX Ol-bearing	1962.5	86.63	39.59	0.004	12.98	0.019	0.177	47.21	0.181	0.007	0.026	0.004
FPYX Ol-bearing	1962.5	86.73	39.95	0.011	12.78	0.017	0.171	46.88	0.200	0.007	0.024	0.014

Table 3: EMPA on chromite from the main Bushveld Complex. *UG2-W* was done by Opoubou-Lando (2010) at the Waterval Mine. UG1-U and UG2-U was done by Eales and Reynolds (1986) in the Union section. The LZ (Lower Zone) was analysed by Cameron (1978). UMT377 and TMT 870 was analysed by EDS at the University of the Witwatersrand.

Analysis No.	TiO2	V2O5	Al2O3	Cr2O3	FeO	MnO	MgO	NiO
UG2-W	0.97		15.62	44.10	28.61			0.22
UG2-W	1.08		15.60	45.30	28.87			0.14
UG2-W	1.28		16.20	43.89	29.86			0.26
UG2-W	1.13		16.43	42.75	28.69			0.16
UG2-W	1.00		18.88	43.68	28.57			0.15
UG2-W	1.08		18.35	43.94	28.91			0.14
UG1-U	1.31		12.74	42.63	36.10			0.18
UG1-U	1.45		13.94	43.55	31.60			0.22
UG1-U	1.20		13.56	42.94	34.00			0.19

UG2-U	1.75		11.91	42.43	37.81			0.22
UG2-U	1.78		12.98	37.21	40.14			0.22
UG2-U	1.50		17.00	43.75	28.34			0.19
UG2-U LZ	0.77		19.65	36.05	36.00			
LZ	0.59		14.80	41.73	46.50			
LZ	0.48		17.61	45.00	24.60			
LZ	0.44		15.59	49.29	25.70			
UMT-377 - 998 m	3.42	0.32	6.54	34.69	49.35	0.60	2.24	0.22
TMT-870	0.31		27.47	35.45	26.14	0.54	9.16	0.22

Table 4: EMPA on olivine grains from hole ZF116 on Zwartfontein.

Hole	depth, m	Mg #	rock	SiO2	TiO2	FeO	CaO	MnO	MgO	NiO	Cr2O3	CoO	Total
ZF116	1226	82.6	HZB	39.57	0.008	16.51	0.042	0.242	44.08	0.516		0.026	101.05
ZF116	1226	82.7	HZB	39.70	0.006	16.47	0.038	0.235	44.35	0.515	0.002	0.026	101.35
ZF116	1226	82.5	HZB	39.73	0.016	16.67	0.044	0.245	44.23	0.507	0.002	0.029	101.48
ZF116	1226	82.6	HZB	39.81	0.010	16.60	0.043	0.238	44.32	0.517	0.003	0.026	101.58
ZF116	1227	83.2	HZB	39.30	0.009	16.14	0.033	0.240	44.70	0.463	0.004	0.025	100.94
ZF116	1227	82.1	HZB	37.80	0.006	16.86	0.038	0.239	43.51	0.497	0.004	0.030	99.134
ZF116	1227	83.2	HZB	38.59	0.007	15.95	0.036	0.239	44.29	0.439	0.001	0.022	99.583
ZF116	1227	83.3	HZB	38.20	0.008	15.87	0.031	0.239	44.30	0.410	0.001	0.026	99.106
ZF116	1227	83.1	HZB	37.20	0.010	15.86	0.038	0.246	43.70	0.460	0.003	0.023	97.617
ZF116	1227	82.9	HZB	37.40	0.000	16.09	0.033	0.236	43.84	0.450	0.004	0.026	98.107
ZF116	1227	82.1	HZB	38.07	0.007	16.83	0.031	0.240	43.46	0.507	0.002	0.031	99.113
ZF116	1227	83.1	HZB	37.86	0.004	16.02	0.037	0.243	44.09	0.371	0.001	0.021	98.656
ZF116	1227	83	HZB	37.84	0.006	16.02	0.040	0.240	43.90	0.478	0.003	0.025	98.562
ZF116	1227	83.2	HZB	37.69	0.005	15.97	0.029	0.240	44.10	0.477	0.002	0.023	98.626
ZF116	1227	82.8	HZB	37.95	0.003	16.28	0.029	0.236	43.93	0.488	0.002	0.028	98.925
ZF116	1227	83.1	HZB	38.74	0.008	16.02	0.038	0.240	44.33	0.482	0.002	0.024	99.894
ZF116	1227	83.1	HZB	39.22	0.005	16.10	0.042	0.239	44.46	0.474	0.000	0.027	100.57
ZF116	1227	83.1	HZB	38.97	0.007	16.14	0.029	0.239	44.36	0.484	0.002	0.025	100.27
ZF116	1227	82.8	HZB	38.07	0.007	16.47	0.042	0.243	43.56	0.494	0.002	0.028	98.905
ZF116	1228	82.6	HZB	37.66	0.005	16.43	0.038	0.240	43.27	0.486	0.001	0.028	98.838
ZF116	1228	82.4	HZB	38.07	0.007	16.46	0.038	0.240	43.64	0.486	0.003	0.029	99.192
ZF116	1228	82.5	HZB	38.06	0.009	16.47	0.038	0.240	43.67	0.489	0.003	0.027	99.012
ZF116	1240	82.9	FPYX	38.79	0.007	17.06	0.035	0.251	43.71	0.205	0.004	0.028	100.09
ZF116	1240	82.3	FPYX	38.82	0.005	16.77	0.025	0.251	43.89	0.202	0.002	0.028	99.995
ZF116	1240	82.9	FPYX	37.77	0.006	16.09	0.033	0.262	43.77	0.195	0.002	0.025	98.145
ZF116	1240	82.5	FPYX	38.25	0.010	16.59	0.029	0.251	43.88	0.207	0.002	0.026	99.235
ZF116	1240	82.4	FPYX	38.79	0.009	16.68	0.039	0.243	43.88	0.215	0.004	0.028	99.827

		83.	FPY	38.1	0.00	15.2	0.02	0.24	44.6	0.19		0.02	
ZF116	1240	9	X	4	6	7	7	5	9	4	0.003	3	98.61
			FPY	38.1	0.01	17.0	0.03	0.25	43.4	0.21		0.03	
ZF116	1240	82	X	3	2	0	8	2	8	5	0.022	0	99.19
		83.	FPY	36.6	0.00	15.3	0.03	0.25	44.4	0.20		0.02	
ZF116	1240	8	X	0	7	1	1	5	1	3	0.008	5	96.85
		82.	FPY	38.0	0.00	16.8	0.02	0.25	43.6	0.20		0.02	
ZF116	1240	2	X	4	3	1	9	9	0	3	0.001	9	98.98
		83.	FPY	38.3	0.00	15.5	0.03	0.25	44.6	0.18		0.02	
ZF116	1240	6	X	8	4	6	0	7	6	4	0.001	1	99.10
		82.	FPY	38.5	0.00	16.6	0.03	0.25	44.0	0.19		0.02	
ZF116	1240	5	X	1	5	3	6	7	7	9	0.002	6	99.74
		82.	FPY	37.7	0.01	16.5	0.04	0.25	43.8	0.20		0.02	
ZF116	1240	5	X	4	0	2	5	1	6	7	0.003	8	98.67
		82.	FPY	37.7	0.00	16.6	0.02	0.25	43.9	0.20		0.02	
ZF116	1240	5	X	1	7	0	6	1	4	5	0.002	9	98.77
		82.	FPY	38.6	0.00	16.6	0.03	0.25	44.1	0.20		0.02	
ZF116	1240	5	X	3	8	5	9	2	3	7	0.003	9	99.95
		82.	FPY	38.2	0.00	16.5	0.02	0.24	44.0	0.20		0.02	
ZF116	1240	6	X	8	5	2	1	9	3	2	0.001	8	99.34
		82.		39.7	0.00	16.8	0.02	0.31	44.3	0.23		0.02	101.5
ZF116	1572	4	HZB	7	4	8	5	0	3	8	0.002	5	8
		82.		39.7	0.00	16.9	0.02	0.30	44.3	0.23		0.02	101.6
ZF116	1572	3	HZB	5	5	6	2	9	4	9	0.001	5	5
		82.		39.7	0.00	16.8	0.02	0.31	44.3	0.23		0.02	101.6
ZF116	1572	4	HZB	8	4	7	4	0	4	5	0.002	6	0
		82.		39.8	0.00	16.8	0.01	0.30	44.5	0.23		0.02	101.8
ZF116	1572	5	HZB	4	5	8	9	8	1	3	0.001	6	2
		82.		39.8	0.00	16.8	0.01	0.30	44.2	0.23		0.02	101.6
ZF116	1572	4	HZB	8	5	8	6	4	8	1	0.002	6	3
		82.		39.8	0.00	16.8	0.01	0.30	44.2	0.23		0.02	101.5
ZF116	1572	4	HZB	5	8	4	8	6	2	2	0.002	4	1